U.S. Coast Guard Research and Development Center
1082 Shennecossett Road, Groton, CT 06340-6048

Report No. CG-D-05-05

LEEWAY DIVERGENCE

FINAL REPORT
JANUARY 2005

Prepared for:

U.S. Department of Homeland Security
United States Coast Guard
Operations (G-O)
Washington, DC 20593-0001

N O T I C E

This document is disseminated under the sponsorship of the Department of Homeland Security in the interest of information exchange. The United States Government assumes no liability for its contents or use thereof.

The United States Government does not endorse products or manufacturers. Trade or manufacturers' names appear herein solely because they are considered essential to the object of this report.

This report does not constitute a standard, specification, or regulation.

Marc B. Mandler, Ph.D
Technical Director
United States Coast Guard
Research & Development Center
1082 Shennecossett Road
Groton, CT 06340-6048

Technical Report Documentation Page

1. Report No.	2. Government Accession Number	3. Recipient's Catalog No.
CG-D-05-05	ADA435435	

4. Title and Subtitle	5. Report Date
LEEWAY DIVERGENCE	January 2005
	6. Performing Organization Code Project No. 1012.3.16
7. Author(s) Arthur A. Allen	8. Performing Organization Report No.
9. Performing Organization Name and Address U.S. Coast Guard Research and Development Center 1082 Shennecossett Road Groton, CT 06340-6048	10. Work Unit No. (TRAIS) 11. Contract or Grant No.
12. Sponsoring Organization Name and Address U.S. Department of Homeland Security United States Coast Guard Operations (G-O) Washington, DC 20593-0001	13. Type of Report & Period Covered Final 14. Sponsoring Agency Code Commandant (G-OPR) U.S Coast Guard Headquarters Washington, DC 20593-0001

15. Supplementary Notes

The technical point of contact is Arthur Allen, 860-441-2747, email: aallen@rdc.uscg.mil

16. Abstract (MAXIMUM 200 WORDS)

Understanding leeway divergence is key to accurately determining maritime search areas. The downwind and crosswind components of leeway drift as a function of wind speed have been reported on in the literature for 23 categories of leeway drift objects. Two additional leeway drift object categories were analyzed in this report. The optimal relationships between downwind and crosswind components of leeway coefficients and leeway speed and divergence angle values are derived empirically using the 25 categories that contained both sets of coefficients. Downwind and crosswind leeway coefficients were generated for an additional 38 leeway categories based on the estimates from standard error relationships. The entire set of downwind and crosswind leeway component coefficients is presented for 63 leeway categories.

The crosswind component of leeway has been observed to be either positive (right of the downwind direction) or negative (left of the downwind directions) for the duration of each individual drift run. For four drift object categories, forty-nine sign changes of the crosswind leeway component occurred during 1332.2 hours of sampling. This represents a frequency of sign change in the crosswind components of 4% per hour, independent of leeway category or wind speed. Crosswind leeway component sign changes at 4% per hour have a significant impact on the final search area probability distribution modeled by Monte Carlo simulations.

17. Key Words		18. Distribution Statement
Leeway	Leeway divergence	This document is available to the U.S. public through the National Technical Information Service, Springfield, VA 22161
Leeway angle	Crosswind component	
Downwind component	Divergence angle	
Search and Rescue	SAR	

19. Security Class (This Report)	20. Security Class (This Page)	21. No of Pages	22. Price
UNCLASSIFIED	UNCLASSIFIED		

Form DOT F 1700.7 (8/72) Reproduction of form and completed page is authorized

ACKNOWLEDGEMENTS

The comments of Penny Herring, Dr. Jennifer Dick-O'Donnell, LT Harlan Wallace, Gary Hover, LT Gregory Purvis, J. R. Frost, R. Quincy Robe, Richard Schaefer, M. J. Lewandowski and Vonnie Summers are appreciated and helped to improve this report.

EXECUTIVE SUMMARY

The hunt for a drifting object in the maritime environment typically requires the determination of search areas. It is well established that survivors and their craft drift generally downwind due to leeway effects. It is now understood from a series of field studies conducted during the 1990s that leeway drift is not always directly downwind, but that there is often a significant component of drift perpendicular to the downwind direction. This perpendicular motion is the crosswind component of leeway drift. The crosswind component of leeway causes an object's drift to diverge from the downwind direction. Understanding this behavior, defined as **leeway divergence**, is key to accurately determining search areas. This study discusses the importance of the leeway crosswind components and develops a Downwind Leeway (DWL) and Crosswind Leeway (CWL) component model for incorporating the effect of leeway divergence into search planning tools and determination of search areas.

This report is a follow on to Allen and Plourde (1999) with a particular emphasis on the relationship among leeway angle, divergence angle, and crosswind components of leeway, and their roles in describing and modeling leeway motion. This report also provides the background and framework for on-going efforts to incorporate crosswind components of leeway into the search area determination model first introduced in Allen and Plourde (1999) and into manual search planning methods.

In the past, the unclear relationship between leeway angle and leeway divergence, and the lack of crosswind information, has limited accurate representation of leeway behavior in search planning tools. This report clarifies leeway divergence terms, discusses crosswind behavior, and ultimately presents DWL and CWL of leeway drift, as a function of wind speed, for 63 categories of leeway drift objects.

The net displacement from the downwind direction is dependent on the magnitude and frequency of sign changes of the crosswind component of leeway. Allen and Plourde (1999) provided values for leeway speed as function of wind speed and divergence angle for 63 leeway categories. Leeway data for 25 of these 63 categories are available allowing direct computation of the DWL and CWL coefficients using linear regression analysis. For the other 38 categories, no actual leeway drift data are available. Using the data for the 25 leeway categories, Chapter 2 of the report develops a statistically derived method to determine the remaining 38 sets of DWL and CWL coefficients. Chapter 3 then presents the entire set of downwind and crosswind leeway coefficients for both the unconstrained and constrained DWL and CWL component regression models. It is proposed that incorporating these coefficients into DWL and CWL component search planning models will result in better-centered and better-sized search areas than those search areas developed without using the downwind and crosswind leeway components.

The investigations in Chapter 5 show that the frequency of CWL sign change appears to be independent of wind speed. The frequency of the sign change was shown to vary between leeway object categories but was not consistent with the general configuration of the individual leeway object types. The overall observed frequency of these sign changes in crosswind components based on the leeway drift of all four leeway object categories combined was approximately 4-6% per hour. It was further shown that varying the sign change frequency between 0% and 50% per hour has a significant impact on final search area probability

distribution, but varying the sign change frequency between 4% and 6% per hour does not affect the distribution. Based on past search area modeling, it appears that a 4-6% sign change frequency provides a search area distribution consistent with those generated by existing SAR planning tools. Accordingly, a "generic" value of 4% change in CWL sign per hour is recommended for use in stochastic, leeway-drift models until further work in this area provides a more complete picture of CWL sign change.

Recommendations

1) Tables 3-1 and 3-2 provide a complete set of DWL and CWL coefficients for the 63 categories of leeway objects in the taxonomy developed by Allen and Plourde (1999). Although 38 sets of DWL and CWL coefficients were statistically derived from the empirical data, the Table 3-1 and 3-2 coefficients should be used in numerical search planning tools to determine the downwind and crosswind components of leeway (as a function of wind speed adjusted to the standard 10-meter height) in calculating search area distributions.
2) Incorporate into numerical search planning tools the use of a simple statistical model of switching between positive and negative crosswind component equations using a sign change frequency of 4% per hour, independent of wind speed or leeway category.
3) Incorporate into manual search planning tools the use of divergence angles provided by Allen and Plourde (1999) divided by an "adjustment factor" determined here to be 1.35.
4) Continue efforts to fully understand and model the drift of survivors and survivor craft by studying targets over more drift runs and in a variety of wind conditions. The conditions should include wind speeds less than three meters per second (m/s) and greater than 20 m/s, and periods of rapid wind direction shifts. With more drift runs the question of initial distribution between left and right divergence can be addressed. Collecting leeway data under a variety of wind conditions will also allow the observation of changes between left and right divergence. Data collection for the 38 leeway categories for which data are not available will allow direct computation and verification of the DWL and CWL coefficients for these categories.
5) Further refine the collection of leeway data collected in the field to minimize the effect that the installed or attached instrumentation has on drift of the search test object. The use of current meters placed directly onboard the test object may lessen the impact on the leeway object of crosswind component sign-change. However, these directly mounted current meters should be verified against the more standard technique of a tethered current meter, which is well away from any local flow distortion effects. Additional insight into the behavior and dynamics of an object changing crosswind component sign might come with further information of the wave field and from leeway dynamics modeling studies.

TABLE OF CONTENTS

LIST OF ILLUSTRATIONS

LIST OF TABLES

LIST OF ACRONYMS

AMM	Automated Manual Method
CANSARP	Canadian Search and Rescue Prediction
CASP	Computer Assisted Search Planning
CDF	Cumulative Distribution Function
CWL	Crosswind Leeway
DWL	Downwind Leeway
GDOC	Geographic Display Operations Computer
LKP	Last Known Position
PIW	Person in the water
PVD	Progressive Vector Diagrams
SAR	Search and Rescue

(This page intentionally left blank.)

CHAPTER 1.

PRESENT UNDERSTANDING OF LEEWAY DRIFT

1.1. Introduction to Leeway – Concepts and Terminology

The starting point for a maritime search for survivors and survivor craft is the determination of search areas where there is a high probability of locating these Search and Rescue (SAR) targets. The search areas are based upon an evaluation of Last Known Position (LKP) of the target, surface currents, and leeway drift. This report focuses on **leeway drift**, the movement of the leeway object relative to the ocean's surface caused by the wind. **Leeway object** is defined as any vessel, life raft, person in the water (PIW) or object of interest (e.g. debris from a ship sinking or airplane crash) that is subject to leeway drift. The overall geographic location of the object is determined by the leeway drift (motion relative to the upper surface layer of the ocean) added to the movement of the upper layer of water in the ocean caused by wind-driven surface currents, tidal currents, and long-term ocean currents.

The National Search and Rescue Supplement to the International Aeronautical and Maritime Search and Rescue Manual defines Leeway as "the movement of a search object through water caused by winds blowing against exposed surfaces"(National Search and Rescue Committee, 2000). Exposed surface of the object means that portion above the water. It is important to note, however, that there are two mechanisms by which the wind causes an object to drift relative to the surface layer of the ocean. The first of these is the drag force exerted on the object by the wind that pushes the object through the water. If the profile the object presents to the wind is in any way asymmetric, then this force will have both a downwind component and a crosswind component. In addition, surface gravity waves may contribute to the leeway drift of the object. The surface gravity waves are, of course, generated by the wind and generally propagate in a downwind direction but may also be moving at an angle to the downwind direction. Thus, the wave induced leeway drift can be in either the downwind direction, cross wind direction or both. As both physical mechanisms are driven by surface winds, the composite leeway drift correlates well with surface wind speed and direction, and is modeled as a function of wind speed using linear regression techniques. The leeway drift of an object is often expressed as a percentage of the wind speed adjusted to the 10-meter reference height for oceanic surface wind measurements.

The leeway drift phenomenon has been the subject of a number of field investigations and studies. A comprehensive explanation of the leeway drift and review of leeway drift observations and experiments, as well as techniques and models for predicting leeway drift, are provided by Allen and Plourde (1999). A thorough summary and review of the results of the various leeway experiments as reported in the works cited above are provided in Chapter 2 of the Allen and Plourde report.

Although the larger component of leeway drift is in the downwind direction, there is often a significant component of drift perpendicular to the downwind direction. This motion perpendicular to the downwind direction is the crosswind component of leeway drift. The crosswind component of leeway drift causes the object's drift trajectory to diverge from the downwind direction. Understanding this behavior, defined as **leeway divergence**, is key to accurately determining search areas. The divergence from the downwind direction is dependent

on both the object and its environment. Drifting objects generally present an asymmetric profile to the wind. This asymmetric profile leads to a net side force caused by the pressure differential of the wind on the object (Hodgins and Hodgins, 1998), which in turn results in a motion perpendicular to the downwind direction. This divergence from the downwind direction is accounted for by specifying a **leeway angle**, that is the angle between the wind direction and the direction of movement of the leeway object designated **"**Lα**"** in Figure 1-1.

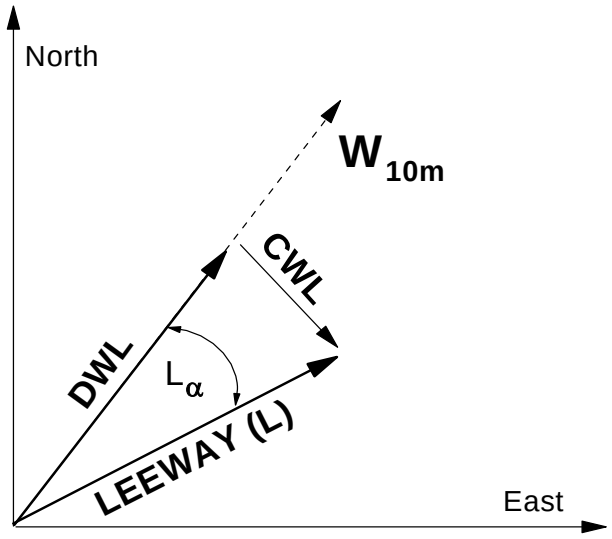

$\mathbf{W_{10m}}$ = Wind velocity vector adjusted to 10 m height,
L = Leeway velocity vector,
Lα = Leeway angle,

$\frac{|\mathbf{L}|}{|\mathbf{W}_{10m}|}$ = Leeway rate,

DWL = $|\mathbf{L}|\cos(L\alpha)$ = Downwind Leeway component,

CWL = $|\mathbf{L}|\sin(L\alpha)$ = Crosswind Leeway component.

Figure 1-1. The relationship between the leeway speed and leeway angle and the downwind and crosswind components of leeway.

The nature and relationship of the various leeway parameters are represented in Figure 1-1. The corresponding definitions used in this report can be summarized as follows:

The **Leeway rate** is the ratio of the leeway speed of the drifting object to the 10-meter surface wind speed. Leeway rate is always a positive value

Leeway velocity vector (**L**) of a drifting object is the two-dimensional representation of the rate of the leeway object's motion through the water and the direction of motion relative to the wind velocity vector as shown in Figure 1-1.

Leeway speed and **leeway angle** are the polar coordinate representation for the leeway velocity vector. **Leeway speed** is the rate of travel of the leeway object relative to the surface of the ocean. **Leeway angle** is the angle between the wind direction and the direction of leeway drift for a single sampling period for a particular drift object. Leeway angles to the right of the wind direction are designated as positive; leeway angles to the left of the wind direction are designated as negative.

$\mathbf{W_{10m}}$ is the surface wind speed adjusted to a height 10 meters above the water. This is the standard meteorological convention for determining "surface winds." At a 10-meter height, it is assumed that the wind velocity is steady and not subject to the frictional boundary layer effects of the ocean surface.

Downwind leeway (DWL**)** and **Crosswind leeway (**CWL**)** are the components of the **leeway velocity vector** expressed in rectangular coordinates. Downwind leeway is the component in the direction of the wind. Crosswind leeway is the component perpendicular to the wind direction.

A key parameter investigated in the report is the **Divergence angle**. As stated above, leeway angle refers to the angle between the direction of drift and downwind direction for a *single sampling* period for a *particular* drift object. Over a number of sampling periods, leeway objects of a given type may exhibit a range of leeway angles. In this report, **divergence angle** refers to the *representative range of* leeway angles for a category of leeway objects. Divergence angle has been calculated using different methods in different studies. It is calculated by obtaining the net leeway angle over time for a specific leeway object's drift trajectory, and then averaging again for a series of leeway drift trajectories of a number of leeway objects in a leeway category, to determine the mean leeway angle and standard deviation of the leeway angle for the category. Divergence angle is then calculated as twice the standard deviation of the leeway angle, or mean plus one standard deviation of the leeway angle, or mean plus two standard deviations of the leeway angle depending on the particular study. A more comprehensive discussion of how divergence angle has been determined for this study is presented in Section 1.2.

Figure 1-2 shows a typical plot of leeway object trajectories for a particular type of leeway object (Life rafts with deep ballast, canopy, light loading, no drogue. In this case, the plotted trajectories indicate leeway angles ranging from approximately -20^o (20^o to the left of the downwind direction) through $+15^o$ (15^o to the right of the downwind direction). The divergence angle specified by Allen and Plourde (1999) for this class is 20^o as indicated by the dashed lines.

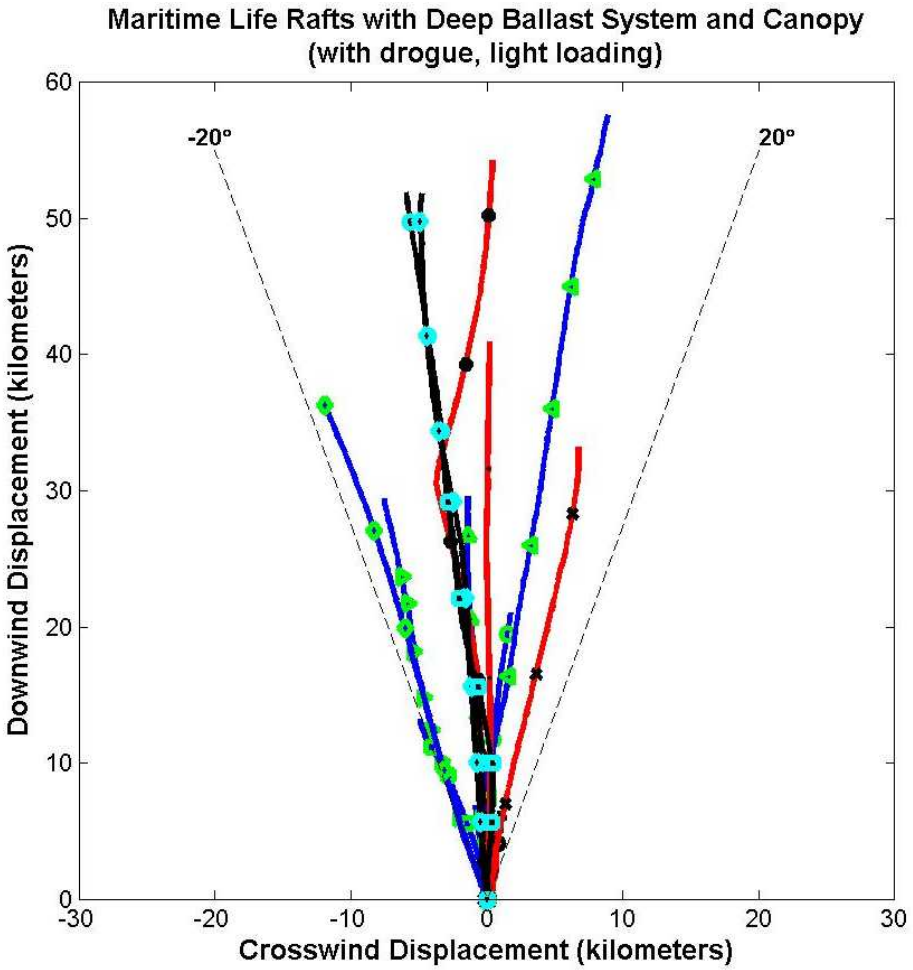

Figure 1-2. Progressive vector diagrams (PVD) of trajectories relative to the downwind direction for twenty experimental drift runs of 4-6 person maritime life raft with deep-ballast system and canopy, light loading, no drogue. Markers are placed along the PVDs at 6-hour intervals. The twenty-degree divergence angles for this leeway category specified by Allen and Plourde (1999) are shown as dashed lines.

Two problems exist with the relationship between leeway angle and divergence angle. The first is there is no one method for converting leeway angle statistics or analysis to a divergence angle estimate for a given leeway object category. Allen and Plourde (1999) used three different methods to develop divergence angle values based on the various leeway drift data sets. The second problem is there are inconsistencies in how present search-planning tools (e.g. the Coast Guard Computer Assisted Search Planning and Automated Manual Solution models) specify and incorporate the divergence angle concept in computing search areas.

These problems are avoided by using downwind and crosswind leeway (DWL and CWL) components as a function of wind speed, rather than the more-traditional use of leeway and leeway angle to compute the leeway drift over time. This approach is more consistent with the dynamics of leeway, as the physical mechanisms determining the downwind and crosswind components are different. It also provides a more accurate method of determining leeway at low

wind speeds and is computationally easier to implement in SAR planning tools. To capitalize on this advantage, Allen and Plourde demonstrated how DWL and CWL components could be calculated by linearly regressing the downwind and crosswind leeway components against wind speed. For given leeway object categories where leewaydrift data sets existed, DWL and CWL regression equations were developed. The DWL and CWL regression equations each require a separate leeway speed coefficient (the value that $\mathbf{W_{10m}}$ is multiplied by to compute leeway speed which corresponds to the slope of the linear regression), a Y-intercept term, and Standard Error of the Estimate ($S_{y/x}$).

However, implementation of the DWL and CWL component approach is not completely straightforward. First of all, the determination of the DWL and CWL regression equations for a given category requires the existence of an adequate leeway drift data set. Secondly, although there is a clear correlation between wind speed and DWL, the correlation between wind speed and CWL is less obvious (as demonstrated by Allen and Plourde (1999). There appear to be other factors beside wind speed that influence the crosswind component of leeway drift. Thirdly, there are a number of factors that influence whether a leeway object will initially drift to the right or left of the wind, and observations indicate that the crosswind component can randomly change direction under certain conditions. The phenomena of CWL direction and CWL direction change have been largely unexplored. Each of these issues will be addressed in detail in this report.

1.2. Previous Studies Of Leeway Angle And Leeway Divergence

The relationship between wind speed, leeway angle and leeway divergence angle has been addressed in a number of previous studies starting in 1960. Chapline (1960); Hufford and Broida (1974); Nash and Willcox (1985, 1991); Fitzgerald, Finlayson and Allen (1994); Allen (1996); Allen and Fitzgerald (1997); and Kang (1999) all reported leeway drift that was not directly downwind. Chapline (1960) also observed that those vessels with large underwater lateral planes had an increased tendency to move off the downwind direction. He reported relative wind direction for sailing vessels of 9 to 13 points (101 to 146 degrees), but did not include what their leeway angle or direction was. However, for fishing sampans, he reported relative wind direction of 10 points (112 ½ degrees) and a leeway motion directly abeam. Chapline provided the first reported leeway angle (2 points or 22 ½ degrees) for a commercial fishing vessel – Hawaii sampan.

Hufford and Broida (1974) provided leeway data including Leeway angle in tabular form for four small craft (12 to 21 ft) and a 12-foot rubber raft. Four of the five targets were tested with and without (w/o) drogues; a 15-foot Barge was tested only without a drogue. Hufford and Broida's data for the four small craft were analyzed and are presented in Table 1-1 and Figure 1-3.

Table 1-1. Leeway angle (in degrees) four small craft studied by Hufford and Broida (1974).

Hufford & Broida (1974)	Number of samples	Speed (m/s)	Leeway Angle				Abs. Angle	
			mean	s.dev.	min	max	mean	s.dev.
four small craft	73	1.1 – 5	4.8	32.2	-105	73	26.1	19.3
	127	5 – 9.8	4.9	25.7	-60	67	20.7	15.7
	200	1.5 – 9.8	4.8	28.2	-105	73	22.8	17.2
Three craft with drogues	38	2.8 – 9.8	9.3	21.1	-38	55	17.6	14.7
Four craft without drogues	162	1.1 – 8.4	3.8	29.6	-105	73	24.0	17.6

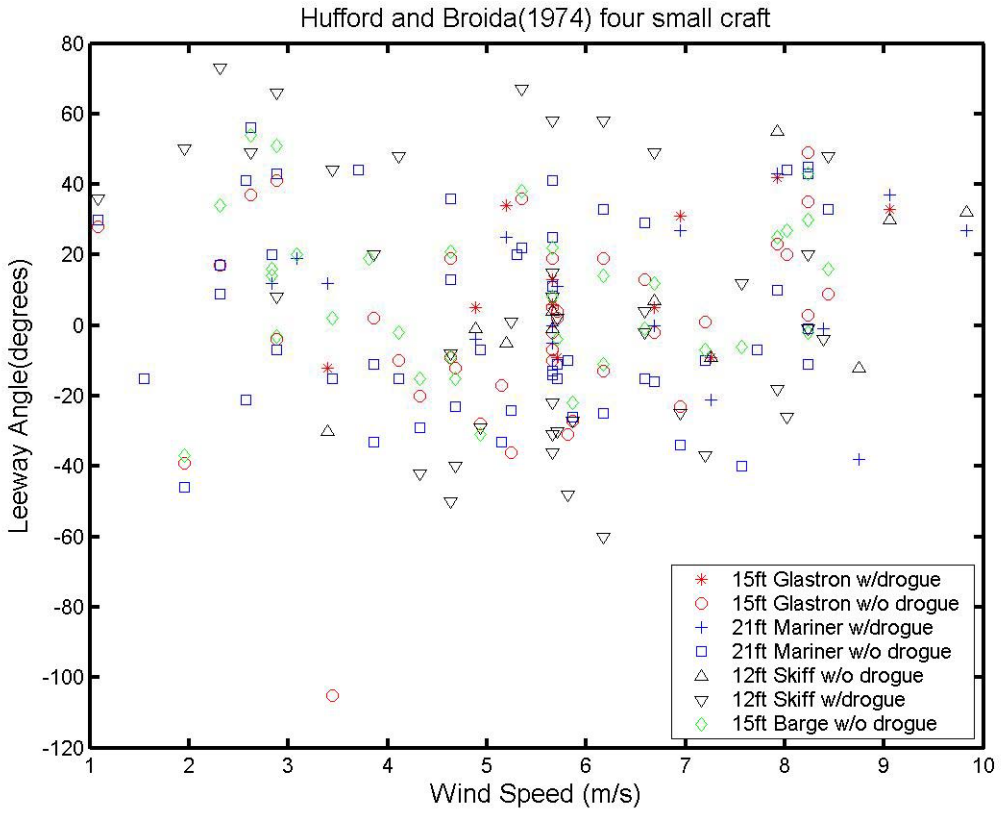

Figure 1-3. Leeway angle versus wind speed from Hufford and Broida (1974), data set for four small craft.

Hufford and Broida (1974) was one of the first attempts to scientifically observe and correlate wind speed to leeway. Since experimental technique and analysis were being developed, Hufford and Broida (1974) did not include a sample size later found to be necessary for a more rigorous examination of leeway. From the spread of points in Figure 1-3, there is no apparent correlation between wind speed and leeway angle.

Allen and Plourde (1999) conducted a comprehensive review of previous leeway observations and experiments reported in the literature to determine the types of leeway objects studied to date, the methods used during these studies, and the present level of understanding of leeway behavior including the factors influencing the crosswind component of leeway and leeway divergence. This effort was focused on determining the source and validity of the key parameters (i.e., Leeway Rate and Divergence Angle) used to model leeway drift for various categories of leeway objects in the SAR Planning Tools employed by the SAR community.

Allen and Plourde (1999) investigated and reviewed the guidance provided by the National SAR Manual for use of leeway direction ("maximum angle off downwind"). The apparent source of this information is Hufford and Broida (1974), and Nash and Willcox (1985), but no specific references are cited, and it appears that the wording combines ideas from multiple sources. They then investigated in detail how leeway divergence was handled in the then-current versions of National SAR Manual and three SAR planning tools: the U. S. Coast Guard's Geographic Display Operations Computer (GDOC) Automated Manual Method (AMM), the U. S. Coast Guard's Computer Aided Search Planning (CASP) model, and the Canadian Search and Rescue Prediction (CANSARP) program. They also introduced a new model (designated AP98) that uses linear regression equations and variance of both the downwind and crosswind components of leeway (DWL and CWL) to predict the drift of SAR targets. AP98 incorporates many features of leeway behavior that have recently been observed in experiments, the most significant of which is the inclusion of crosswind components of leeway to express the divergence of the leeway-object's trajectory from the downwind direction. A sensitivity study conducted as part of Allen and Plourde (1999) showed that significant reductions in search area size (which could lead to more efficient and more successful searches) could be achieved with the new AP98 DWL and CWL component model.

Allen and Plourde (1999) also devised and presented a comprehensive taxonomy for describing and categorizing the sixty-three types of leeway objects (vessels, life rafts and other drifting objects). This taxonomy will facilitate assigning Leeway Rate and Divergence Angles to "new" categories of leeway objects based on existing leeway data. This taxonomy provides an orderly framework for organizing and relating the leeway parameters derived from observations and experiments on specific types of leeway objects, and applying them to similar types of leeway objects for which data are not available. It also provides a structure for incorporating new types of leeway objects (e.g. vessels, survival craft, and objects of maritime interest) that may be introduced into maritime service as opposed to simply adding them to an ever-growing, unstructured list. The highest level, Level I, provides the major categories of leeway objects (e.g., Persons in Water, Vessels, Life Rafts, Debris, etc.). These major categories are then divided into sub-categories in Level II and Level III based on the specific configurations of the leeway objects. The taxonomy as used in this report is depicted in Figure 1-4 below.

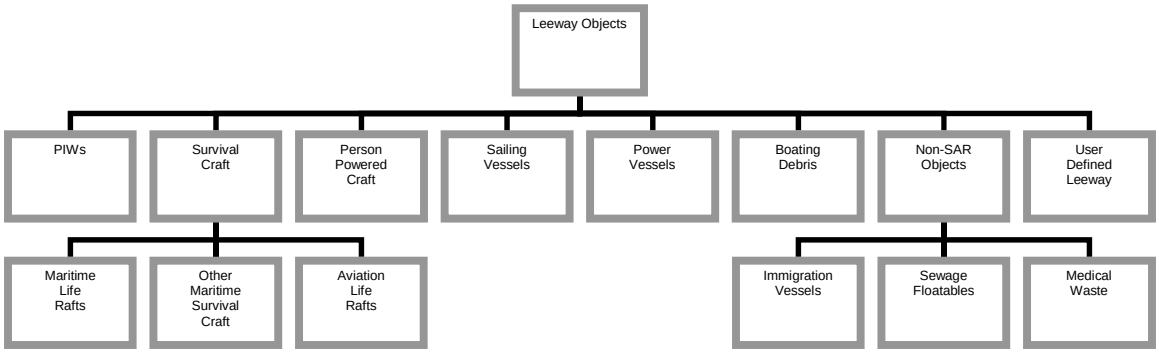

Figure 1-4. Leeway object taxonomy devised by Allen and Plourde (1999).

Finally, Allen and Plourde presented coefficients for determining leeway speed as a function of 10-meter wind speed (specifically the Slope and Y-intercept for the Leeway speed vs. $\mathbf{W_{10m}}$ linear regression), the Divergence angles, and the Standard Error of the leeway speed vs. wind speed linear regression for the sixty-three categories of leeway objects, with references identifying the origins of the values provided. These coefficients are organized in Table 8-1 of the Allen and Plourde (1999) according to the new taxonomy, and can be used by SAR planners in determining leeway using the currently available search planning tools. Table 8-1 of the Allen and Plourde report represents a significant step forward in organizing the current knowledge of leeway drift, and forms the basis of the work described in this report. A portion of the table covering Persons in the Water (PIW) and Survival Craft is reproduced below as Table 1-2.

Table 1-2. Excerpt from the Comprehensive Table of Leeway Coefficients, Allen and Plourde (1999) (Table 8-1).

Table 8-1
Recommended Leeway Speed and Direction Values for Search Planning Tools

Leeway		Target	Class	Leeway Speed (cm/s)		Diver-gence	$S_{y/x}$	Reference
Level 1	Level 2	Level 3	Level 4	Slope (%) $\mathbf{W_{10m}}$	Y-intercept (cm/s)	Angle (deg)	cm/s	Notes
PIW				1.1	3.5	40	> 15	[1]
	Vertical			0.5	3.8	24	> 10	[2]
	Sitting			1.2	0.2	24	1.38	[3]
	Horizontal	Survival Suit	face up	1.4	5.3	40	1.85	[4]
		Scuba Suit	face up	0.7	4.3	40	5.92	[5]
		Deceased	face down	1.5	4.0	40	> 10	[6]
Survival Craft	Maritime Life Rafts	No Ballast Systems and Canopy		4.2	1.6	38	> 15	[7]
			no canopy, no drogue	5.7	10.9	32	10.4	[8]
			no canopy, w/ drogue	4.4	- 10.3	38	4.1	[9]
			canopy, no drogue	3.7	5.7	32	2.1	[10]
			canopy, w/ drogue	3.0	0.0	38	>15	[11]
		Shallow Ballast Systems and Canopy		2.9	- 0.2	30	> 15	[12]
			no drogue	3.2	- 1.0	30	0.9	[13]
			with drogue	2.5	0.7	30	4.2	[14]
			Capsized	1.7	- 5.2	11	2.1	[15]
		Deep Ballast Systems & Canopies	(See Table 8-1A for Levels 4-6)	3.0	0.8	18	7.9	[16]
	Other Maritime Survival Craft	life capsule		3.8	- 4.1	30	1.4	[29]
		USCG Sea Rescue Kit		2.5	- 2.1	10	4.0	[30]
	Aviation Life Rafts	no ballast, w/canopy	4-6 person, w/o drogue	3.7	5.7	32	2.1	[31]
		Evac/ Slide	46-person	2.8	- 0.6	20	4.0	[32]

The five methods used by Allen and Plourde in determining divergence angle for the sixty-three categories of leeway objects are summarized in Table 1-3.

As briefly described in Section 1.1, a number of different approaches were utilized by various investigators to calculate or assign divergence angle values for all of the categories of leeway objects included in the new taxonomy. Actual leeway angle values were available to derive leeway divergence angles for 35 of the categories. For the leeway object categories with available leeway-angle values, three methods were used to estimate the relationship between leeway-angle statistics and divergence angle:

1) Twice the standard deviation of the leeway angle was used for data sets with mean leeway angle close to zero and with little or no bifurcation of the data set about the abscissa of leeway angle as function wind speed (± two standard deviations include approximately 95% of the distribution of observed leeway angles for a data set with normal-like distribution). This method was used for 18 leeway object categories (indicated by **2SD** in Table 1-3).
2) Mean of the leeway angle plus twice the standard deviation was used for sets with a non-zero mean, but limited to one side of the abscissa due to data constraints. This method was used for 9 leeway object categories (indicated by **Mean+2SD** in Table 1-3).
3) Mean of the leeway angle plus one standard deviation for sets with data collected on both tacks, showing bifurcation at higher wind speeds. (These later two types of leeway-angle data sets require an inclusion of a mean angle or mean of the absolute angle (if the bifurcation is symmetrical) plus either one or two standard deviations. The appropriate method depends on the nature of the leeway angle data set available. Which relationship is applied is based on the discretion of the researcher.) This method was used for 8 of the leeway object categories (indicated by **Mean+1SD** in Table 1-3).

When there were sufficient data, the data set was sorted by wind speed, and leeway angle statistics were determined for only those values above a wind speed threshold, typically 5 m/s (~10 Kt). This was done to reduce the effect of the wide scatter in leeway angle as wind speed approaches zero.

Non-statistical methods were used to estimate divergence angle when leeway-angle data were not available in the original reports. For three leeway object categories, leeway divergence angles were visually estimated (indicated by **Int** in Table 1-3) from figures showing leeway angle versus wind speed (Allen and Plourde (1999) on Nash and Wilcox (1991).

For 25 categories of leeway objects, divergence angles were assigned (extrapolated) by using the divergence angle values from other leeway categories that were similar in configuration (size, draft, and shape) to the category of object for which no values are presently available (indicated by **Ext** in Table 1-3). Where more than one neighboring category contained a divergence angle, the category with the greater divergence angle was used. A complete summary of the divergence angles obtained and methods used is provided in Table 1-3.

Table 1-3. Divergence angles for sixty-three categories of leeway objects and methods used in their determination by Allen and Plourde (1999).

#	Leeway Object Category	Div. Ang.	Method Used
1	PIW	40	Ext
2	PIW, Vertical	24	Ext
3	PIW, Sitting	24	2SD
4	PIW, Horizontal, Survival Suit	40	Mean + 1SD
5	PIW, Horizontal, Scuba Suit	40	Ext
6	PIW, Horizontal, Deceased	40	Ext
7	Life Raft, No Ballast	38	Ext
8	Life Raft, No Ballast, no canopy, no drogue	32	Mean + 1SD
9	Life Raft, No Ballast, no canopy, w/ drogue	38	Mean + 1SD
10	Life Raft, No Ballast, canopy, no drogue	32	Ext
11	Life Raft, No Ballast, canopy, w/ drogue	38	Ext
12	Life Raft, Shallow Ballast, canopy	30	Ext
13	Life Raft, Shallow Ballast, canopy, no drogue	30	Mean + 2SD
14	Life Raft, Shallow Ballast, canopy, with drogue	30	Mean + 1SD
15	Life Raft, Shallow Ballast, canopy, capsized	11	Ext
16	Life Raft, Deep Ballast, canopy	18	2SD
17	Life Raft, Deep Ballast & Canopy, 4-6 pers	20	2SD
18	Life Raft, D. Ballast & Canopy, 4-6 pers., no drogue	20	2SD
19	Life Raft, D. Ballast & Canopy, 4-6 pers., no drogue, light load	20	2SD
20	Life Raft, D. Ballast & Canopy, 4-6 pers, no drogue, heavy load	20	2SD
21	Life Raft, Ballast & Canopy, 4-6 pers., drogue	16	2SD
22	Life Raft, Ballast & Canopy, 4-6 pers., drogue, light load	32	2SD
23	Life Raft, Ballast & Canopy, 4-6 pers., drogue, heavy load	27	2SD
24	Life Raft, Ballast & Canopy, 15-25 pers	14	2SD
25	Life Raft, Ballast &Canopy, 15-25 pers. no drogue, light load	12	2SD
26	Life Raft, Ballast and Canopy, 15-25 pers. drogue, heavy load	12	2SD
27	Life Raft, Capsized	16	Ext
28	Life Raft, Swamped	11	Ext
29	Survival Craft, Life Capsule	30	2SD
30	Survival Craft, USCG Sea Rescue Kit	10	2SD
31	Survival Craft, Aviation Life Raft, 4-6 pers, canopy, no drogue	32	Ext
32	Survival Craft, Aviation Life Raft, Evac Slide, 4-6 pers	20	2SD
33	Sea Kayak w/person on aft deck	20	2SD
34	Surfboard w/ person	20	Ext
35	Windsurfer w/ person and mast and sail in water	16	2SD
36	Sailing Vessel, Monohull, full keel, deep draft	65	Ext
37	Sailing Vessel, Monohull, fin keel, shoal draft	65	Ext
38	Power Vessel, Skiff, flat bottom Boston Whaler	30	Int
39	Power Vessel, V-hull, Std configuration	20	2SD
40	Power Vessel, V-hull, Swamped	20	Ext
41	Sports Boat, Cuddy Cabin, modified V-hull	25	Int
42	Sport Fisher, Center Console, Open Cockpit	30	Int
43	Commercial Fishing Vessels	65	Ext
44	Commercial Fishing Vessels, Sampans	65	Ext
45	Commercial Fishing Vessels, Side-stern troller	65	Ext
46	Commercial Fishing Vessels, Longliners	65	Ext
47	Commercial Fishing Vessels, Junk	65	Mean + 1SD
48	Commercial Fishing Vessels, Gill Netter	45	Mean + 1SD

Table 1-3 (continued). Divergence angles for sixty-three categories of leeway objects and methods used in their determination by Allen and Plourde (1999).

#	Leeway Object Category	Div. Ang.	Method Used
49	Coastal Freighter	65	Ext
50	Boating Debris, F/V Debris	14	Ext
51	Boating Debris, Bait/Wharf Box	42	Mean + 1SD
52	Boating Debris, Bait/Wharf Box, lightly loaded	20	Mean + 1SD
53	Boating Debris, Bait/Wharf Box, fully loaded	44	Mean + 1SD
54	Non SAR objects, Immigration Vessel, Cuban refugee, sail	23	Mean + 2SD
55	Non SAR objects, Immigration Vessel, Cuban refugee, no sail	45	Mean + 2SD
56	Non SAR Object, Sewage Floatable	7	Mean + 2SD
57	Non SAR Object, Medical Waste,	14	Ext
58	Non SAR Object, Medical Waste, Vials	14	Ext
59	Non SAR Object, Medical Waste, Vials, Large	13	Mean + 2SD
60	Non SAR Object, Medical Waste, Vials, Small	14	Mean + 2SD
61	Non SAR Object, Medical Waste, Syringes,	7	Ext
62	Non SAR Object, Medical Waste, Syringes, Large	7	Mean + 2SD
63	Non SAR Object, Medical Waste, Syringes, Small	7	Mean + 2SD

In summary, Allen and Plourde (1999) and previous studies provide a variety of information and data on leeway angle. For some leeway objects, the mean leeway angle was clearly not zero. While this may be partially explained by limited data sets that were biased by logistical considerations, some objects clearly were observed to drift off the downwind direction in a consistent manner. Without a clear definition of divergence angle, or a single acceptable method of using leeway angle statistics to determine divergence angle, Allen and Plourde (1999) and previous studies used three different methods to provide an estimate of divergence angle from the leeway-angle statistics.

1.3. Objectives Of The Present Study

To properly model leeway divergence, the following factors should be addressed: (1) the positive and negative magnitudes of crosswind leeway components as functions of wind speed adjusted to the 10-meter height; (2) the confidence bounds of the two functions that relate crosswind leeway to wind speed; (3) the factors that influence the percentage of objects, for each leeway category, to drift either to the right of or the left of the downwind direction, and (4) the frequency that a drifting object changes crosswind direction, shifting from positive to negative crosswind leeway, or vice-versa.

Coefficients for the downwind and crosswind components of leeway drift as a function of wind speed have been developed through linear regression techniques using data reported in the literature for twenty-three categories of leeway drift objects (Allen (1996); Allen and Fitzgerald (1997); Kang (1999); Allen and Plourde (1999); and Allen, Robe and Morton (1999)). Two additional leeway categories, two configurations of 20-person maritime life rafts, are analyzed in this report (Appendix A) to provide coefficients of downwind and crosswind components of leeway for 10-meter-height wind speed. The crosswind component of leeway has been observed to be either persistently positive (right of the downwind direction) or persistently negative (left of the downwind direction) for the duration of each individual drift run.

In this report, we lay the groundwork to model the leeway drift of all 63 categories of leeway objects reported in Allen and Plourde (1999) using the DWL and CWL component approach. The relationship between DWL and CWL components and leeway speed/divergence angle is established in Chapter 2. We use the 23 categories of leeway objects (plus the two additional categories analyzed in Appendix A) that contained values for both the downwind and crosswind components of leeway and leeway speed and divergence angle. We assume that the relationship between DWL and CWL components and leeway speed/divergence angle established for the 25 leeway categories holds true for additional 38 leeway categories, provided by Allen and Plourde (1999) that contain values for leeway speed and divergence angle only. Thus, assuming this consistency, a procedure is established for estimating the downwind and crosswind components of leeway for these additional 38 leeway categories. Future numerical search planning tools will use downwind and crosswind components of leeway rather than leeway speed and divergence angle. Therefore, the entire set of downwind and crosswind components of leeway for all 63 categories are provided in tabular form (Tables 3-1 and 3-2) in Chapter 3.

Chapter 4 addresses the factors influencing the change in sign of the crosswind leeway component. Though the physics of drifting object, crosswind direction change was not investigated, statistical review showed that changes in crosswind motion do occur. Further statistical analysis was conducted to determine any correlation between various factors and the change in crosswind leeway motion. A sensitivity study of search area distributions with different change frequencies in crosswind direction was conducted to identify a specific sign change frequency that can be used in SAR planning models.

Chapter 5 is the report summary, with recommendations for incorporating this new leeway modeling approach in SAR planning tools, and further refining leeway determination methodology.

CHAPTER 2.

METHOD FOR ESTIMATING DOWNWIND AND CROSSWIND COMPONENTS OF LEEWAY FROM LEEWAY SPEED AND DIVERGENCE ANGLE

2.1. Approach Used In Determining Downwind And Crosswind Components Of Leeway

Allen and Plourde (1999) present a complete set of values for calculating leeway drift for sixty-three categories of leeway objects. Allen and Plourde's Table 8-1 includes leeway speed (expressed as a percentage of the wind speed adjusted to a height of 10 meters ($\mathbf{W_{10m}}$)), divergence angle and standard error of the estimate ($S_{y/x}$). Present manual and numerical search planning tools use the leeway speed and divergence angle for determining the leeway drift of leeway objects. However, there are inherent limitations when using leeway speed and divergence angle for prediction of an object's leeway behavior. Specifically, the use of leeway speed and leeway angle does not account for the fact that different physical mechanisms govern the downwind component of leeway drift (DWL) and the crosswind component of leeway drift (CWL). Although both DWL and CWL would be difficult to model analytically because of the complex physics involved, a statistical model can account for this difference. In addition, the prediction of leeway drift using leeway speed and divergence angle as a function of wind becomes unreliable at low wind speeds (less than 5 m/s). Expressing leeway behavior in terms of downwind and crosswind components of leeway as functions of $\mathbf{W_{10m}}$ overcomes these limitations.

New tools that use numerical methods to estimate search distribution areas will use downwind and crosswind component (DWL and CWL) of leeway as functions of $\mathbf{W_{10m}}$, rather than leeway speed as a function of $\mathbf{W_{10m}}$ and divergence angle. Developing linear regression leeway values for DWL and CWL is a straightforward process. Allen and Plourde (1999) developed these values for 23 leeway object categories. Two additional categories were analyzed here, with those DWL and CWL linear regression values presented in Appendix A. This leaves 38 categories in the Allen and Plourde leeway taxonomy without DWL and CWL linear regression values because there are no actual leeway drift data available for regression analysis. The purpose of this chapter is to present a scheme for estimating the DWL and CWL linear regression coefficients for these 38 categories.

Two variations of linear-regression analysis can be used to derive the coefficients for the downwind and crosswind components of leeway versus $\mathbf{W_{10m}}$. Normally, linear regressions are unconstrained, and have a slope term (here, leeway speed coefficient) and a y-intercept term. A variant is where the regression is constrained to pass through the origin.

The advantage of an unconstrained linear regression is a better statistical representation of a data set than represented by a constrained linear regression (that is, a better fit of the regression line to the data) over a greater range. For the data examined here, the unconstrained regression generally has a better "fit" at low and high wind speeds. However, because an unconstrained regression yields a y-intercept term, this could mean that leeway drift occurs in the absence of any wind, going against the traditional concept of leeway. Additional rules, guidance or procedures must account for the zero-wind speed (with undefined wind direction) case. In

numerical search-planning tools using Monte-Carlo simulation, this could result in a significant processing burden to account for an extremely rare event. Though the constrained linear regression does not provide as good a "fit" at lower wind speed, it does, by its very nature, reflect zero leeway at zero wind speed. In practice, SAR Planners are developing models that use both approaches; therefore, both methods of statistical regression were determined.

The procedures of Neter, Kutner, Nachtsheim and Wasserman (1996) were used for determining the unconstrained linear regression and the constrained linear regression. Both unconstrained and constrained linear regressions of the downwind and crosswind components of leeway were determined and are presented in Chapter 3.

As described above, the coefficients for downwind and crosswind leeway versus $\mathbf{W_{10m}}$ equations for twenty-three of the sixty-three leeway categories have been determined experimentally and can be found in the literature (Allen, 1996; Allen and Fitzgerald, 1997; Allen and Plourde, 1999; Allen et al. 1999; and Kang 1999). The DWL and CWL as functions of $\mathbf{W_{10m}}$ for two additional leeway categories are analyzed from experimental data and are presented in Appendix A. The two additional categories are maritime life rafts (deep ballast, canopy, 15-25 person capacity) with either no-drogue with light loading or the same rafts with a drogue and heavy loading. In addition, there were a number of leeway categories with experimentally observed leeway drift data for which unconstrained regression analysis have been completed, but no analysis showing constrained linear regressions. The analyses of the constrained linear regression for these leeway categories are presented in Appendix B.

In order to present a complete set of coefficients for all sixty-three leeway categories, the remaining thirty-eight categories required development of the coefficients for the downwind and crosswind component leeway equations. A relationship between the downwind and crosswind regression coefficients and leeway speed and divergence angle values (presented by Allen and Plourde (1999)) was derived from the DWL and CWL coefficients previously developed for the twenty-five categories for which leeway drift data were available. The relationships between the standard errors of the leeway speed equation derived from experimental leeway field data and the DWL and CWL equations were also estimated. The methodology and assumptions used to develop the 38 additional sets of regression coefficients is described in detail below.

2.2. Estimation Of Downwind And Crosswind Coefficients Based On Leeway Speed And Divergence Angle

The regression coefficients for downwind and crosswind components of leeway for the thirty-eight categories without data were estimated as follows. First, we assume that the slopes of the regression lines for the DWL and CWL regressions (that is the leeway speed coefficients for both components) are related to the slope of the overall leeway speed vs. wind speed regression. The slope of the leeway speed vs. wind speed regression (designated Slope (%)$\mathbf{W_{10m}}$ **in Table 1-2**) is the coefficient by which the wind speed is multiplied to compute leeway speed in the traditional method of calculating leeway drift. Based on the geometry presented in Figure 1-1, it is assumed that a similar relationship holds for computing DWL and CWL, and that linear regression coefficients can be determined for DWL and CWL. The component leeway speed coefficients are designated as DWL Slope and CWL Slope. It is further assumed that DWL Slope and CWL Slope are linearly related to Leeway Speed Slope by the cosine and sine of an

angle proportional to the Divergence angle, since the Divergence angle is a statistical representation of the Leeway angles observed for a certain category of leeway objects. The Divergence Angle is adjusted by a second coefficient of proportionality designated as the Adjustment Factor to provide this angle. The relationship is shown in equation form below:

$$\text{Predicted DWL slope} = \text{Leeway speed slope x cosine}\left(\frac{\text{Divergence Angle}}{\text{Adjustment Factor}}\right) \qquad 2\text{-}1$$

$$\text{Predicted CWL slope} = \text{Leeway speed slope x sine}\left(\frac{\text{Divergence Angle}}{\text{Adjustment Factor}}\right) \qquad 2\text{-}2$$

The divergence angles used to determine the Adjustment Factor and DWL and CWL slopes are those presented for the 25 leeway categories for which both leeway components and leeway speed regressions versus wind speed have been completed. These values are available in Table 8-1 in Allen and Plourde (1999). The approach used in this chapter is to determine the Adjustment Factor based on "tuning" Equations 2-1 and 2-2 to provide the best overall statistical fit for the 25 leeway categories for which data are available, and assume that the same Adjustment Factor applies to the remaining 38 leeway object categories for which data are not available.

The optimum Adjustment Factor was determined empirically as follows. The Adjustment Factor was varied from 1.0 to 2.0 and the values of Predicted DWL and CWL Slope computed using equations 2-1 and 2-2. The predicted values of DWL and CWL were then compared to the actual values of the DWL and CWL Slope obtained from the linear regressions using the actual data for the twenty-five leeway categories. A linear unconstrained regression of the predicted values of DWL and CWL against the actual values of DWL and CWL were calculated.

If equations 2-1 and 2-2 were perfect predictors of DWL and CWL, the regressions of Predicted DWL and CWL Slope against Actual DWL and CWL Slope would have linear regression slopes of 1.0, zero intercepts, r^2 of 1.0 and $S_{y/x}$ of 0.0. Note: The coefficient of determination (r^2) is the ratio of the variability in the dependent variable explained by regression line to the original variability about the mean observations. The r^2 is an estimate of the variance accounted for by the regression. The standard error of estimate ($S_{y/x}$) is an estimator for the standard deviation of the dependent variable about the regression line. Further explanations of r^2 and $S_{y/x}$ can be found in Chapter 3 of Allen (1996). The Absolute Slope Difference from 1.0 for the linear regression slopes for the Predicted vs. Actual Slope regressions versus Adjustment Factor (varied from 1.0 to 2.0) are plotted in Figure 2-1. The coefficients of the regression of the predicted DWL and CWL Slopes versus actual DWL and CWL Slopes are shown in Table 2-1.

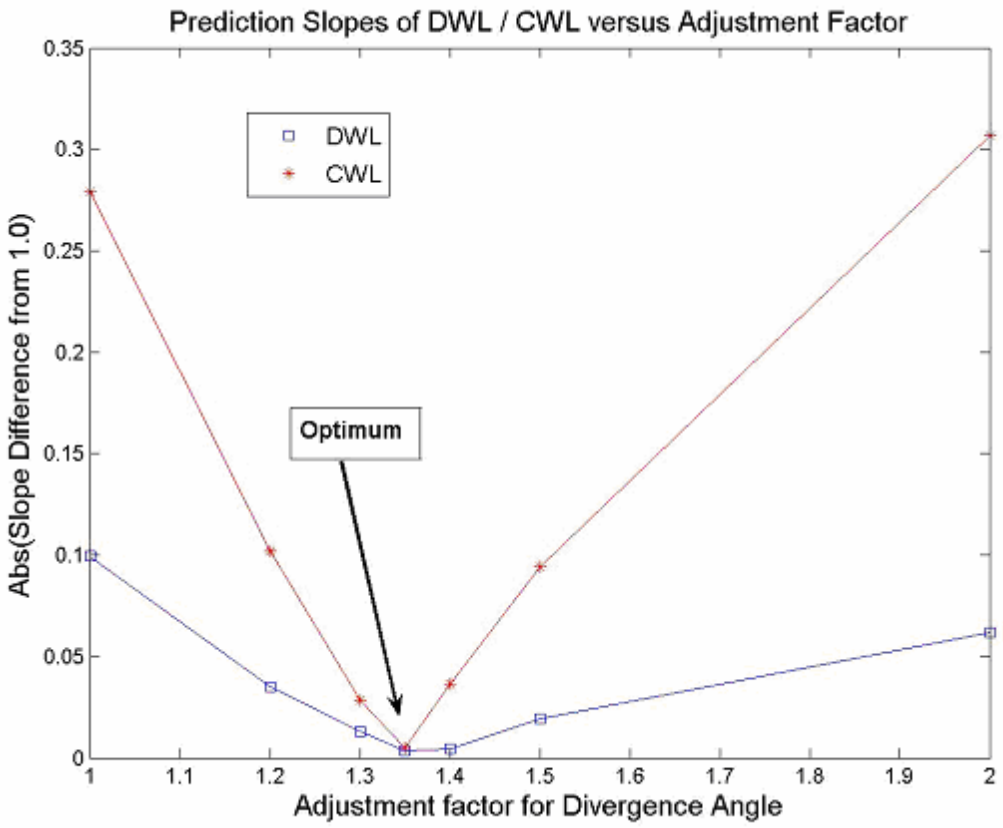

Figure 2-1. The absolute difference from one of the slope coefficients of the regression of the downwind and crosswind components of leeway against the actual coefficients of the downwind and crosswind components of leeway as a function of the adjustment factor.

Table 2-1. Coefficients of Linear Unconstrained Regression of Predicted DWL versus Actual DWL Predicted CWL versus Actual CWL for 25 Leeway Categories.

Adjustment Factor	Leeway Variable	Slope	y-intercept	r^2	$S_{y/x}$
1.0	DWL	0.9006	0.0025	0.9515	0.2909
	CWL	1.2791	0.1348	0.5102	0.8194
1.2	DWL	0.9650	-0.0701	0.9564	0.2949
	CWL	1.1021	0.0995	0.5106	0.7055
1.3	DWL	0.9871	-0.0951	0.9549	0.3070
	CWL	1.0286	0.0878	0.5107	0.6583
1.35	DWL	**0.9964**	**-0.1057**	**0.9538**	**0.3136**
	CWL	**0.9951**	**0.0829**	**0.5107**	**0.6368**
1.4	DWL	1.0047	-0.1152	0.9527	0.3202
	CWL	0.9636	0.0785	0.5108	0.6166
1.5	DWL	1.0191	-0.1315	0.9504	0.3330
	CWL	0.9057	0.0710	0.5108	0.5795
2.0	DWL	1.0619	-0.1805	0.9412	0.3799
	CWL	0.6934	0.0482	0.5109	0.4436

As indicated in Figure 2-1 and Table 2-1, the optimum prediction of DWL and CWL occurs (the Absolute Slope Difference from 1.0 is minimized) when the Adjustment Factor is set at 1.35. The optimum Adjustment Factor turned out to be the same for both DWL and CWL. The regression fit for the DWL slope with an adjustment factor of 1.35 is excellent with an r^2 of 0.95. The regression fit for the CWL component with an adjustment factor of 1.35 is only fair with an r^2 of 0.51. The predicted versus actual slope coefficients of DWL and CWL along with the linear unconstrained regressions and their 95% prediction limits are shown in Figures 2-2 and 2-3.

Assuming that the same relationship (Equations 2-1 and 2-2) and Adjustment Factor applies to all leeway object categories, slope coefficients (leeway speed coefficients) for DWL and CWL for the remaining 38 leeway categories were computed using the following equations.

Predicted DWL Slope = Leeway speed slope x cosine (Divergence Angle/1.35) 2-3

Predicted CWL Slope = Leeway speed slope x sine (Divergence Angle/1.35) 2-4

The Y-intercepts for both DWL and CWL are assigned to zero, since we have no experimental data. Hence, the DWL and CWL regression equations for the 38 categories for which no data are available are inherently constrained.

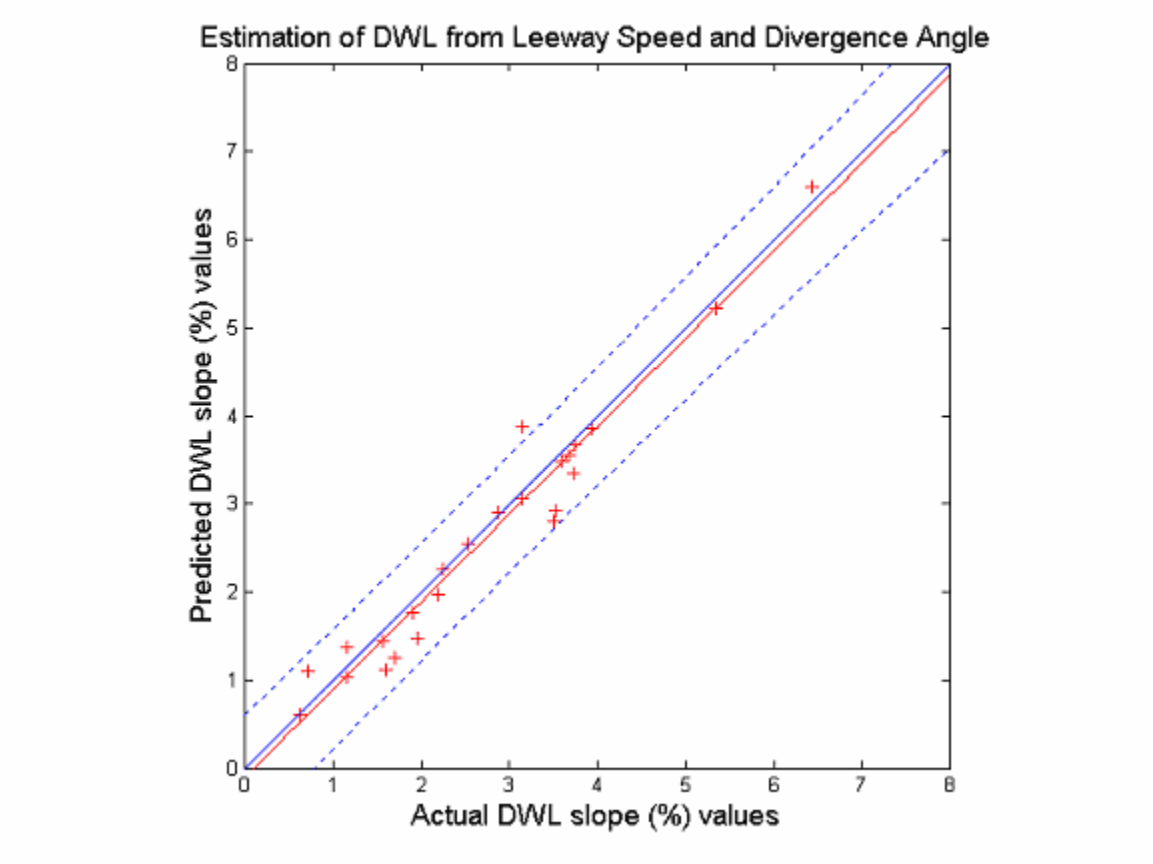

Figure 2-2. Predicted versus actual coefficients of the downwind components of leeway using an adjustment factor of 1.35.

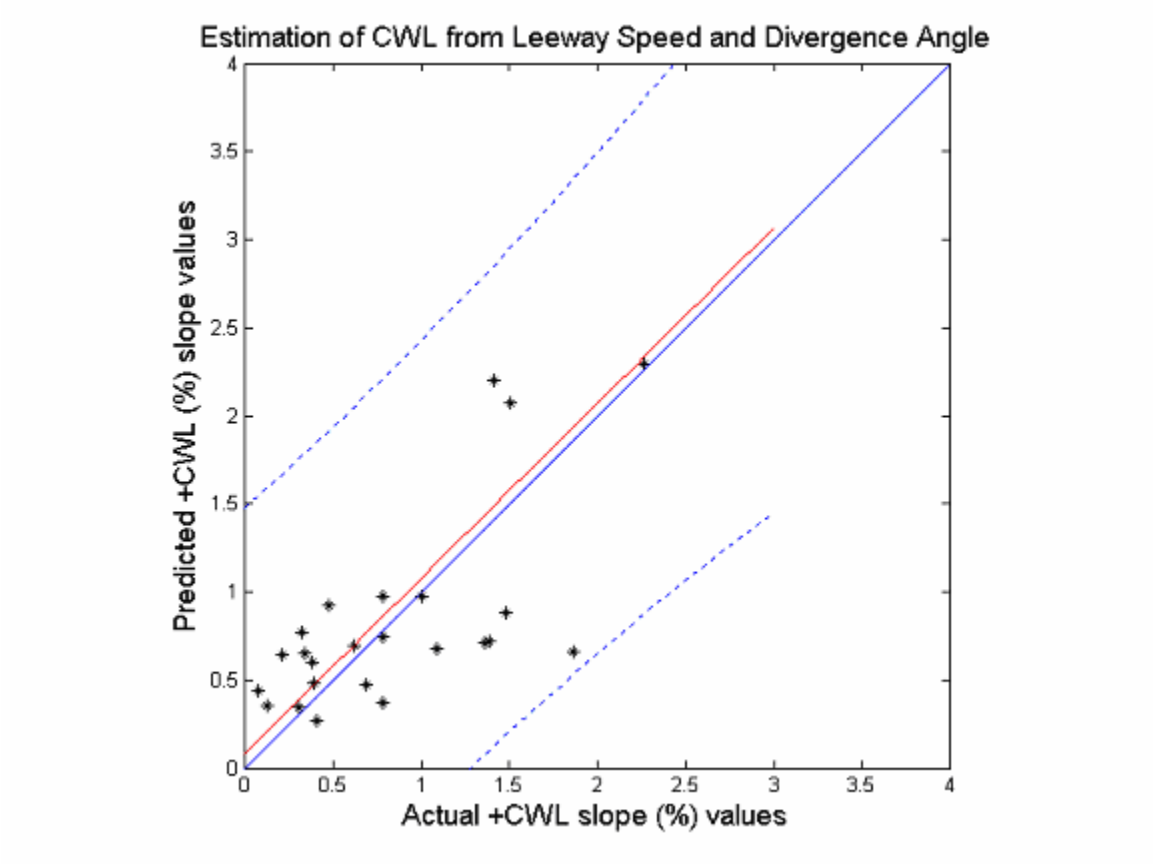

Figure 2-3. Predicted versus actual coefficients of the crosswind components of leeway using an adjustment factor of 1.35.

2.3. Estimation Of Standard Error Terms ($S_{y/x}$)

Section 2.2 describes how estimates of DWL and CWL slope were derived for the 38 leeway object categories for which data are not available. For these categories, the Y-intercept has been set at zero (in the absence of any data). However, to complete the two-component linear regression model for the 38 categories, a value for the Standard Error of Estimate ($S_{y/x}$) must be determined. This was accomplished by determining a linear regression relationship between the Standard Error values used in the traditional leeway drift modeling approach (which uses leeway speed and leeway angle) and the Standard Error values computed using the DWL and CWL component approach which have been computed for 25 leeway object categories. Unconstrained linear regressions and their respective 95% prediction limits were calculated and are presented in Figures 2-4 and 2-5. The red lines show the DWL and CWL Slope vs. traditional Leeway Speed Slope linear regressions. The green lines represent the 95% prediction limits.

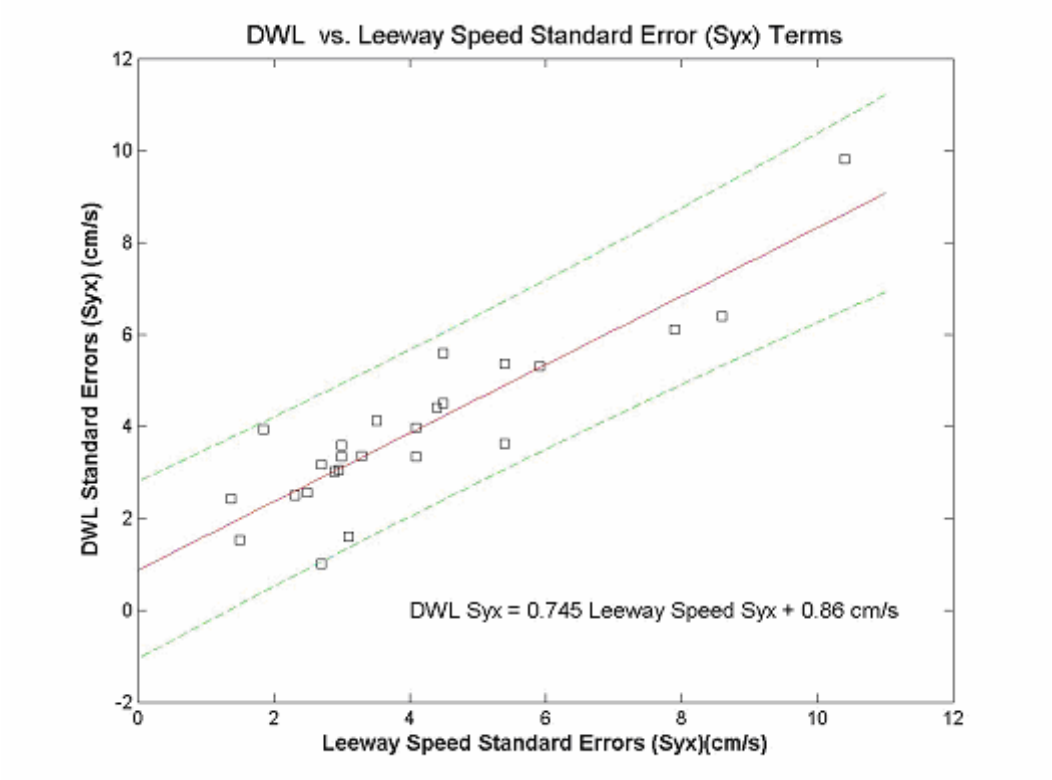

Figure 2-4. Standard error of estimate ($S_{y/x}$) for the downwind components of leeway equations versus standard error of estimate ($S_{y/x}$) of the leeway speed equations.

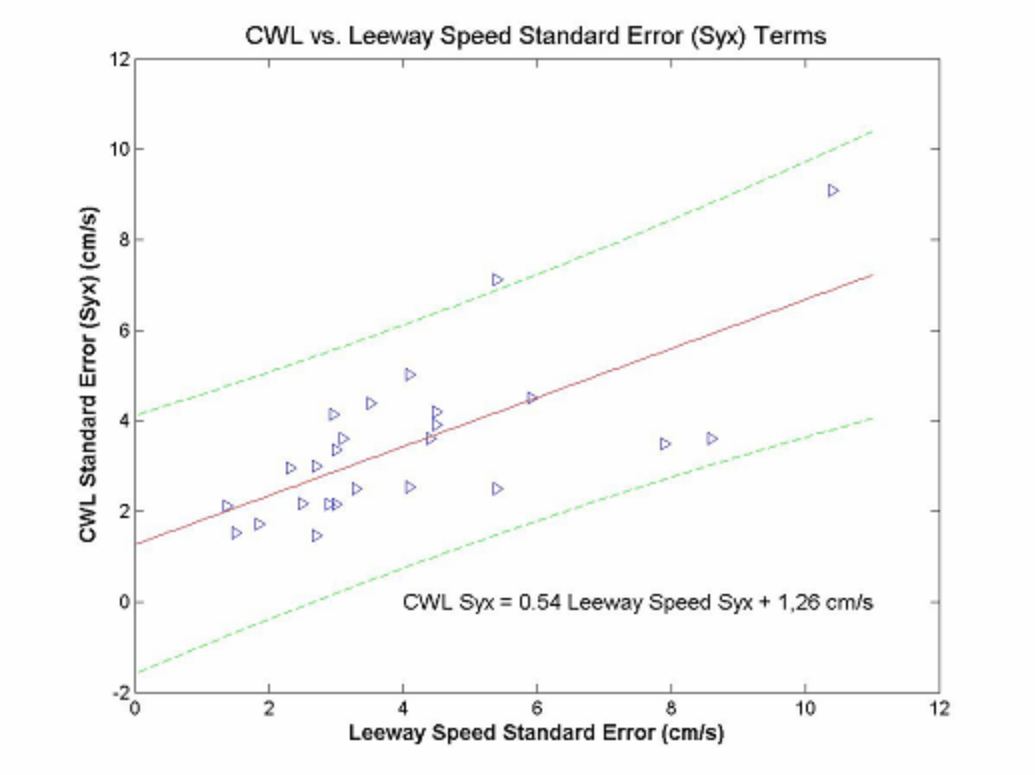

Figure 2-5. Standard error of estimate ($S_{y/x}$) for the crosswind components of leeway equations versus the standard error of the estimate ($S_{y/x}$) of the leeway speed equations.

The DWL and CWL Estimated S_{yx} linear regression equations were as follows:

Estimated S_{yx} for DWL equation = Leeway speed's S_{yx} * 0.745 + 0.86 cm/s 2-5

(r^2 = 0.79 and S_{yx} = 0.86 cm/s)

Estimated S_{yx} for CWL equation = Leeway speed's S_{yx} * 0.54 + 1.26cm/s 2-6

(r^2 = 0.48 and S_{yx} = 1.27 cm/s)

Assuming that this same statistical relationship holds for the 38 leeway object categories for which no data are available, the S_{yx} regression equations (2-5 and 2-6) can also be used to estimate the $S_{y/x}$ terms for the DWL and CWL equations of the remaining thirty-eight leeway categories using the traditional method S_{yx} values provided in Table 8-1 in Allen and Plourde (1999).

It is important to note that the Predicted DWL and CWL slope values, and Predicted S_{yx} values should be considered as first-order estimates at best, and ideally should have been computed using actual data. However, these estimates can be used to provide a complete, workable set of DWL and CWL regression coefficients, which will be employed to provide a complete set of DWL and CWL prediction equations in the next chapter of this report.

(This page intentionally left blank.)

CHAPTER 3.

COMPILING A COMPREHENSIVE SET OF DOWNWIND AND CROSSWIND LEEWAY COEFFICIENTS

The methodology outlined in Chapter 2, was used to produce estimates of the predicted leeway speed slope and predicted $S_{y/x}$ values for determining downwind and crosswind components for thirty-eight leeway categories for which actual leeway data are not available. The Y-intercept value in the DWL and CWL linear regression equations has been set at zero. In addition, the actual DWL and CWL linear regression values have been computed by applying linear regression analysis to actual data as reported in Allen and Plourde (1999) (for 23 leeway object categories) and in Appendix A of this report (for 2 additional leeway categories). Together, these linear regression coefficients constitute a complete set for implementing a DWL and CWL linear regression model for predicting leeway drift for all 63 leeway object categories in the Allen and Plourde (1999) taxonomy.

This complete set of "optimally estimated" linear regression coefficients is provided in Tables 3-1 and 3-2 for the unconstrained and constrained linear regression models, respectively. Both sets are provided as both approaches are being used by SAR Planners in modeling leeway drift. The difference between the two sets in Table 3-1 and 3-2 are described as follows:

1) Table 3-1 Unconstrained Values - The unconstrained linear regression approach provides a statistically "pure" set of leeway linear regression coefficients, providing the best statistical fit with actual data. However, it produces non-zero leeway drift at zero wind speed, which contradicts the traditional assumption of zero leeway at zero wind speed. This also introduces the need for additional computational rules or procedures for zero-wind case predictions.
2) Table 3-2 – Constrained Values – The constrained linear regression approach requires that the regression line pass through the origin, which reflects the traditional assumption of zero leeway at zero wind speed. This approach is more computationally efficient (i.e., does not require additional computational rules for the zero-wind case), but does not fit the actual data as well, and can produce less accurate predictions at wind speeds that approach the higher and lower limits of wind speeds recorded in the actual data sets.

Both Tables 3-1 and 3-2 are similar in organization to Table 8-1 of Allen and Plourde (1999) which presented a complete set of leeway drift coefficients (Slope, Divergence angle, and $S_{y/x}$) for computing leeway drift for all 63 leeway categories using traditions (non-component) leeway models. Values in Table 3-2 that differ from the corresponding value in Table 3-1 are shown in **bold**.

Tables 3-1 and 3-2 are organized as follows:

The first four columns in Tables 3-1 and 3-2 delineate the leeway object for which the coefficients are used and reflect the leeway taxonomy introduced by Allen and Plourde (1999). The bold horizontal lines separate Level 1 categories.

The fifth column of Table 3-1 and 3-2 gives slope coefficients (in units of cm/s per m/s, which corresponds to a %) of the downwind component of leeway versus 10-m wind speed ($\mathbf{W_{10m}}$) linear regression equation

Downwind Leeway (cm/s) = [Slope (%) x $\mathbf{W_{10m}}$(m/s)] + y-intercept (cm/s) 3-1

The sixth column is the y-intercept term (cm/s) of equation 3-1. The seventh column is the standard error of estimate ($S_{y/x}$, in units of cm/s) for equation 3-1, that was directly determined for those 25 categories for which experimental data were available, or estimated using equation 2-5 for the 38 categories for which data are unavailable. Note that in Table 3-1, the y-intercept is always set to zero.

The eighth and ninth columns are the coefficients (slope and y-intercept, respectively) of the positive crosswind component of leeway versus 10-m wind speed ($\mathbf{W_{10m}}$) linear regression equation.

Positive crosswind Leeway (cm/s) = [Slope (%) x $\mathbf{W_{10m}}$(m/s)] + y-intercept (cm/s) 3-2

Again note that in Table 3-2 the y-intercept is set to zero.

The tenth column is the standard error of estimate ($S_{y/x}$, in units of cm/s) for equation 3-2 that was directly determined for those 25 categories for which experimental data were available, or estimated using equation 2-6 for the 38 categories for which data are unavailable.

The eleventh and twelfth columns of Table 3-1 and 3-2 are the coefficients (slope and y-intercept, respectively) of the negative crosswind component of leeway versus 10-m wind speed ($\mathbf{W_{10m}}$) unconstrained linear regression equation.

Negative crosswind Leeway (cm/s) = [Slope (%) x $\mathbf{W_{10m}}$(m/s)] + y-intercept (cm/s) 3-3

Again note that in Table 3-2 the y-intercept is set to zero.

The thirteenth column is the standard error of estimate ($S_{y/x}$, in units of cm/s) for equation 3-3that was directly determined for those 25 categories for which experimental data were available, or estimated using equation 2-6 for the 38 categories for which data are unavailable.

In Table 3-1, the fourteenth column is the wind speed (m/s) at the intersection of the two crosswind regression equations. The fifteenth column contains the rule for applying the crosswind components for winds speeds below the intersection wind speed. If column fifteen is negative-one (-1) then the negative crosswind equation alone is used when the wind speed is below the intersection wind speed. If column fifteen is positive-one (+1) then the positive crosswind equation alone is used when the wind speed is below the intersection wind speed. If column fifteen is zero (0), then both crosswind equations are used equally for all wind speeds. Because Table 3-2 represents the constrained regression, these two columns are omitted.

The last column includes reference notes for that leeway category. Reference notes follow each table.

Table 3-1. Unconstrained linear regression values for downwind and crosswind components of leeway values.

Leeway Target Category				DWL			+CWL			-CWL			J	R	Note
Level 1	**Level 2**	**Level 3**	**Level 4**	**Slope**	**Y**	**$S_{y/x}$**	**Slope**	**Y**	**$S_{y/x}$**	**Slope**	**Y**	**$S_{y/x}$**			
PIW				0.96	0.0	12.0	0.54	0.0	9.4	- 0.54	0.0	9.4	0	0	[1]
	Vertical			0.48	0.0	8.3	0.15	0.0	6.7	- 0.15	0.0	6.7	0	0	[2]
	Sitting			1.60	-3.98	2.42	0.13	0.33	2.11	- 0.13	-0.33	2.11	0	0	[3]
	Horizontal	Survival Suit		1.71	1.12	3.93	1.36	-3.30	1.71	- 0.13	-2.65	1.62	0	0	[4]
		Scuba Suit		0.63	0.0	5.3	0.31	0.0	4.5	- 0.31	0.0	4.5	0	0	[5]
		Deceased		1.30	0.0	8.3	0.74	0.0	6.7	- 0.74	0.0	6.7	0	0	[6]
Survival Craft	Maritime Life Rafts			3.70	0.0	12.0	1.98	0.0	9.4	- 1.98	0.0	9.4	0	0	[7]
		No Ballast Systems	no canopy, no drogue	5.34	9.91	9.82	2.26	1.04	9.08	-2.26	-1.04	9.08	0	0	[8]
			no canopy, w/ drogue	3.15	-4.47	4.0	1.51	0.0	5.0	- 1.51	0.0	5.0	0	0	[9]
			Canopy, no drogue	3.39	0.0	2.4	1.49	0.0	2.4	- 1.49	0.0	2.4	0	0	[10]
			Canopy, w/ drogue	2.65	0.0	12.0	1.42	0.0	9.4	- 1.42	0.0	9.4	0	0	[11]
		Shallow Ballast Systems & Canopy		2.68	0.0	12.0	1.10	0.0	9.4	- 1.10	0.0	9.4	0	0	[12]
			no drogue	2.96	0.0	1.5	1.21	0.0	1.7	- 1.21	0.0	1.7	0	0	[13]
			with drogue	2.31	0.0	4.0	0.95	0.0	3.5	- 0.95	0.0	3.5	0	0	[14]
			Capsized	1.68	0.0	2.4	0.24	0.0	2.4	- 0.24	0.0	2.4	0	0	[15]
		Deep Ballast Systems & Canopies (See Table 2-1A for Levels 3-6)		3.52	-2.5	6.1	0.62	-3.0	3.5	-0.45	-0.2	3.6	2.62	-1	[16]
	Other Maritime	Life Capsule		3.52	0.0	1.9	1.44	0.0	2.0	-1.44	0.0	2.0	0	0	[29]
		Life Capsule		3.52	0.0	1.9	1.44	0.0	2.0	-1.44	0.0	2.0	0	0	[29]
		USCG Sea Rescue Kit		2.48	0.0	3.8	0.32	0.0	3.4	-0.32	0.0	3.4	0	0	[30]
	Aviation Life Rafts	No Ballast w/canopy 4-6 person w/o drogue		3.39	0.0	2.4	1.49	0.0	2.4	-1.49	0.0	2.4	0	0	[31]
		Evac/Slide 46-person		2.71	0.0	3.8	0.72	0.0	3.4	-0.72	0.0	3.4	0	0	[32]

Slope = Slope of $\mathbf{W_{10m}}$ (%); Y = Y-intercept (cm/s); $S_{y/x}$ = Std. Error of Estimate (cm/s); J = Junction $\mathbf{W_{10m}}$ (m/s) for **+/- CWL** equations;
R = Rule (–1, 0, +1) for applying CWL equation below Junction $\mathbf{W_{10m}}$; Note = Number of reference note following table.

Table 3-1. (continued). Unconstrained linear regression values for downwind and crosswind components of leeway values.

Sub-Table 3-1A. Sub-table for maritime life rafts with deep ballast systems and canopies.

Leeway Target Category				DWL			+CWL			-CWL			J	R	Note
Level 3	**Level 4**	**Level 5**	**Level 6**	**Slope**	**Y**	**$S_{y/x}$**	**Slope**	**Y**	**$S_{y/x}$**	**Slope**	**Y**	**$S_{y/x}$**			
Maritime Life Rafts with Deep Ballast Systems and Canopies	4-6 person capacity			3.50	-1.8	6.4	0.78	-3.6	3.6	-0.47	-0.1	3.9	2.80	-1	[17]
		without drogue		3.75	-2.3	4.4	0.78	-3.6	3.6	-0.47	-0.1	3.9	2.80	-1	[18]
			light loading	3.75	-2.32	4.51	1.00	-5.31	3.91	-0.47	-0.14	3.91	3.52	-1	[19]
			heavy loading	3.59	-1.92	2.56	0.48	-0.16	2.17	-0.48	0.16	2.17	0	0	[20]
		With drogue		1.91	0.9	1.6	0.78	-3.6	3.6	-0.47	-0.1	3.9	2.80	-1	[21]
			light loading	1.95	-0.53	3.59	0.21	1.29	2.15	-0.21	-1.29	2.15	0	0	[22]
			heavy loading	2.19	-0.96	1.01	1.39	-7.9	1.46	-1.39	7.9	1.46	0	0	[23]
	15-25 person capacity			3.68	-4.96	5.37	0.34	-1.85	2.50	-0.49	1.58	2.63	4.13	-1	[24]
		w/o drogue	light loading	3.93	-3.30	3.01	0.38	-3.33	2.16	-0.59	1.59	2.28	5.07	-1	[25]
		with drogue	heavy loading	3.15	-4.49	3.35	0.39	-1.80	2.50	-0.38	2.98	1.64	6.28	1	[26]
	Capsized			0.88	0.0	2.5	0.18	0.0	2.4	- 0.18	0.0	2.4	0	0	[27]
	Swamped			0.99	0.0	2.4	0.14	0.0	2.3	- 0.14	0.0	2.3	0	0	[28]

Slope = Slope of $\mathbf{W_{10m}}$ (%); Y = Y-intercept (cm/s); $S_{y/x}$ = Std. Error of Estimate (cm/s); J = Junction $\mathbf{W_{10m}}$ (m/s) for **+/- CWL** equations;
R = Rule (–1, 0, +1) for applying CWL equation below Junction $\mathbf{W_{10m}}$; Note = Number of reference note following table.

Table 3-1. (continued). Unconstrained linear regression values for downwind and crosswind components of leeway values.

Leeway Target Category				DWL			+CWL			-CWL			J	R	Note
Level 1	**Level 2**	**Level 3**	**Level 4**	**Slope**	**Y**	**$S_{y/x}$**	**Slope**	**Y**	**$S_{y/x}$**	**Slope**	**Y**	**$S_{y/x}$**			
Person-Powered Craft	Sea Kayak W/ Person on aft deck			1.16	11.12	4.12	0.41	0.00	4.39	-0.41	0.00	4.39	0	0	[33]
	Surf board w/ person			1.93	0.0	8.3	0.51	0.0	6.7	-0.51	0.0	6.7	0	0	[34]
	Windsurfer Mast & sail in water			2.25	5.03	2.50	0.69	-1.30	2.96	-0.69	1.30	2.96	0	0	[35]
Sailing Vessels	Mono-hull	Full Keel	Deep Draft	2.00	0.0	8.3	2.23	0.0	6.7	-2.23	0.0	6.7	0	0	[36]
		Fin Keel	Shoal Draft	2.67	0.0	8.3	2.98	0.0	6.7	-2.98	0.0	6.7	0	0	[37]
Power Vessels	Skiffs	Flat Bottom	Boston whaler	3.15	0.0	2.2	1.29	0.0	2.2	-1.29	0.0	2.2	0	0	[38]
		V-hull	Std. Conf.	2.87	3.98	3.33	0.32	-2.93	2.53	-0.62	1.03	3.05	4.2	-1	[39]
			Swamped	1.65	0.0	3.1	0.39	0.0	2.9	-0.39	0.0	2.9	0	0	[40]
	Sport Boats	Cuddy Cabin	Modified V-hull	6.54	0.0	3.0	2.19	0.0	2.8	-2.19	0.0	2.8	0	0	[41]
	Sport Fisher	Center Console	Open cockpit	5.55	0.0	3.3	2.27	0.0	3.0	-2.27	0.0	3.0	0	0	[42]
	Commercial Fishing Vessels			2.47	0.0	12.0	2.76	0.0	9.4	-2.76	0.0	9.4	0	0	[43]
		Hawaiian Sampans		2.67	0.0	8.3	2.98	0.0	6.7	-2.98	0.0	6.7	0	0	[44]
		Japanese Side-stern Troller		2.80	0.0	8.3	3.13	0.0	6.7	-3.13	0.0	6.7	0	0	[45]
		Japanese Longliners		2.47	0.0	8.3	2.76	0.0	6.7	-2.76	0.0	6.7	0	0	[46]
		Korean F/V		1.80	0.0	3.79	2.01	0.0	3.3	-2.01	0.0	3.3	0	0	[47]
		Gill-netter w/rear reel		3.72	-0.87	3.33	1.41	2.00	3.36	-1.41	-2.00	3.36	0	0	[48]
	Coastal Freighter			1.87	0.0	8.3	2.09	0.0	6.7	-2.09	0.0	6.7	0	0	[49]
Boating Debris	F/V debris			1.97	0.0	8.3	0.36	0.0	6.7	-0.36	0.0	6.7	0	0	[50]
	Bait/wharf box			0.72	15.18	5.59	1.86	-5.26	4.20	-1.86	5.26	4.20	0	0	[51]
	Holds a cubic meter of ice	Lightly loaded		2.53	9.01	3.05	1.09	-2.76	4.14	-1.09	2.76	4.14	0	0	[52]
		Full loaded		1.15	7.94	3.17	1.48	-0.32	2.99	-1.48	0.32	2.99	0	0	[53]

Slope = Slope of $\mathbf{W_{10m}}$ (%); Y = Y-intercept (cm/s); $S_{y/x}$ = Std. Error of Estimate (cm/s); J = Junction $\mathbf{W_{10m}}$ (m/s) for +/- CWL equations; R = Rule (–1, 0, +1) for applying CWL equation below Junction $\mathbf{W_{10m}}$; Note = Number of reference note following table.

Table 3-1 (continued). Unconstrained linear regression values for downwind and crosswind components of leeway values.

Leeway Target Category				DWL			+CWL			-CWL			J	R	Note
Level 1	Level 2	Level 3	Level 4	Slope	Y	$S_{y/x}$	Slope	Y	$S_{y/x}$	Slope	Y	$S_{y/x}$			
Non-SAR Objects	Immigration Vessel		w/o sail	1.56	8.30	1.53	0.078	2.70	1.52	-0.078	-2.70	1.52	0	0	[54]
	Cuban refugee raft		w/ sail	6.43	-3.47	3.63	2.22	0.00	7.12	-2.22	0.00	7.12	0	0	[55]
	Sewage Floatables Tampon Applicator			1.79	0.0	3.1	0.16	0.0	2.9	-0.16	0.0	2.9	0	0	[56]
	Medical Waste			2.75	0.0	12.0	0.50	0.0	9.4	-0.50	0.0	9.4	0	0	[57]
		Vials		3.64	0.0	12.0	0.67	0.0	9.4	-0.67	0.0	9.4	0	0	[58]
			Large	4.34	0.0	3.1	0.74	0.0	2.9	-0.74	0.0	2.9	0	0	[59]
			Small	2.95	0.0	5.4	0.54	0.0	4.5	-0.54	0.0	4.5	0	0	[60]
		Syringes		1.79	0.0	12.0	0.16	0.0	9.4	-0.16	0.0	9.4	0	0	[61]
			Large	1.79	0.0	3.1	0.16	0.0	2.9	-0.16	0.0	2.9	0	0	[62]
			Small	1.79	0.0	2.4	0.16	0.0	2.3	-0.16	0.0	2.3	0	0	[63]
User Defined Leeway				[64]	[65]	[66]	[67]	[68]	[69]	[70]	[71]	[72]	[73]	[74]	

Slope = Slope of $\mathbf{W_{10m}}$(%); Y = Y-intercept (cm/s); $S_{y/x}$ = Std. Error of Estimate (cm/s); J = Junction $\mathbf{W_{10m}}$ (m/s) for +/- CWL equations; R = Rule (–1, 0, +1) for applying CWL equation below Junction $\mathbf{W_{10m}}$; Note = Number of reference note following table.

[1] Slope, y-intercept, and Syx for DWL and CWL estimated from leeway speed and divergence angle values, Allen and Plourde's (1999) Table 8-1, by the procedure outlined in section 2.2.

[2] Slope, y-intercept, and Syx for DWL and CWL estimated from leeway speed and divergence angle values from Allen and Plourde's (1999) Table 8-1, by the procedure outlined in sections 2.2 and 2.3.

[3] Slope, y-intercept, and Syx for DWL and +CWL are from Allen et al. (1999). The values for –CWL are assumed by Allen et al. (1999) to be equivalent to the values for +CWL.

[4] same as [3]

[5] Slope, y-intercept, and Syx for DWL and +CWL from Kang (1999). The values for –CWL are assumed by Kang (1999) to be equivalent to the values for +CWL.

[6] Slope, y-intercept, and Syx for DWL and CWL estimated from leeway speed and divergence angle values from Allen and Plourde's (1999) Table 8-1, by the procedure outlined in sections 22.2 and 2.3.

[7] same as [6]

[8] Slope, y-intercept, and Syx for DWL and +CWL from Allen and Plourde's (1999) re-analysis of Hufford and Broida's (1974) leeway data. The values for –CWL were assumed by Allen and Plourde (1999) to be equivalent to the values for +CWL.

[9] same as [8]

[10] Slope, y-intercept, and Syx for DWL and CWL estimated from leeway speed and divergence angle values from Allen and Plourde's (1999) Table 8-1, by the procedure outlined in sections 2.2 and 2.3.

[11] same as [10]

[12] same as [10]

[13] same as [10]

[14] same as [10]

[15] same as [10]

[16] Slope, y-intercept, and Syx) for DWL, +CWL and -CWL are from Allen and Plourde (1999).

[17] same as [16]

[18] same as [16]

[19] same as [16]

[20] Slope, y-intercept, and Syx for DWL, and +CWL are from Allen and Plourde (1999). The values for –CWL are assumed by Allen and Plourde (1999) to be equivalent to the values for +CWL.

[21] Slope, y-intercept, and Syx for DWL, +CWL and -CWL are from Allen and Plourde (1999).

[22] Slope, y-intercept, and Syx for DWL, and +CWL are from Allen and Plourde (1999). The values for –CWL are assumed by Allen and Plourde (1999) to be equivalent to the values for +CWL.

[23] same as [22]

[24] Slope, y-intercept, and Syx) for DWL, +CWL and -CWL are from Allen and Plourde (1999).

[25] Slope, y-intercept, and Syx) for DWL, +CWL and -CWL are from this report, Appendix A.

[26] same as [25]

[27] Slope, y-intercept, and Syx) for DWL and CWL were estimated from the leeway speed and divergence angle values from Allen and Plourde's (1999) Table 8-1, by the procedure outlined in sections 2.2 and 2.3.

[28] same as [27]

[29] same as [27]

[30] same as [27]

[31] same as [27]

[32] same as [27]

[33] Slope, y-intercept, and Syx) for DWL and +CWL are from Allen et al. (1999). The values for –CWL are assumed by Allen et al. (1999) to be equivalent to the values for +CWL.

[34] Values (slope, y-intercept, and Syx) for DWL and CWL were estimated from the leeway speed and divergence angle values from Allen and Plourde's (1999) Table 8-1, by the procedure outlined in sections 2.2 and 2.3.

[35] Values (slope, y-intercept, and Syx) for DWL and -CWL are from Allen et al. (1999). The values for +CWL are assumed by Allen et al. (1999) to be equivalent to the values for -CWL.

[36] Values (slope, y-intercept, and Syx) for DWL and CWL were estimated from the leeway speed and divergence angle values from Allen and Plourde's (1999) Table 8-1, by the procedure outlined in sections 2.2 and 2.3.

[37] same as [36]

[38] same as [36]

[39] Values (slope, y-intercept, and Syx) for DWL, +CWL and -CWL are from Allen and Fitzgerald (1997).

[40] Values (slope, y-intercept, and Syx) for DWL and CWL were estimated from the leeway speed and divergence angle values from Allen and Plourde's (1999) Table 8-1, by the procedure outlined in sections 2.2 and 2.3.

[41] same as [40]

[42] same as [40]

[43] same as [40]

[44] same as [40]

[45] same as [40]

[46] same as [40]

[47] same as [40]

[48] Values (slope, y-intercept, and Syx) for DWL, and -CWL are from Allen (1996). The values for +CWL are assumed by Allen (1996) to be equivalent to the values for –CWL.

[49] Values (slope, y-intercept, and Syx) for DWL and CWL were estimated from the leeway speed and divergence angle values from Allen and Plourde's (1999) Table 8-1, by the procedure outlined in sections 2.2 and 2.3.

[50] same as [49]

[51] Values (slope, y-intercept, and Syx) for DWL and +CWL are from Allen et al. (1999). The values for –CWL are assumed by Allen et al. (1999) to be equivalent to the values for +CWL.

[52] same as [51]

[53] same as [51]

[54] Values (slope, y-intercept, and Syx) for DWL, and -CWL are from Allen (1996). The values for +CWL are assumed by Allen (1996) to be equivalent to the values for –CWL.

[55] same as [54]

[56] Values (slope, y-intercept, and Syx) for DWL and CWL were estimated from the leeway speed and divergence angle values from Allen and Plourde's (1999) Table 8-1, by the procedure outlined in sections 2.2 and 2.3. Sewage floatables include tampon applicators.

[57] Values (slope, y-intercept, and Syx) for DWL and CWL were estimated from the leeway speed and divergence angle values from Allen and Plourde's (1999) Table 8-1, by the procedure outlined in sections 2.2 and 2.3.

[58] same as [57]

[59] same as [57]

[60] same as [57]

[61] same as [57]

[62] same as [57]

[63] same as [57]

[64] User defined slope coefficient (percent) for the regression of the downwind component of leeway versus W10m. The values usually assigned range from 0.5 to 7.0%, or a default value of 3%.

[65] User defined y-intercept coefficient (cm/s) for the regression of downwind component of leeway versus W10m. This value is usually assigned a value of zero.

[66] User defined standard error of estimate term, Sy/x (cm/s) for the regression of downwind component of leeway versus W10m. The values usually assigned range from 1 to 15 cm/s, or a default value of 10 cm/s.

[67] User defined slope coefficient (percent) for the regression of the positive crosswind component of leeway versus W10m. The values usually assigned range from 0.5 to 3.0%, or a default value of 1.5%.

[68] User defined y-intercept coefficient (cm/s) for the regression of positive crosswind component of leeway versus W10m. This value is usually assigned a value of zero.

[69] User defined standard error of estimate term, Sy/x (cm/s) for the regression of positive crosswind component of leeway versus W10m. The values usually assigned range from 1 to 15 cm/s, or a default value of 10 cm/s.

[70] User defined slope coefficient (percent) for the regression of the negative crosswind component of leeway versus W10m. The values usually assigned range from 0.5 to 3.0%, or a default value of 1.5%.

[71] User defined y-intercept coefficient (cm/s) for the regression of negative crosswind component of leeway versus W10m. This value is usually assigned a value of zero.

[72] User defined standard error of estimate term, Sy/x (cm/s) for the regression of negative crosswind component of leeway versus W10m. The values usually assigned range from 1 to 15 cm/s, or a default value of 10 cm/s.

[73] User defined value for the wind speed (m/s) where the two regression equations of the crosswind components of leeway versus W10m intersect. This value is usually assigned a value of zero.

[74] User defined value for the rule (-1,0, +1) for choosing which crosswind component of leeway equation versus W10m is used below the wind junction speed given in 73. This value is usually assigned a value of zero.

Table 3-2. Constrained linear regression values for downwind and crosswind components of leeway values.

Leeway Target Category				DWL			+CWL			-CWL			Note
Level 1	**Level 2**	**Level 3**	**Level 4**	**Slope (%)**	**Y**	**$S_{y/x}$ (cm/s)**	**Slope**	**Y**	**$S_{y/x}$ (cm/s)**	**Slope**	**Y**	**$S_{y/x}$ (cm/s)**	
PIW				0.96	0.0	12.0	0.54	0.0	9.4	- 0.54	0.0	9.4	[1]
	Vertical			0.48	0.0	8.3	0.15	0.0	6.7	- 0.15	0.0	6.7	[2]
	Sitting			**1.09**	**0.0**	**2.84**	**0.17**	**0.0**	**2.11**	**-0.17**	**0.0**	**2.11**	[3]
	Horizontal	Survival Suit		**1.87**	**0.0**	**3.95**	**0.98**	**0.0**	**1.82**	**- 0.57**	**0.0**	**1.63**	[4]
		Scuba Suit		0.63	0.0	5.3	0.31	0.0	4.5	- 0.31	0.0	4.5	[5]
		Deceased		1.30	0.0	8.3	0.74	0.0	6.7	- 0.74	0.0	6.7	[6]
Survival Craft	Maritime Life Rafts			**3.56**	0.0	12.0	**1.59**	0.0	9.4	**- 1.59**	0.0	9.4	[7]
		No Ballast Systems	no canopy, no drogue	**7.10**	**0.0**	**10.39**	**2.45**	**0.0**	**8.86**	**-2.45**	**0.0**	**8.86**	[8]
			no canopy, w/ drogue	**2.53**	**0.0**	**3.93**	**1.51**	**0.0**	**5.02**	**- 1.51**	**0.0**	**5.02**	[9]
			canopy, no drogue	3.39	0.0	2.4	1.49	0.0	2.4	- 1.49	0.0	2.4	[10]
			canopy, w/ drogue	**1.21**	0.0	12.0	**0.92**	0.0	9.4	**- 0.92**	0.0	9.4	[11]
		Shallow Systems and Canopy	Ballast	2.68	0.0	12.0	1.10	0.0	9.4	- 1.10	0.0	9.4	[12]
			no drogue	2.96	0.0	1.5	1.21	0.0	1.7	- 1.21	0.0	1.7	[13]
			with drogue	2.31	0.0	4.0	0.95	0.0	3.5	- 0.95	0.0	3.5	[14]
			Capsized	1.68	0.0	2.4	0.24	0.0	2.4	- 0.24	0.0	2.4	[15]
		Deep Ballast Systems & Canopies (See Table 3-2A for Levels 4-6)		**3.28**	**0.0**	**6.20**	**0.32**	**0.0**	**3.66**	**-0.43**	**0.0**	**3.64**	[16]
	Other	Life Capsule		3.52	0.0	1.9	1.44	0.0	2.0	-1.44	0.0	2.0	[29]
	Maritime	USCG Sea Rescue Kit		2.48	0.0	3.8	0.32	0.0	3.4	-0.32	0.0	3.4	[30]
	Aviation Life Rafts	No Ballast w/canopy 4-6 person w/o drogue		3.39	0.0	2.4	1.49	0.0	2.4	-1.49	0.0	2.4	[31]
		Evac/Slide 46-person		2.71	0.0	3.8	0.72	0.0	3.4	-0.72	0.0	3.4	[32]

Slope = Slope of $\mathbf{W_{10m}}$ (%); Y = Y-intercept (cm/s); $S_{y/x}$ = Std. Error of Estimate (cm/s); Note = Number of reference note following table. **Bolded** values differ from Table 3-1.

Table 3-2 (continued). Constrained linear regression values for downwind and crosswind components of leeway values.

Sub -Table 3-2A (Sub-table for Maritime Life Rafts with Deep Ballast Systems and Canopies)

Leeway Target Category				DWL			+CWL			-CWL			Note
Level 3	**Level 4**	**Level 5**	**Level 6**	**Slope (%)**	**Y**	**$S_{y/x}$ (cm/s)**	**Slope (%)**	**Y**	**$S_{y/x}$ (cm/s)**	**Slope (%)**	**Y**	**$S_{y/x}$ (cm/s)**	
Maritime Life Rafts with Deep Ballast Systems and Canopies	4-6 person capacity			**3.32**	**0.0**	**6.43**	**0.42**	**0.0**	**3.86**	**-0.48**	**0.0**	**3.91**	[17]
		without drogue		**3.52**	**0.0**	**4.54**	**0.47**	**0.0**	**4.05**	**-0.48**	**0.0**	**3.91**	[18]
			light loading	**3.53**	**0.0**	**4.60**	**0.47**	**0.0**	**4.23**	**-0.48**	**0.0**	**3.91**	[19]
			heavy loading	**3.35**	**0.0**	**2.67**	**0.49**	**0.0**	**1.80**	**-0.49**	**0.0**	**1.80**	[20]
		with drogue		**2.00**	**0.0**	**1.67**	**0.30**	**0.0**	**2.97**	**-0.30**	**0.0**	**2.97**	[21]
			light loading	**1.91**	**0.0**	**3.59**	**0.30**	**0.0**	**2.19**	**-0.30**	**0.0**	**2.19**	[22]
			heavy loading	**2.08**	**0.0**	**1.05**	**0.34**	**0.0**	**3.00**	**-0.34**	**0.0**	**3.00**	[23]
	15-25 person capacity			**3.19**	**0.0**	**5.59**	**0.15**	**0.0**	**2.57**	**-0.34**	**0.0**	**2.67**	[24]
		w/o drogue	light loading	**3.62**	**0.0**	**3.16**	**0.07**	**0.0**	**2.33**	**-0.43**	**0.0**	**2.23**	[25]
		with drogue	heavy loading	**2.70**	**0.0**	**3.67**	**0.20**	**0.0**	**2.58**	**-0.09**	**0.0**	**1.76**	[26]
	Capsized			0.88	0.0	2.5	0.18	0.0	2.4	- 0.18	0.0	2.4	[27]
	Swamped			0.99	0.0	2.4	0.14	0.0	2.3	- 0.14	0.0	2.3	[28]

Slope = Slope of $\mathbf{W_{10m}}$ (%); Y = Y-intercept (cm/s); $S_{y/x}$ = Std. Error of Estimate (cm/s); Res. to Gybe = Resistance to jibing (1 = low, 2 = moderate, 3 = high); Note = Number of reference note following table. **Bolded** values differ from Table 3-1.

Table 3-2 (continued). Constrained linear regression values for downwind and crosswind components of leeway values.

Leeway Target Category				DWL			+CWL			-CWL			Note
Level 1	**Level 2**	**Level 3**	**Level 4**	**Slope (%)**	**Y**	**$S_{y/x}$ (cm/s)**	**Slope (%)**	**Y**	**$S_{y/x}$ (cm/s)**	**Slope (%)**	**Y**	**$S_{y/x}$ (cm/s)**	
Person-Powered Craft	Sea Kayak W/ Person on aft deck			**2.97**	**0.0**	**6.29**	**0.41**	**0.0**	**4.39**	**-0.41**	**0.00**	**4.39**	[33]
	Surf board w/ person			1.93	0.0	8.3	0.51	0.0	6.7	-0.51	0.0	6.7	[34]
	Windsurfer Mast & sail in water			**3.18**	**0.0**	**3.17**	**0.45**	**0.0**	**3.00**	**-0.45**	**0.0**	**3.00**	[35]
Sailing Vessels	Mono-hull	Full Keel	Deep Draft	2.00	0.0	8.3	2.23	0.0	6.7	-2.23	0.0	6.7	[36]
		Fin Keel	Shoal Draft	2.67	0.0	8.3	2.98	0.0	6.7	-2.98	0.0	6.7	[37]
Power Vessels	Skiffs	Flat Bottom	Boston whaler	3.15	0.0	2.2	1.29	0.0	2.2	-1.29	0.0	2.2	[38]
		V-hull	Std. Conf.	**3.27**	**0.0**	**3.71**	**0.004**	**0.0**	**2.77**	**-0.52**	**0.0**	**3.07**	[39]
			Swamped	1.65	0.0	3.1	0.39	0.0	2.9	-0.39	0.0	2.9	[40]
	Sport Boats	Cuddy Cabin	Modified V-hull	6.54	0.0	3.0	2.19	0.0	2.8	-2.19	0.0	2.8	[41]
	Sport Fisher	Center Console	Open cockpit	5.55	0.0	3.3	2.27	0.0	3.0	-2.27	0.0	3.0	[42]
	Commercial Fishing Vessels			2.47	0.0	12.0	2.76	0.0	9.4	-2.76	0.0	9.4	[43]
		Hawaiian Sampans		2.67	0.0	8.3	2.98	0.0	6.7	-2.98	0.0	6.7	[44]
		Japanese Side-stern Troller		2.80	0.0	8.3	3.13	0.0	6.7	-3.13	0.0	6.7	[45]
		Japanese Longliners		2.47	0.0	8.3	2.76	0.0	6.7	-2.76	0.0	6.7	[46]
		Korean F/V		1.80	0.0	3.79	2.01	0.0	3.3	-2.01	0.0	3.3	[47]
		Gill-netter w/rear reel		**3.55**	**0.0**	**3.35**	**1.78**	**0.0**	**3.43**	**-1.78**	**0.0**	**3.43**	[48]
	Coastal Freighter			1.87	0.0	8.3	2.09	0.0	6.7	-2.09	0.0	6.7	[49]
Boating Debris	F/V debris			1.97	0.0	8.3	0.36	0.0	6.7	-0.36	0.0	6.7	[50]
	Bait/wharf box			**2.63**	**0.0**	**7.83**	**1.20**	**0.0**	**4.60**	**-1.20**	**0.0**	**4.60**	[51]
	holds a cubic meter of ice	lightly loaded		**3.95**	**0.0**	**4.85**	**0.65**	**0.0**	**4.29**	**-0.65**	**0.0**	**4.29**	[52]
		full loaded		**2.03**	**0.0**	**3.45**	**1.44**	**0.0**	**2.99**	**-1.44**	**0.0**	**2.99**	[53]

Slope = Slope of $\mathbf{W_{10m}}$ (%); Y = Y-intercept (cm/s); $S_{y/x}$ = Std. Error of Estimate (cm/s); Note = Number of reference note following table.
Bolded values differ from Table 3-1.

Table 3-2 (continued). Constrained linear regression values for downwind and crosswind components of leeway values.

Leeway Target Category				DWL			+CWL			-CWL			Note
Level 1	**Level 2**	**Level 3**	**Level 4**	**Slope (%)**	**Y**	**$S_{y/x}$ (cm/s)**	**Slope (%)**	**Y**	**$S_{y/x}$ (cm/s)**	**Slope (%)**	**Y**	**$S_{y/x}$ (cm/s)**	
Non-SAR Objects	Immigration Vessel Cuban refugee raft		w/o sail	**3.21**	**0.0**	**2.92**	**0.62**	**0.0**	**1.71**	**-0.62**	**0.0**	**1.71**	[54]
			w/ sail	**5.80**	**0.0**	**3.66**	2.22	0.00	7.12	-2.22	0.00	7.12	[55]
	Sewage Floatables Tampon Applicator			1.79	0.0	3.1	0.16	0.0	2.9	-0.16	0.0	2.9	[56]
	Medical Waste			2.75	0.0	12.0	0.50	0.0	9.4	-0.50	0.0	9.4	[57]
		Vials		3.64	0.0	12.0	0.67	0.0	9.4	-0.67	0.0	9.4	[58]
			Large	4.34	0.0	3.1	0.74	0.0	2.9	-0.74	0.0	2.9	[59]
			Small	2.95	0.0	5.4	0.54	0.0	4.5	-0.54	0.0	4.5	[60]
		Syringes		1.79	0.0	12.0	0.16	0.0	9.4	-0.16	0.0	9.4	[61]
			Large	1.79	0.0	3.1	0.16	0.0	2.9	-0.16	0.0	2.9	[62]
			Small	1.79	0.0	2.4	0.16	0.0	2.3	-0.16	0.0	2.3	[63]
User Defined Leeway				[64]	[65]	[66]	[67]	[68]	[69]	[70]	[71]	[72]	

Slope = Slope of $\mathbf{W_{10m}}$ (%); Y = Y-intercept (cm/s); $S_{y/x}$ = Std. Error of Estimate (cm/s); Note = Number of reference note following table.
Bolded values differ from Table 3-1.

[1] Slope and Syx for DWL and CWL estimated from leeway speed and divergence angle values from Allen and Plourde's (1999) Table 8-1, by the procedure outlined in section 2.2 and 2.3 of this report.

[2] same as [1]

[3] Slope and Syx for DWL and +CWL are from Allen et al. (1999). The values for –CWL are assumed by Allen et al. (1999) to be equivalent to the values for +CWL.

[4] same as [3].

[5] Slope and Syx for DWL and +CWL from Kang (1999). The values for –CWL are assumed by Kang (1999) to be equivalent to the values for +CWL.

[6] Slope and Syx for DWL and CWL estimated from leeway speed and divergence angle values from Allen and Plourde's (1999) Table 8-1, by the procedure outlined in section 3.2 and 3.3 of this report.

[7] Slope, and Syx) for DWL and CWL estimated by combining values from the four leeway categories that constitute this category. Methods and values are reported in Appendix B of this report.

[8] Slope and Syx for DWL and +CWL are analysis of Hufford and Broida's (1974) leeway data and are reported in Appendix A of this report. The values for –CWL were assumed to be equivalent to the values for +CWL.

[9] same as [8]

[10] Slope and Syx for DWL and CWL estimated from leeway speed and divergence angle values from Allen and Plourde's (1999) Table 8-1, by the procedure outlined in sections 3.2 and 3.3 of this report.

[11] Slope, and Syx for DWL and CWL estimated by combining values from the four leeway categories that constitute this category. Methods and values are reported in Appendix B of this report.

[12] Slope and Syx for DWL and CWL estimated from leeway speed and divergence angle values from Allen and Plourde's (1999) Table 8-1, by the procedure outlined in section 3.2 and 3.3 of this report.

[13] same as [12]

[14] same as [12]

[15] same as [12]

[16] Methods and values (slope and Syx) for DWL, +CWL and -CWL are reported in Appendix B of this report.

[17] same as [16]

[18] same as [16]

[19] same as [16]

[20] same as [16]

[21] same as [16]

[22] same as [16]

[23] same as [16]

[24] same as [16]

[25] same as [16]

[26] same as [16]

[27] Slope and Syx for DWL and CWL estimated from leeway speed and divergence angle values from Allen and Plourde's (1999) Table 8-1, by the procedure outlined in sections 3.2 and 3.3 of this report.

[28] same as [27]

[29] same as [27]

[30] same as [27]

[31] same as [27]

[32] same as [27]

[33] Slope and Syx for DWL and +CWL from Allen et al. (1999). The values for –CWL are assumed by Allen et al. (1999) to be equivalent to the values for +CWL.

[34] Slope and Syx for DWL and CWL estimated from leeway speed and divergence angle values from Allen and Plourde's (1999) Table 8-1, by the procedure outlined in sections 3.2 and 3.3 of this report..

[35] Slope and Syx for DWL and -CWL are from Allen et al. (1999). The values for +CWL are assumed by Allen et al. (1999) to be equivalent to the values for -CWL.

[36] Slope and Syx for DWL and CWL estimated from leeway speed and divergence angle values from Allen and Plourde's (1999) Table 8-1, by the procedure outlined in sections 3.2 and 3.3 of this report.

[37] same as [36]

[38] same as [36]

[39] Slope and Syx for DWL, +CWL and -CWL from Allen and Fitzgerald (1997).

[40] Slope and Syx for DWL and CWL estimated from leeway speed and divergence angle values from Allen and Plourde's (1999) Table 8-1, by the procedure outlined in sections 3.2 and 3.3 of this report.

[41] same as [40]

[42] same as [40]

[43] same as [40]

[44] same as [40]

[45] same as [40]

[46] same as [40]

[47] same as [40]

[48] Slope and Syx for DWL, and -CWL from Allen (1996). The values for +CWL are assumed by Allen (1996) to be equivalent to the values for –CWL.

[49] Slope and Syx for DWL and CWL estimated from leeway speed and divergence angle values from Allen and Plourde's (1999) Table 8-1, by the procedure outlined in sections 3.2 and 3.3 of this report.

[50] same as [49]

[51] Slope and Syx for DWL and +CWL from Allen et al. (1999). The values for –CWL are assumed by Allen et al. (1999) to be equivalent to the values for +CWL.

[52] same as [51]

[53] same as [51]

[54] Slope and Syx for DWL, and -CWL from Allen (1996). The values for +CWL are assumed by Allen (1996) to be equivalent to the values for –CWL.

[55] same as [54]

[56] Slope and Syx) for DWL and CWL estimated from leeway speed and divergence angle values from Allen and Plourde's (1999) Table 8-1, by the procedure outlined in sections 3.2 and 3.3 of this report.

[57] same as [56]

[58] same as [56]

[59] same as [56]

[60] same as [56]

[61] same as [56]

[62] same as [56]

[63] same as [56]

[64] User defined slope coefficient (percent) for the regression of the downwind component of leeway versus W10m. The values usually assigned range from 0.5 to 7.0%, or a default value of 3%.

[65] User defined y-intercept coefficient (cm/s) for the regression of downwind component of leeway versus W10m. This value is usually assigned a value of zero.

[66] User defined standard error of estimate term, Sy/x (cm/s) for the regression of downwind component of leeway versus W10m. The values usually assigned range from 1 to 15 cm/s, or a default value of 10 cm/s.

[67] User defined slope coefficient (percent) for the regression of the positive crosswind component of leeway versus W10m. The values usually assigned range from 0.5 to 3.0%, or a default value of 1.5%.

[68] User defined y-intercept coefficient (cm/s) for the regression of positive crosswind component of leeway versus W10m. This value is usually assigned a value of zero.

[69] User defined standard error of estimate term, Sy/x (cm/s) for the regression of positive crosswind component of leeway versus W10m. The values usually assigned range from 1 to 15 cm/s, or a default value of 10 cm/s.

[70] User defined slope coefficient (percent) for the regression of the negative crosswind component of leeway versus W10m. The values usually assigned range from 0.5 to 3.0%, or a default value of 1.5%.

[71] User defined y-intercept coefficient (cm/s) for the regression of negative crosswind component of leeway versus W10m. This value is usually assigned a value of zero.

[72] User defined standard error of estimate term, Sy/x (cm/s) for the regression of negative crosswind component of leeway versus W10m. The values usually assigned range from 1 to 15 cm/s, or a default value of 10 cm/s.

CHAPTER 4.

DEVELOPING AN IMPROVED LEEWAY MODEL BASED ON DOWNWIND AND CROSSWIND LEEWAY COMPONENTS

4.1. Leeway Model Implementation

Tables 3-1 and 3-2 present the results of a statistical analysis to derive a workable set of Downwind and Crosswind Leeway (DWL and CWL) component linear regression coefficients based on data from field experiment data for 25 leeway object categories, and estimated empirically for an additional 38 categories. Just as there are various statistical methods for developing these regression equations, there are various modeling techniques that can incorporate results of regression analysis in SAR planning tools. In this section, two versions of a model that utilizes DWL and CWL to compute leeway are proposed and then checked against the original leeway data sets. Both models utilize the coefficients given in Tables 3-1 or 3-2.

Both models share three basic assumptions in their development and implementation. The first assumption is that a specific leeway object has a unique set of leeway equations and retains those equations over the drift durations, unless there is a significant state-changing event. This assumption implies that Monte Carlo simulations would establish "N" sets of leeway equations for each drifting object type where "N" equals the number of replications for that drift object. Then the Monte Carlo simulation would use those equations to establish the leeway velocity components as function of wind speed at each time step over the entire drift period, as long as the drift object did not change configuration (e.g. swamp or capsize). The evidence for each leeway object having a unique set of leeway components is shown in Figures 7-2 and 7-3 of Allen and Plourde (1999), reproduced here as Figure 4-1 (i.e., downwind components of leeway versus $\mathbf{W_{10m}}$ for three separate 4-6 person life rafts with deep ballast system and canopies, no drogue, light loading).

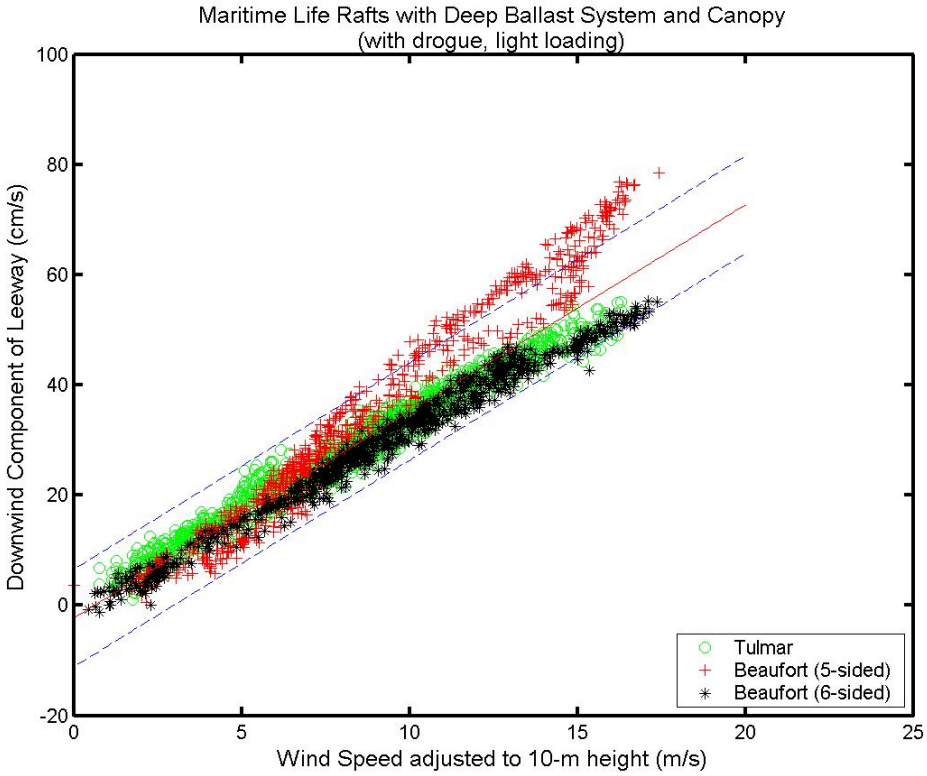

Figure 4-1. Downwind components of leeway versus $\mathbf{W_{10m}}$ for three separate 4-6 person life rafts with deep ballast system and canopies, no drogue, light loading. Also shown is the unconstrained linear regression and its 95% prediction limits.

The second assumption necessary to implement a Monte Carlo simulation using DWL and CWL components is that the distributions of leeway components are normally distributed about the mean linear regression lines of the leeway components versus the 10-meter wind speed. Figure 4-2 shows histogram slices of the downwind components of leeway for all deep-ballasted life rafts at 2 m/s intervals of wind. The downwind leeway data were then grouped by wind speed (plus and minus 0.5 m/s about each two-m/s wind interval), and compared with fitted, normal distributions. For 6-14 m/s the downwind components of leeway closely follow a normal distribution. Only at low wind speeds do the downwind components suggest a non-normal distribution.

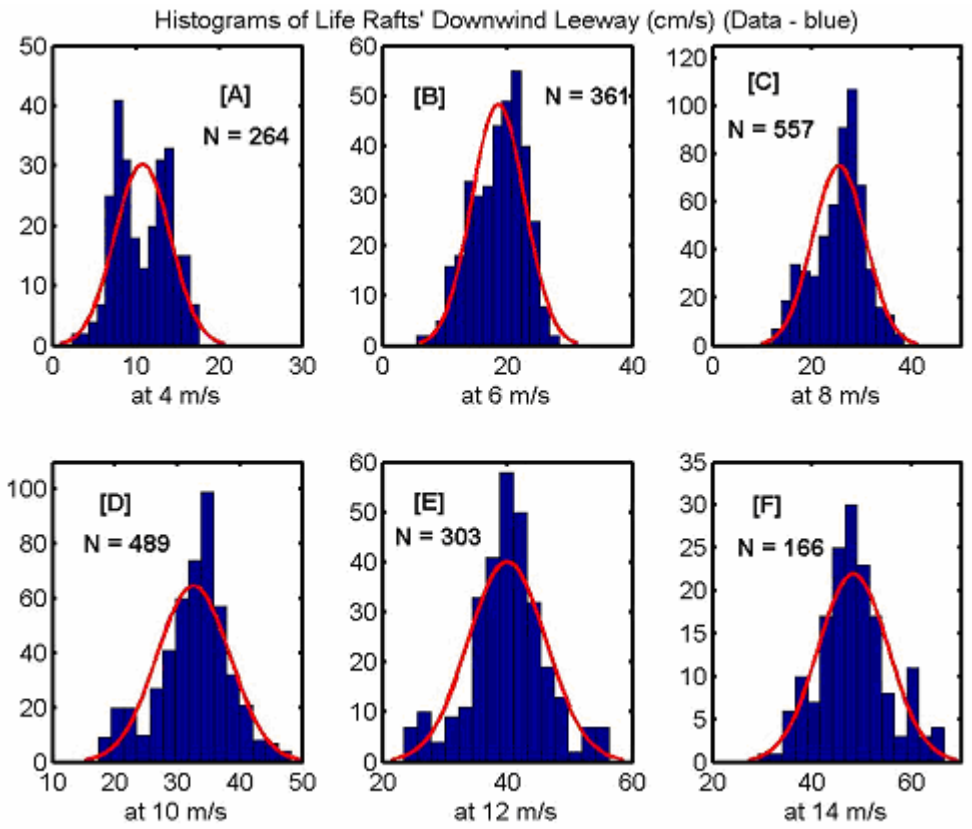

Figure 4-2. Histograms of slices of the downwind leeway components for maritime life rafts with deep ballast systems and canopies compared to normal distributions.

The third assumption is that the Standard Error terms (S_{yx}) most accurately reflect the variance in the leeway components at 10 meters per second of wind. This is based upon the observation that the variance in the leeway components increases with wind speed. The corollary of this assumption is that the Standard Error terms underestimate leeway variance at higher wind speeds and overestimate leeway variance at lower wind speeds. This assertion is illustrated in Figure 4-1 and in Figures 7-21, 7-23, and 7-27 of Allen and Plourde (1999).

It is the application of this third assumption where the two models discussed here differ. The first model uses Table 3-1 coefficients from the linear unconstrained regressions of the leeway components versus wind speed. We have called this the Y-Model (since the unconstrained model has a y-intercept). For each of the three leeway coefficients, the same procedure is followed. N random numbers are drawn from a normal distribution with a mean of zero and standard deviation equal to the S_{yx} term for that leeway component's regression (Table 3-1 columns 7, 10 and 13). To generate N equations (for each component), the random numbers are divided by 20 m/s to generate N new slope offsets and divided by 2 to generate N new Y-intercept offsets.

These two sets of offsets are then added to the regressions' slope and y-intercept terms found in columns 5, 6; 8, 9; and 11, 12 of Table 3-1 to establish N new sets of linear regression leeway equations. Generalized MATLAB® code for this procedure is shown below. In the first line, N randomly generated offsets are drawn from a normal distribution with zero mean and a standard deviation of S_{yx}. In the second line N new slopes are generated. The third line generates N new

Y-intercept terms. The fourth line shows the N equations to generate the leeway component for that wind speed.

```
Model_Y_Offsets          = normrnd(0., Syx,N,1);
Model_Y_slopes           = Regression_Slope + Model_Y_Offsets./20;
Model_Y_y_intercepts     = Regression_Y_intercept  +  Model_Y_Offsets./2;

Model_Y_leeway    = Model_Y_slopes.*Wind_Speed + Model_Y_y_intercepts
```

The second proposed model uses Table 3-2 coefficients from the linear constrained through the origin regressions of the leeway components versus wind speed. We have called this the 0-Model (since the y-intercept of the constrained linear regression is 0). For each of the three linear regression leeway coefficients, N random numbers are drawn from a normal distribution with a mean of zero and standard deviation equal to the S_{yx} term for that leeway component's regression (Table 3-2 columns 7, 10 and 13). To generate N equations (for each component), the random numbers are divided by 10 m/s to generate N new slope offsets. These sets of offsets are then added to the regressions' slope and y-intercept terms found in columns 5, 8 and 11 of Table 3-2 to establish N new sets of linear leeway equations. Generalized MATLAB® code for this procedure is shown below. In the first line, N randomly generated offsets are drawn from a normal distribution with zero mean and a standard deviation of S_{yx}. In the second line N new slopes are generated. The third line, N equations are used to generate the leeway component for that wind speed.

```
Model_0_Offsets      = normrnd(0., Syx,N,1);
Model_0_slopes       = Regression_Slope + Model_0_Offsets./10;

Model_0_leeway       = Model_0_slopes.*Wind_Speed ;
```

4.2 Comparison Of Leeway Models With Data

To check the validity of the two leeway models proposed in Section 4.1, the outputs from the two candidate models are compared with the data on which they are originally based. The largest, most complete leeway data set presently available is the downwind component of leeway for the Maritime Life Rafts with Deep Ballast System and Canopies. This data set includes three different makes of 4-6 person life rafts and one 20-person life raft. There are a total of 4877 10-minute samples in these data sets, which is just under 34 days of data.

There are number of statistical presentations available for comparing experimental data to model generated values. One method of comparison is presented here, while three additional statistical evaluations are provided in Appendix C. Each method has its strengths and weaknesses. The presentation here (Figure 4-3) is a straightforward comparison where model values are simply overlaid on an X-Y plot of empirical data (data in blue). The model values of 1000 leeway drift replications appear as a series of lines, with red representing the 0-Model predictions and green representing the Y-Model predictions. From these two plots, it is clear that both models do an adequate job of reproducing the observed leeway data in the mid-range of wind speeds. At low wind speeds, the Y–Model appears to better account for the observed data (encompassing all

data points). At higher wind speeds, the 0-Model appears to better account for the observed data. It is also clear that the 0-model converges to zero at zero wind speed, but therefore underestimates the leeway data variance at low wind speeds (as shown by the number of data points not encompassed by the red lines). It is not so clear from these two plots how well the two models compare with the data along the regression line and the effects of increasing or decreasing the number (N) of replications. For the plots shown in Figure 4-3, the eye is drawn to the extreme model values that are varied from run to run (at the 1000 N level). This is to say, the plots are dependent on the size of N. When 10,000 replications were used, both models cover a greater range.

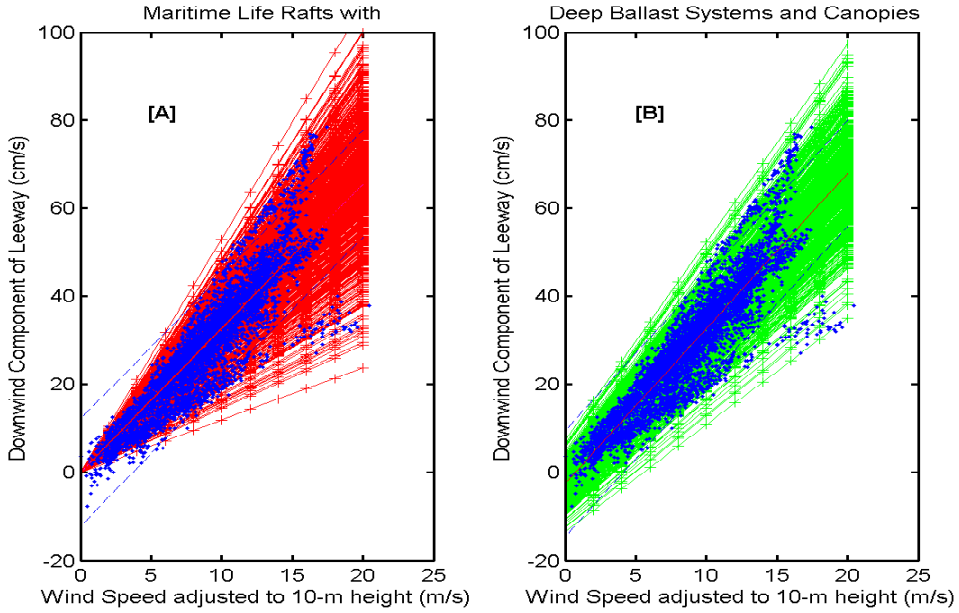

Figure 4-3. Downwind leeway data (blue) from maritime life rafts with deep ballast systems and canopies versus 10-meter wind speed compared with 1000 model generated leeway equation results: (A) 0-model values in red and (B) Y-model values in green.

As stated, additional statistical comparisons are provided in Appendix C. In summary, all comparisons used show that though the 0-Model converges to zero, it doesn't cover the data distribution at low wind speeds as well as the Y-Model. Overall, the Y-Model does a slightly better job than the 0-Model covering the data (particularly at low wind speeds).

(This page intentionally left blank.)

CHAPTER 5.

INVESTIGATING AND ACCOUNTING FOR CHANGES IN THE SIGN OF THE CROSSWIND LEEWAY COMPONENT

5.1. Introduction

Since 1992 there have been over 55 days of leeway drift observations collected on various leeway objects, (Allen and Plourde (1999); Allen, Robe and Morton (1999)). In this total data set, leeway drift objects generally behaved in a certain manner: if the object's drift was initially to the right (or left) of the downwind direction, the drift remained to the right (or left) of the downwind direction for the duration of the drift. However, on a few occasions, the object's drift trajectory changed from right of the downwind to the left downwind or vice versa. This behavior is often referred to as "jibing" or "tacking," using the term associated with sailing, whereby the vessel sails to the left of the downwind or upwind direction, and then to the right. Because of the focus of this report on DWL and CWL components, this phenomenon will be discussed in terms of sign changes of the CWL component.

The frequency of the occurrence of changes in the crosswind component from positive to negative (or vice versa) is an important element for modeling search areas. In the complete absence of changes in the crosswind component sign, search objects will maintain their initial direction of drift relative to the wind direction throughout their entire drift. With no changes in the crosswind component sign, the Monte Carlo initial probability distribution of replications of leeway drift objects will eventually separate from each other over time, about the downwind direction, with replications to the left and replications to the right, delineating two separate high-probability leeway object areas. If the drift of a leeway object changes crosswind component sign frequently, then there will be very little net divergence from the downwind direction, as each replication to the right of the downwind direction will be offset by a replication to the left. Accordingly, the leeway drift will not diverge from the downwind direction, but will be essentially directly downwind. If, however, there are less frequent or even infrequent changes in the sign of the crosswind component, there will be a measurable effect on the probability distribution, with the distribution biased to either side of the downwind direction.

This report does not attempt to describe the dynamics governing the CWL sign change as the physical factors affecting the change may be numerous and subtle, and in general, were not directly measured in leeway experiments. However, a statistical approach may provide practical guidance in dealing with this phenomenon. A statistical analysis of changes and frequency of change in the crosswind drift direction was undertaken, where data were available. This included the identification, description and statistical analysis of changes of the crosswind component observed during the leeway drift field experiments for four categories of leeway drift objects. This analysis resulted in the recommendation of a simple first-order model for estimating frequency of the change in sign of the crosswind leeway component (CWL). The usefulness of this first-order model was investigated in a sensitivity analysis of the effect of the CWL sign-change frequency on Monte Carlo search area distributions.

5.2 Methods Used To Identify And Analyze Crosswind Component Sign Changes

The four leeway categories analyzed for this study were: 5.5-meter V-hull open skiff; 4-6 person deep-ballasted canopied life rafts; 20-person deep-ballasted canopied life rafts; and 1-cubic meter wharf box. These four categories were selected because each category contained 100 or more hours of actual leeway data. These categories had data collected using the direct method of tethered InterOcean® "S4" electromagnetic current meter and an onboard wind-monitoring system (Allen and Plourde (1999)). This provided sufficient quantity and quality of leeway data to document changes in the crosswind component of leeway. It should be noted, however, a tethered S4 current meter may have reduced the occurrences of the leeway object changing direction and the resulting sign change of the crosswind component. Therefore, the analysis presented here represents conservative estimates of the frequency of crosswind component sign changes.

A 5.5 m V-hull open skiff, common to Newfoundland waters (shown in Figure 5-1 [A]), has been extensively studied by Allen and Fitzgerald (1997). A total of 172.5 hours of leeway data have been collected on this leeway drift object. Though Allen and Fitzgerald (1997) reported one confirmed swamping and two suspected swampings of open skiffs during the 1995 field experiments, we report only on the changes in the sign of the crosswind component of leeway for the standard skiff configuration used during these field experiments.

Fitzgerald, Finlayson and Allen (1994), Allen and Plourde (1999) and this report have studied 4-6 person and 20-person deep-ballasted canopied life rafts, (see Figure 5-1 [B] and [C]). There are 656.0 hours of useable leeway data on the 4-6-person life rafts and 268.3 hours of data for the 20-person life rafts. There were three separate types of 4-6 person life rafts and one type of 20-person life raft. Life rafts were primarily set up in one of two configurations: heavily loaded with a drogue attached or lightly loaded with no drogue. Here we used the two data sets for the general combined leeway classes: 4-6 person, deep-ballasted, canopied life rafts; and 20-person, deep-ballasted, canopied life rafts.

Allen, Robe and Morton (1999) collected 102.2 hours of data on a 1-cubic meter wharf box typically used to store ice and bait for commercial fishing vessels, (see Figure 5-1 [D]). These wharf/bait boxes are typically stored on the open deck of the fishing vessels and occasionally act as makeshift life rafts, since they are double-hull plastic. There were six drift runs conducted on the wharf box, three of them with 1-person loading and three with 4-person loading. The combined leeway category for the wharf/bait box was used here.

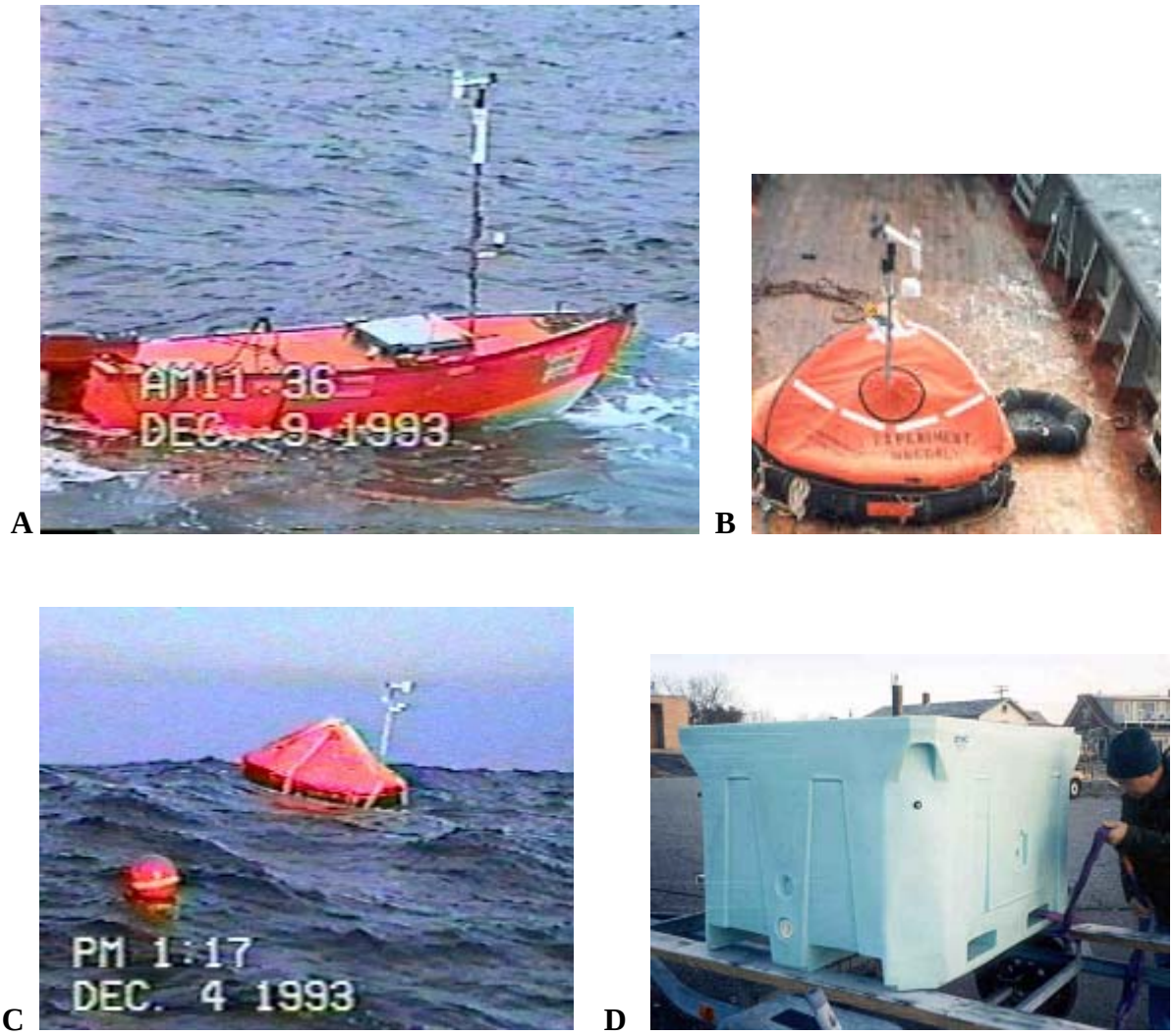

Figure 5-1. The [A] 5.5-meter V-hull, open skiff, [B] Tulmar 4-person life raft, [C] Beaufort 20-person life raft, and [D] 1-cubic meter wharf box.

In investigating the nature and frequency of CWL sign changes, and their dependence on wind speed and leeway object category, a number of graphical analysis techniques were employed. Progressive Vector Diagrams (PVDs) of the downwind and crosswind component of leeway were analyzed for the individual drift runs of the four leeway categories. PVDs are plots of displacement vectors placed tail to head. They show the cumulative displacement of a time series of displacement vectors (i.e. velocity vectors multiplied by their time intervals). PVDs of the downwind and crosswind components of leeway displacement vectors are rotated to the local wind coordinate frame at each time step, thus showing the displacement of the downwind and crosswind leeway drift, relative to the downwind direction. Therefore, in the following PVDs, straight downwind drifts would be straight up from the origin. Deviations to the right of this line indicate positive CWL and deviations to the left indicate negative CWL.

In order to emphasize the deviations from the downwind direction, all of the PVD horizontal axes (crosswind axes) were exaggerated compared to the vertical (downwind axes). A typical

PVD produced during the analysis is shown in Figure 5-2 for a 5.5 m open V-hull skiff. The complete set of PVDs for all four categories is presented in Appendix D.

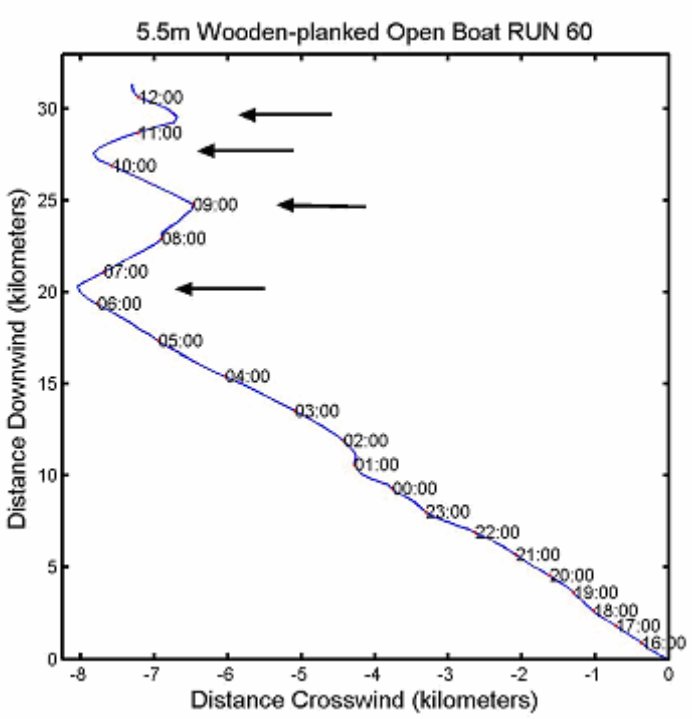

Figure 5-2. Progressive Vector Diagram of the leeway displacement vectors for Drift Run 60, 5.5 m open V-hull skiff starting at 1500 26 November, 1995. Time of day marked along the PVD.

Once the crosswind component sign changes were identified in the PVDs, the CWL time series were analyzed to locate the 10-minute interval most closely associated with the CWL sign change. Time series of the crosswind component of leeway (cm/s) and the wind speed adjusted to the 10-meter height, for the 5.5 m open V-hull skiff, Run 60, are shown in Figure 5-3. The complete set of Time Series Plots for all four categories analyzed is presented in Appendix D.

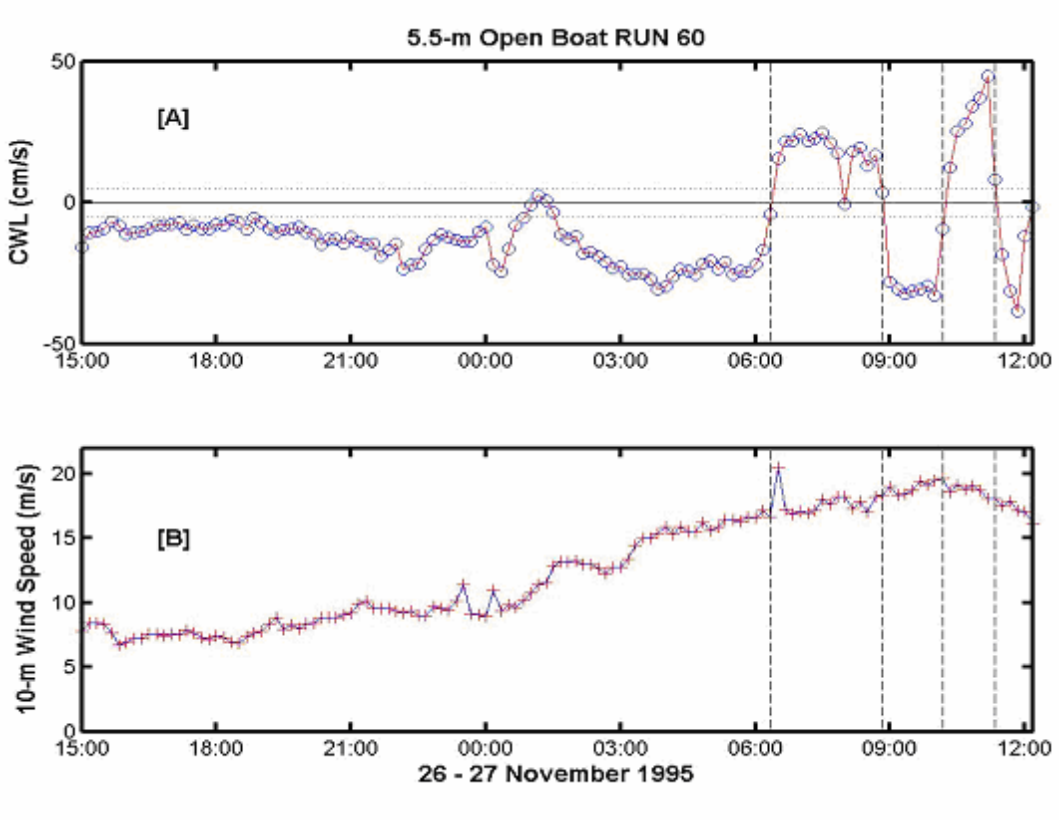

Figure 5-3. Time series of [A] the crosswind component of leeway (cm/s) and [B] the wind speed adjusted to the 10-meter height, during drift run 60, 5.5 m open boat. Vertical-dashed lines indicate CWL sign changes.

5.3 Analysis Of Crosswind Leeway Component Sign Changes

With the 10-minute sampling period identified, the 10-minute-averaged 10-meter wind speed for that period was also extracted from the time series. From these data three histograms were developed. The first histogram is the number of CWL sign changes per 2-meter per second-wide groupings of the 10-meter wind speed. The second histogram is the number of hours of the 10-meter wind speed per 2-meter per second-wide groupings that were sampled. The third histogram shows the values of the first histogram normalized by values of the second histogram, i.e., the frequency (percentage of CWL sign change per hour), per 2-meter per second wide groupings of the 10-meter wind speed. The mean (and standard deviations) of the frequencies grouped by wind speed were then determined, providing a first-order estimate of the frequency of CWL sign changes as function of the 10-meter wind speed for the four leeway categories.

5.3.1 5.5-Meter Open Skiff

Twelve significant changes in sign of the crosswind leeway component of the 5.5 m open-skiff were identified as reported in Section D.1 of Appendix D. For each of these CWL sign changes, the associated 10-meter wind speed is known. Figure 5-4 is the histogram of the number of CWL sign changes by 2 m/s wide groupings of the 10-meter wind speed. Figure 5-5 shows the

hours of leeway data available in the 295.5 hours of leeway data for the 5.5 m open-skiff versus 2 m/s groupings of the 10-meter wind speed ($\mathbf{W_{10m}}$).

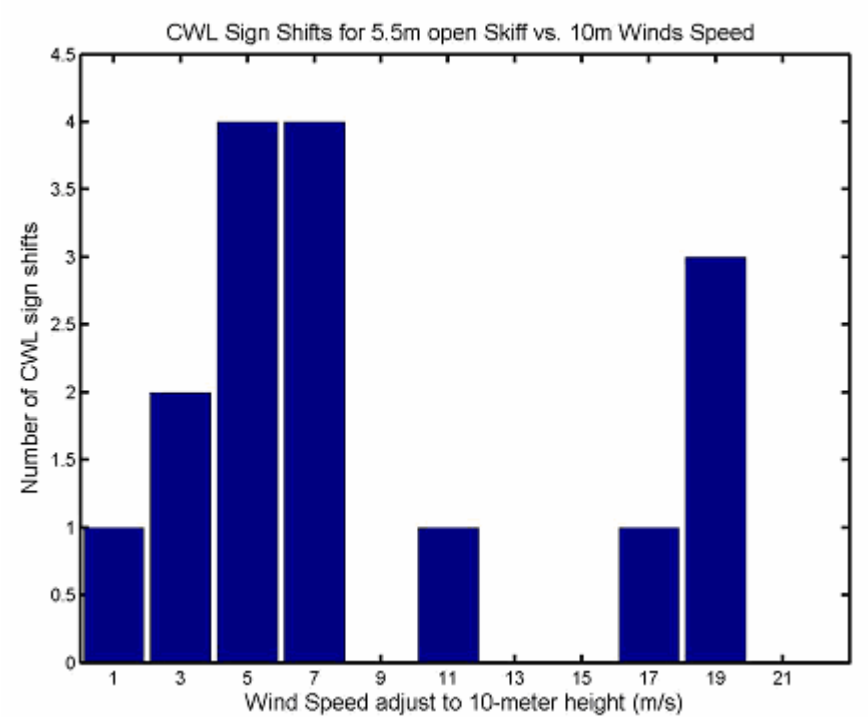

Figure 5-4. Number of significant CWL sign changes versus 2 m/s groupings of $\mathbf{W_{10m}}$ for the 5.5 m open skiff.

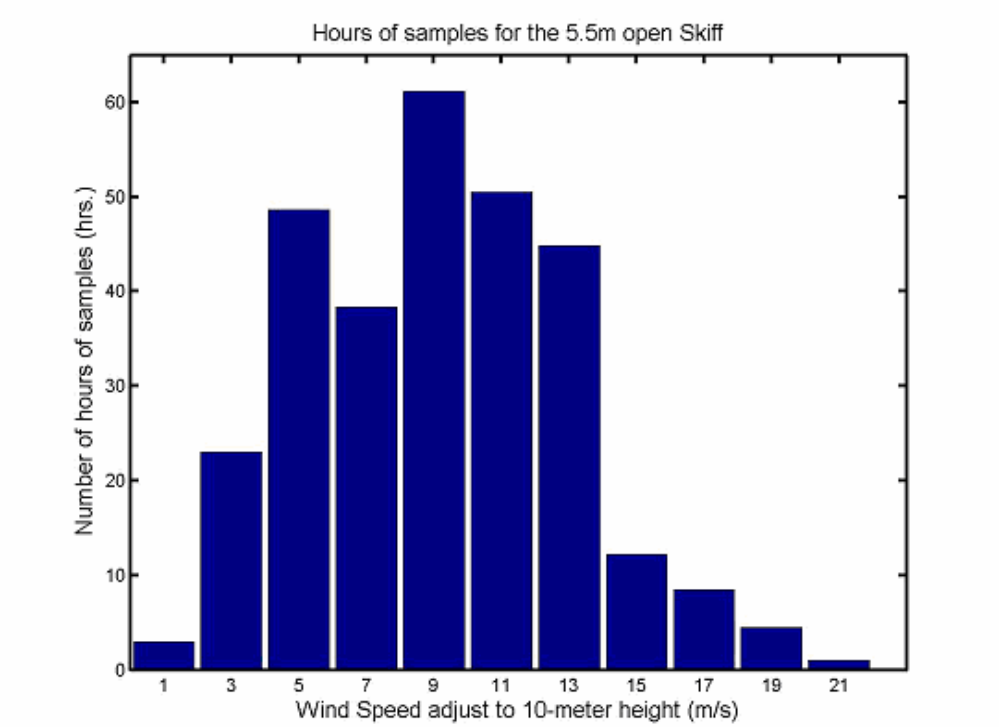

Figure 5-5. Hours of leeway data versus 2 m/s groupings of $\mathbf{W_{10m}}$ for the 5.5m open skiff.

When the values of the first histogram (Figure 5-4, number of CWL sign changes) are normalized by the values of the second histogram (Figure 5-5, hours of data at a given wind speed), the frequency of CWL sign changes per hour was determined for each of the 2 m/s wind speed groupings (Figure 5-6). The mean frequency of CWL sign shifts per hour averaged over the 11 wind speed groupings was 12.8%/hr (std. dev. 20.3%/hr). This mean-frequency line was superimposed on the histogram of the frequency of CWL sign changes in Figure 5-6. However, when a simple average of the sixteen CWL sign changes are normalized by 295.7 hours the result is a 5.4% chance of CWL sign change per hour for this leeway category.

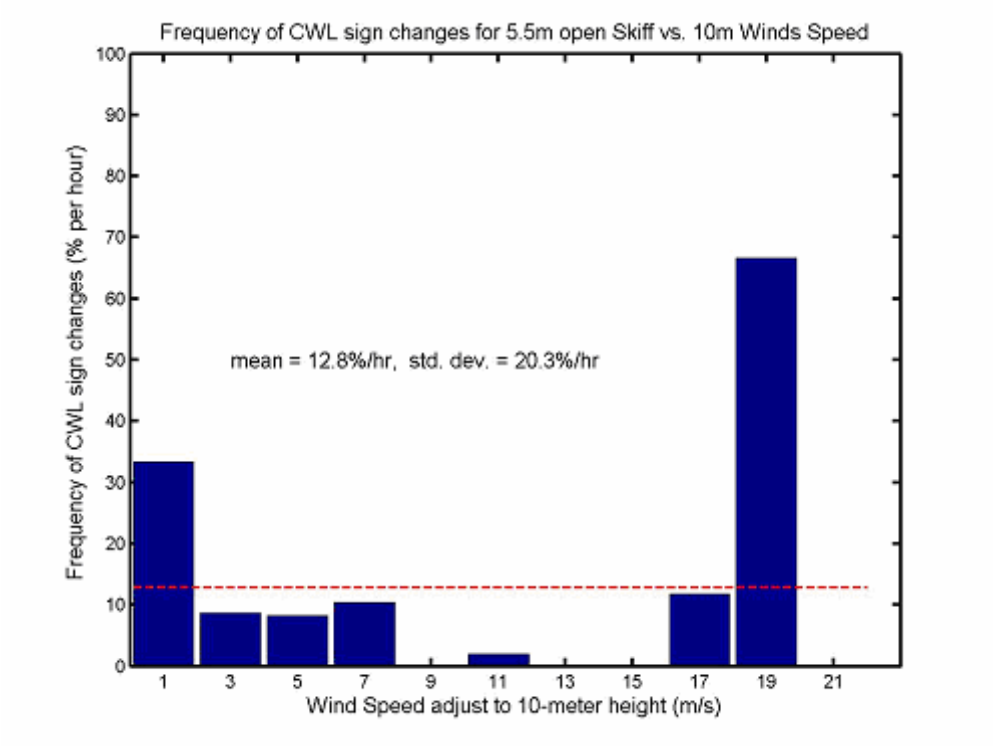

Figure 5-6. Frequency of CWL sign changes (percent per hour) versus 2 m/s groupings of $\mathbf{W_{10m}}$ for the 5.5m open skiff.

This same procedure was used in Sections 5.3.2 through 5.3.4 to investigate and analyze the CWL sign change frequency for each of the other three leeway objects studied.

5.3.2 4-6 Person Life Rafts (with Deep Ballast Systems, Canopy)

Eight significant changes in sign of the crosswind leeway component of the 4-6 person ballasted canopied life rafts were identified as reported in Section D.2 of Appendix D. For each of these CWL sign changes, the associated 10-meter wind speed is known. Figure 5-7 shows the histogram of the number of CWL sign changes by 2 m/s wide groupings of the 10-meter wind speed. Figure 5-8 shows the histogram of the hours of leeway data available for the 660.7 hours of leeway data for the 4-6 person life rafts grouped by the 10-meter wind speed.

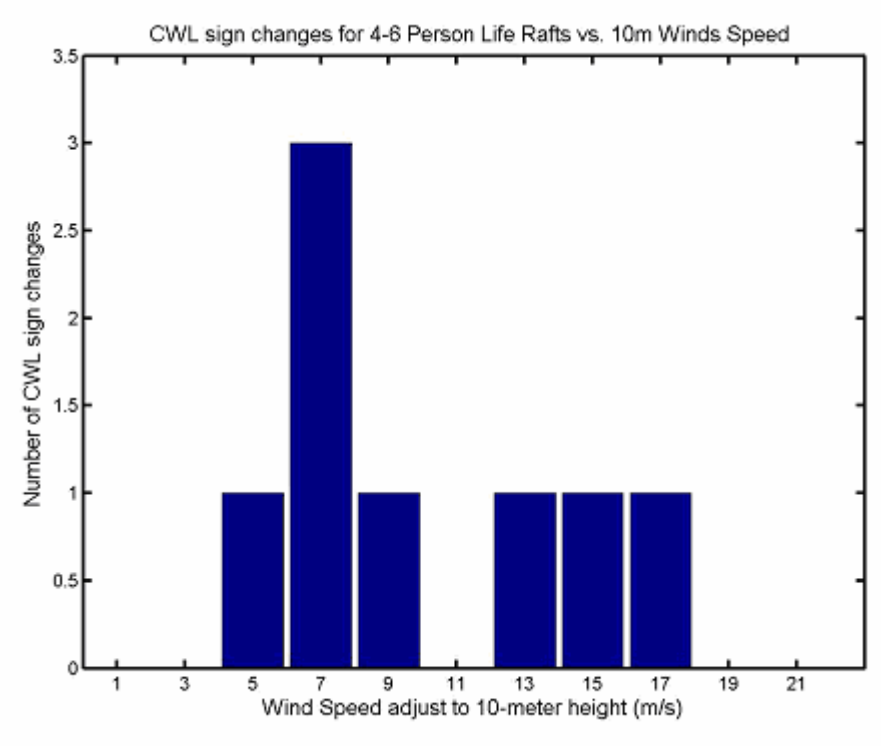

Figure 5-7. Number of significant CWL sign changes versus 2 m/s groupings of $\mathbf{W_{10m}}$ for the 4-6 person life rafts.

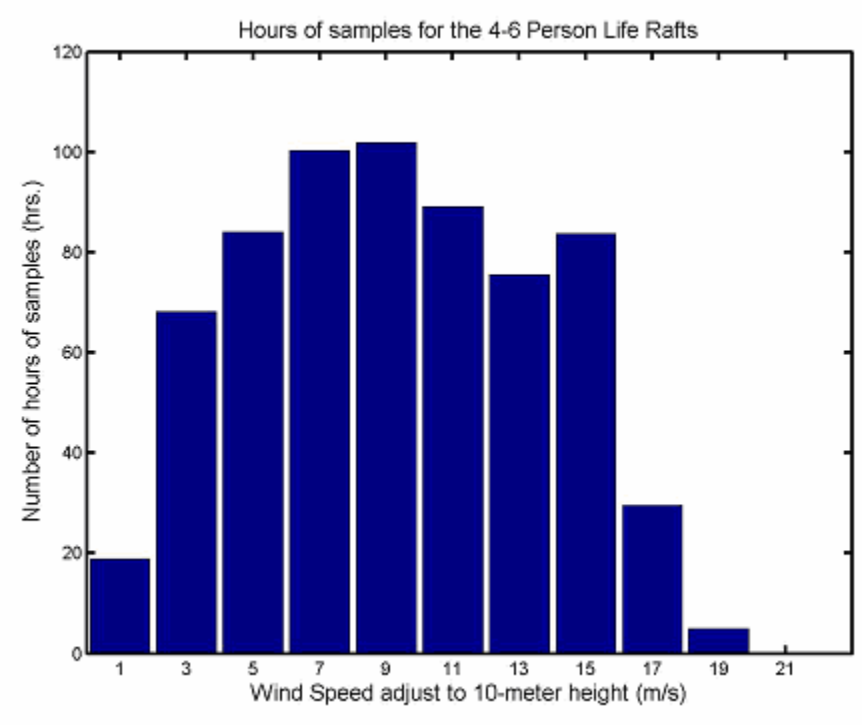

Figure 5-8. Hours of leeway data versus 2 m/s groupings of $\mathbf{W_{10m}}$ for the 4-6 person life raft.

The number of CWL sign changes (Figure 5-7) are normalized by the hours of samples at a given wind speed (Figure 5-8), then hours of samples and the frequency of CWL sign change per hour are determined as function of wind speed for each of the 2 m/s wind speed groupings, as shown in Figure 5-9. The mean of the CWL sign change frequency averaged over the eleven 2 m/s groupings of the 10-meter wind speed was 1.1%/hr with a standard deviation of 1.2%/hr. The mean was superimposed on the histogram of the frequency of CWL sign changes in Figure 5-9. Eight CWL sign changes normalized by 656.0 hours represents a 1.2% chance of CWL sign change per hour for this leeway category.

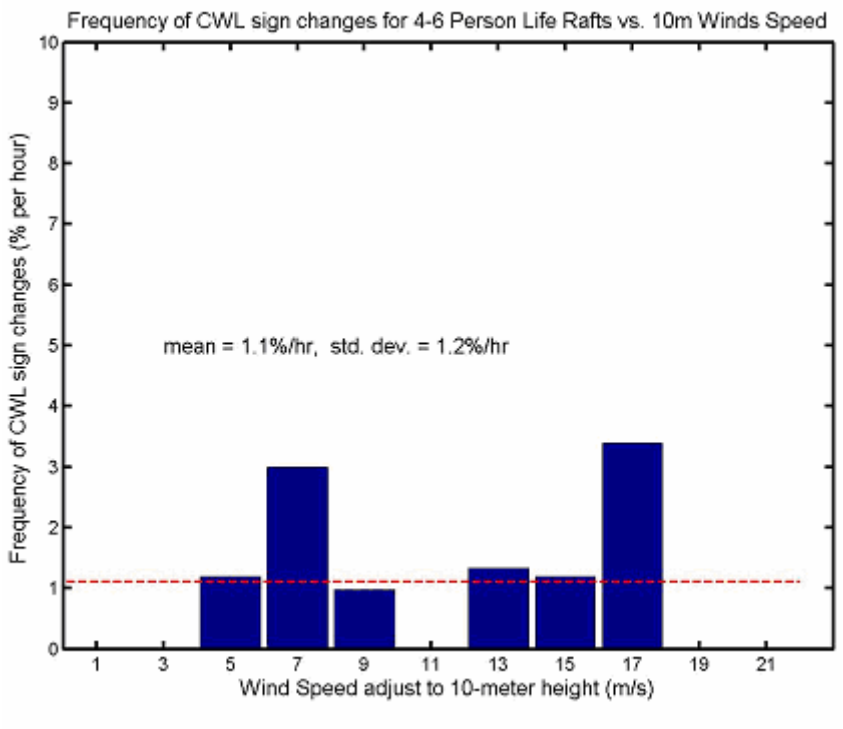

Figure 5-9. Frequency of CWL sign changes (percent per hour) versus 2 m/s groupings of $\mathbf{W_{10m}}$ for the 4-6 person life rafts.

5.3.3 20-Person Life Rafts

Twenty-three significant changes in sign of the crosswind leeway component of the 20-person life rafts were identified as reported in Section D.3 of Appendix D. For each of these CWL sign changes, the associated 10-meter wind speed is known. Figure 5-10 shows the histogram of the number of CWL sign changes by 2 m/s wide groupings of the 10-meter wind speed. Figure 5-11 shows the hours of data available for the 268.3 hours of leeway data for the 20-person life raft versus 2 m/s groupings of the 10-meter wind speed.

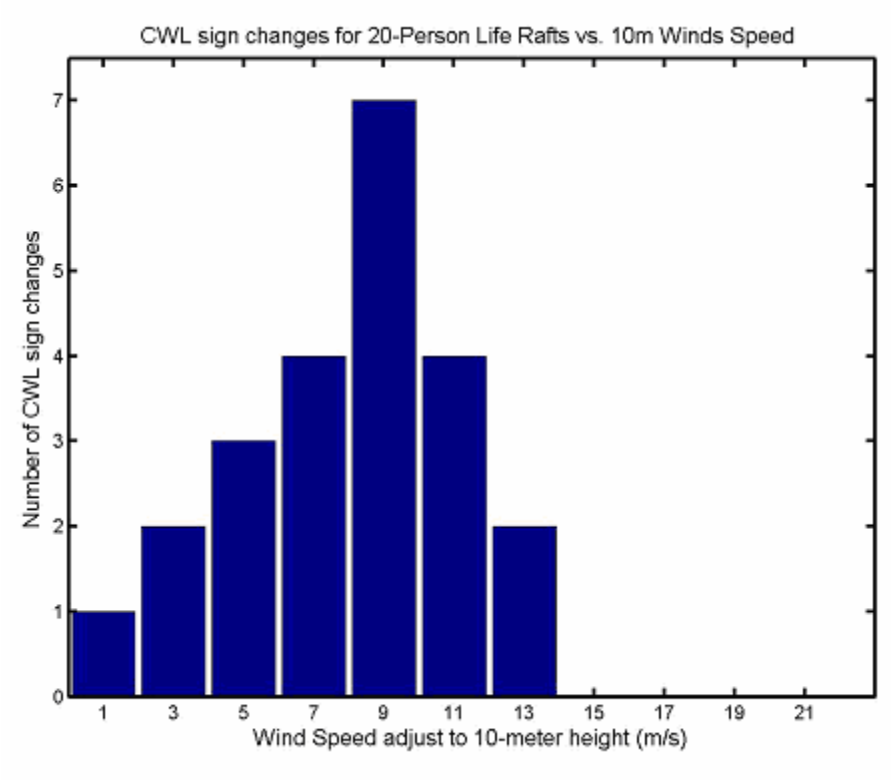

Figure 5-10. Number of significant CWL sign changes versus 2 m/s groupings of $\mathbf{W_{10m}}$ for the 20-person life rafts.

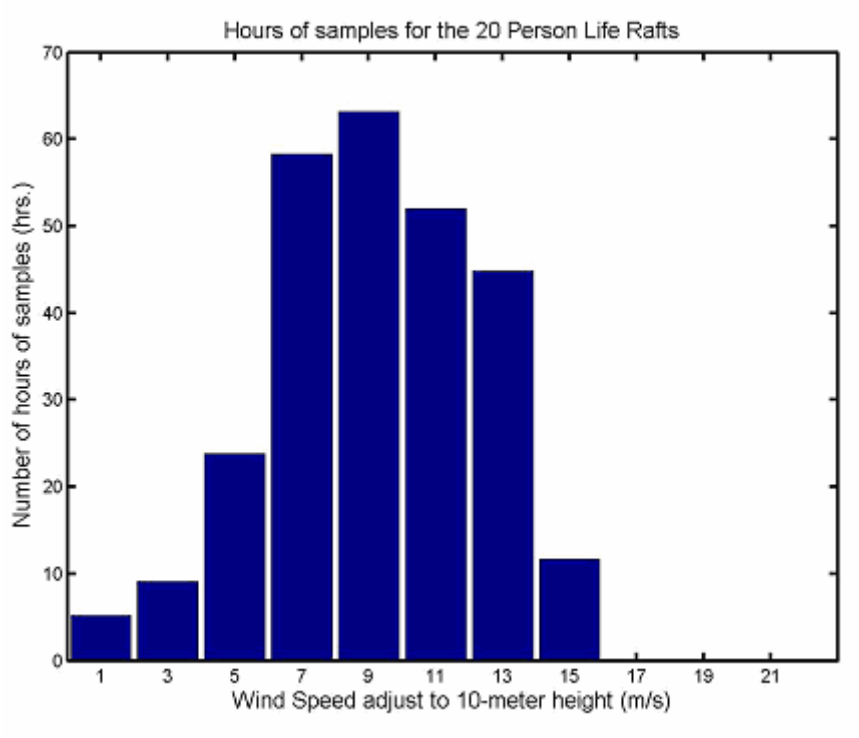

Figure 5-11. Hours of leeway data versus 2 m/s groupings of $\mathbf{W_{10m}}$ for the 20-person life rafts.

The number of CWL sign changes (Figure 5-10) are normalized by the hours of samples at a given wind speed (Figure 5-11), and the frequency of CWL sign changes per hour is determined as function of wind speed for each of the 2 m/s wind speed groupings, as shown in Figure 5-12. The mean of the CWL sign change frequency averaged over the eight 2 m/s groupings of the 10-meter wind speed was 9.3%/hr with a standard deviation of 7.7%/hr. The mean was superimposed on the histogram of the frequency of CWL sign changes in Figure 5-12. Twenty-three CWL sign changes normalized by 268.3 hours represents an 8.6% chance of CWL sign change per hour for this leeway category.

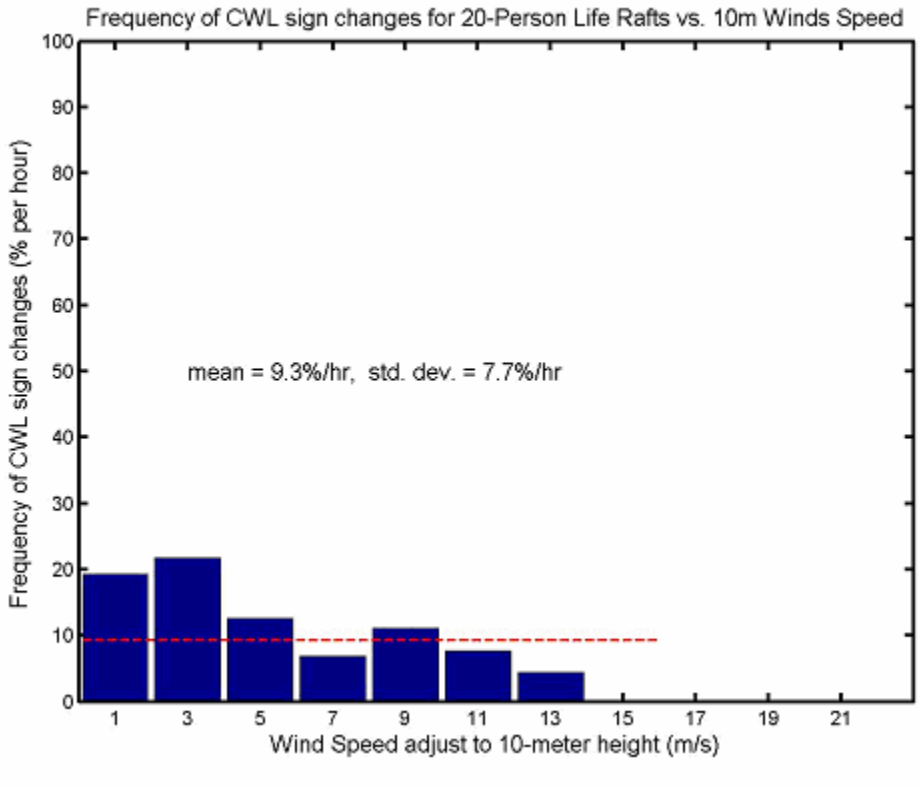

Figure 5-12. Frequency of CWL sign changes (percent per hour) versus 2 m/s groupings of $\mathbf{W_{10m}}$ for the 20-person life rafts.

5.3.4 One-Cubic Meter Wharf Box

Two significant changes in sign of the crosswind leeway component of the 1-cubic meter wharf box were identified as reported in section D.4 of Appendix D. For each of these CWL sign changes, the associated 10-meter wind speed is known. Figure 5-13 is the histogram of the number of CWL sign changes by 2 m/s wide groupings of the 10-meter wind speed. Figure 5-14 shows the hours of data available for the 102.2 hours of leeway data for the 1-cubic meter wharf box versus 2 m/s groupings of the 10-meter wind speed.

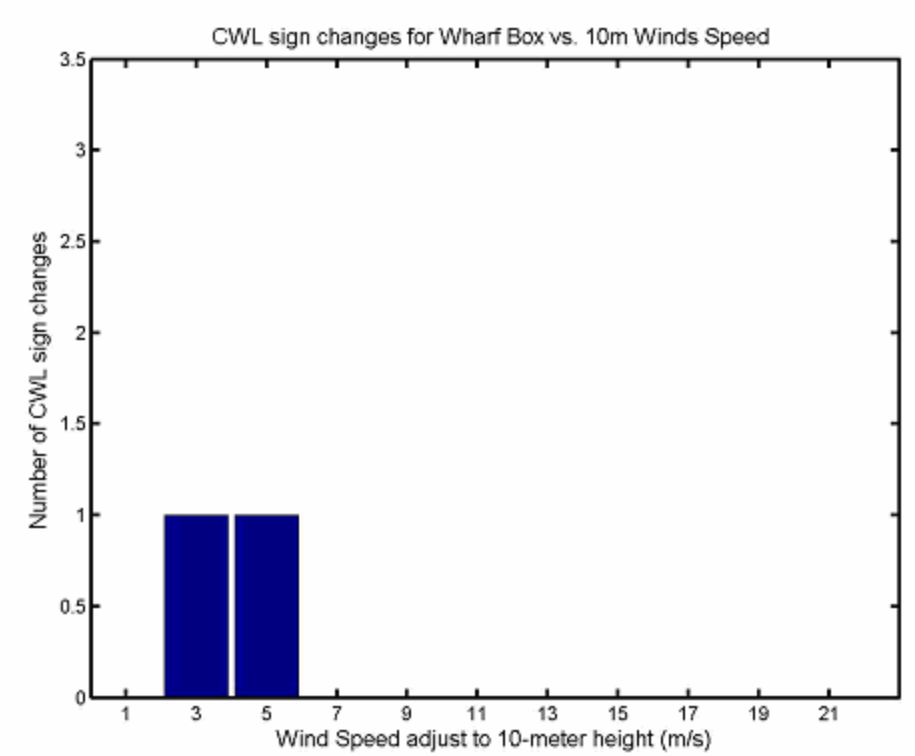

Figure 5-13. Number of significant CWL sign changes versus 2 m/s groupings of $\mathbf{W_{10m}}$ for the 1-cubic meter wharf box.

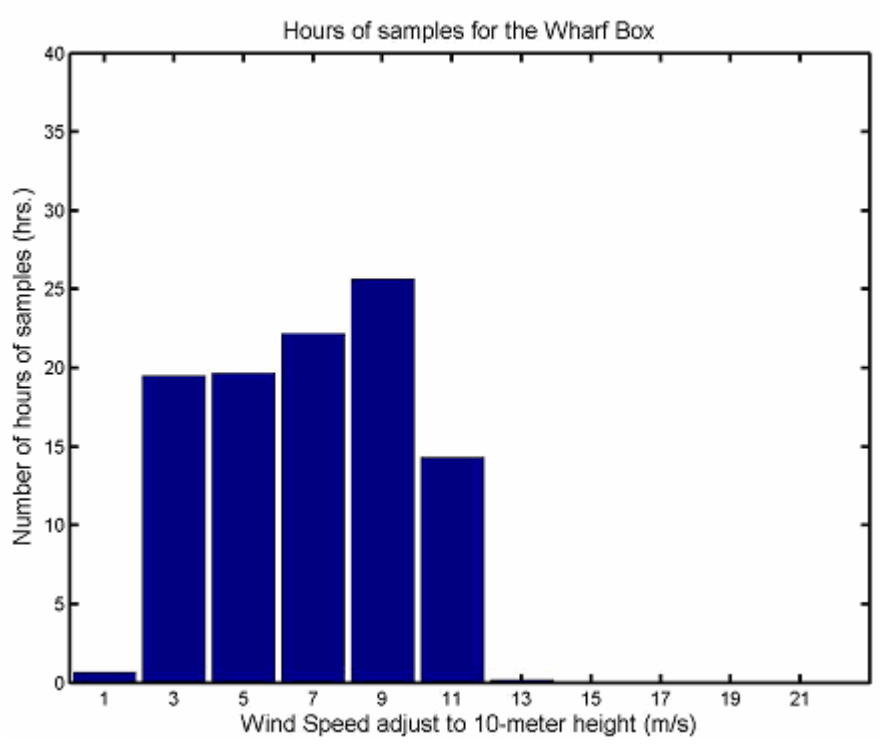

Figure 5-14. Hours of leeway data versus 2 m/s groupings of $\mathbf{W_{10m}}$ for the 1-cubic meter wharf box.

The number of CWL sign changes (Figure 5-13) are normalized by the hours of samples at a given wind speed (Figure 5-14), giving the frequency of CWL sign changes per hour as function of wind speed for each wind speed grouping, as shown in (Figure 5-15). The mean of the CWL sign change frequency averaged over the seven 2 m/s groupings of the 10-meter wind speed was 1.5%/hr with a standard deviation of 2.5%/hr. The mean was superimposed on the histogram of the frequency of CWL sign changes in Figure 5-15. Two CWL sign changes normalized by 102.2 hours represents a 2.0% chance of CWL sign change per hour for this leeway category.

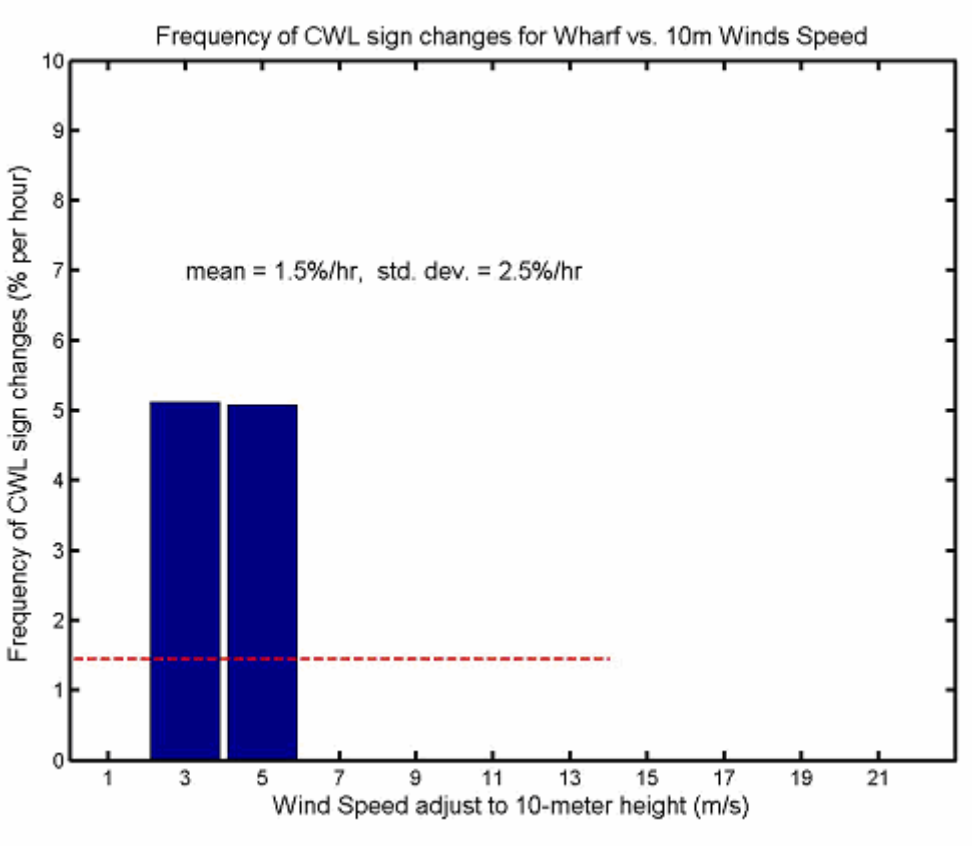

Figure 5-15. Frequency of CWL sign changes (percent per hour) versus 2 m/s groupings of $\mathbf{W_{10m}}$ for the 1-cubic meter wharf box.

5.3.5 Combining Four Leeway Categories Together

The occurrence and frequency of sign changes of the crosswind components of leeway were documented in section 5.3 and analyzed as a function of wind speed for the four leeway object categories studied in sections 5.3.1 to 5.3.4. These four leeway categories all had more than 100 hours of direct leeway sampling with a wind monitoring system mounted onboard the leeway test object.

This analysis was conducted to determine if there is a relationship between the CWL sign change frequency (sign changes per hour) and either wind speed or leeway object category. A summary of statistics of CWL sign changes is presented in Table 5-2. The mean frequency of the CWL sign changes was calculated by equally weighting either the samples or wind speed groupings.

Total means were averaged horizontally (all data combined and weighted equally) or vertically (the four leeway category weighted equally).

Table 5-1. Summary of CWL sign changes statistics.

Leeway Category	CWL sign changes (#)	10-minute Samples (#)	Hours Of Samples (hr)	Freq. CWL sign change [by samples] (%/hr)	Freq. CWL sign change [by 2 m/s wind speed groupings] (%/hr)
5.5 m skiff	16	1774	295.7	5.4*	12.8**
4-6person life raft	8	3936	656.0	1.2*	1.1**
20-person life raft	23	1610	268.3	8.6*	9.3**
Wharf box	2	613	102.2	2.0*	1.5**
4 categories combined together	49	7933	1332.2	3.7* or 4.3***	6.1** or 6.2***

* Averaged by hours of samples (i.e., samples given equal weighting).

** Averaged by 10-meter wind speed bins (i.e., 10-m Wind speed groupings given equal weighting).

*** Averaged by leeway categories (i.e., Leeway categories given equal weighting).

The 4-6 person life rafts and the wharf box displayed a relatively low chance of CWL sign changes while the open skiff and 20-person life rafts had relative high occurrences of CWL sign changes. The histograms (Figures 5-6, 5-9, 5-12 and 5–15) of frequency of CWL sign changes per hour plotted against 2 m/s groupings for the four leeway categories did not show a consistent relationship with wind speed. Nor is there a clear relationship between the leeway object category and frequency of CWL sign change. For instance, the 4-6 person life raft and the wharf box (which have different physical characteristics) both exhibit a sign change frequency on the order of 1%, while the 20–person life raft exhibited a sign change frequency on the order of 8%. Apparently, sign change frequency is independent of leeway object configuration. In considering the results of this analysis, there appears to be no clear-cut relationship with either wind speed or leeway drift object category.

With the limited data presently available, it is impossible to relate the data in Table 5-2 for these four leeway categories to all 63-leeway categories of Allen and Plourde (1999) or across wind speed. Therefore, the next step in the investigation was to examine the generic average frequency of CWL sign change for all leeway categories at all wind speeds This is accomplished by treating the four categories of leeway objects in Section 5.3 as a single category, combining all the changes in CWL sign together to create a generalized histogram for the frequency of CWL sign change.

Repeating the procedure used in Section 5.3, the number of CWL sign changes (Figure 5-16) were normalized by the hours of samples at a given wind speed (Figure 5-17), giving the frequency of CWL sign changes per hour as function 2 m/s groupings of the 10 meter wind speed, (Figure 5-18). The mean of the CWL sign change frequency, as function of 10-meter wind speed, was determined to be 6.1% per hr with a standard deviation of 8.7% per hr. The mean was superimposed on the histogram of the frequency of CWL sign changes in Figure 5-18.

A total of forty-nine CWL sign changes normalized by a total of 1332.2 hours of data represents a 3.7% chance of CWL sign change per hour for these four combined leeway categories.

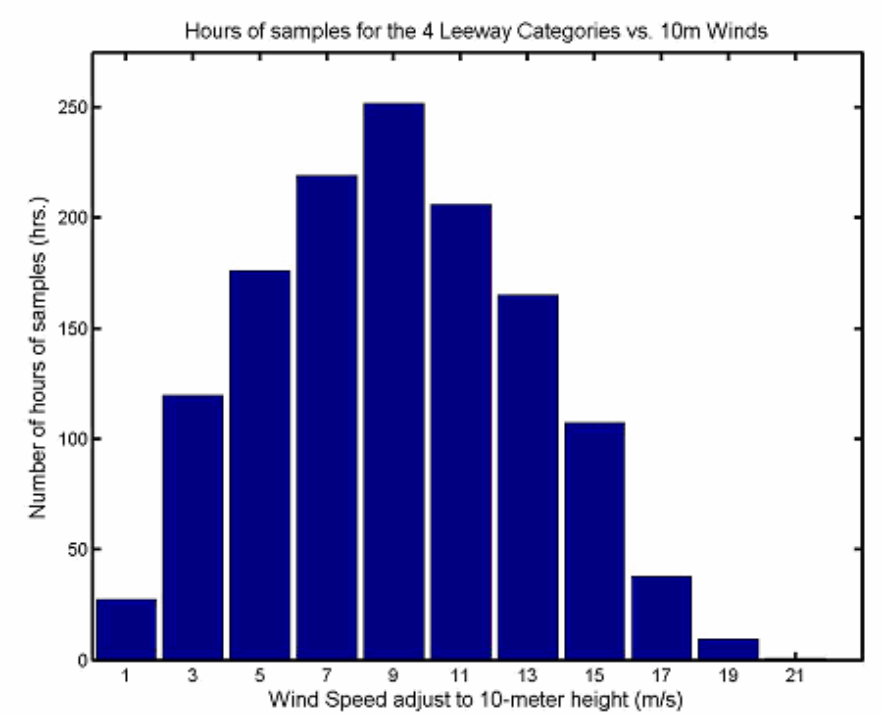

Figure 5-16. Histogram of the number of significant change of signs in the crosswind component of leeway for the four leeway categories combined versus 2 m/s groupings of the 10-meter wind speed (m/s).

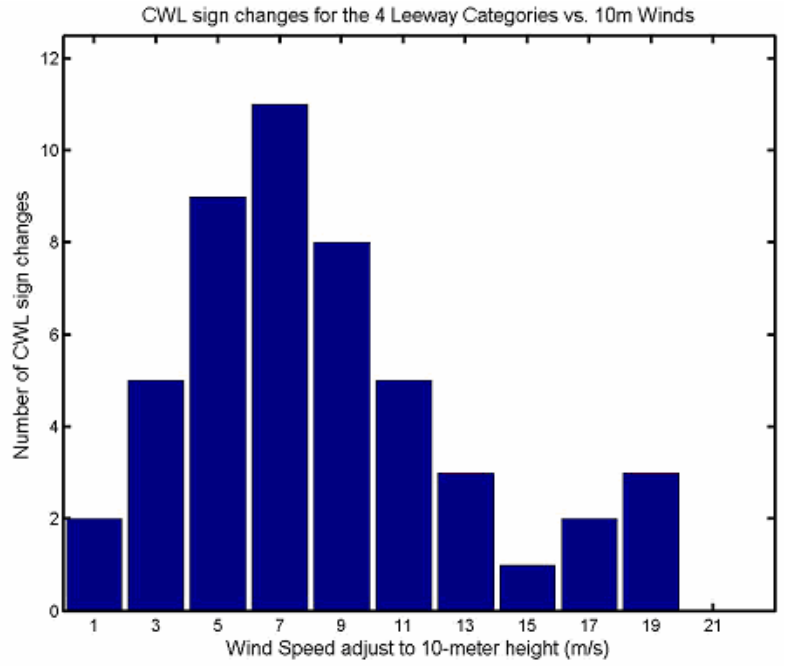

Figure 5-17. Histogram of the hours of leeway data for the four leeway categories combined versus 2 m/s groupings of the10-meter wind speed (m/s).

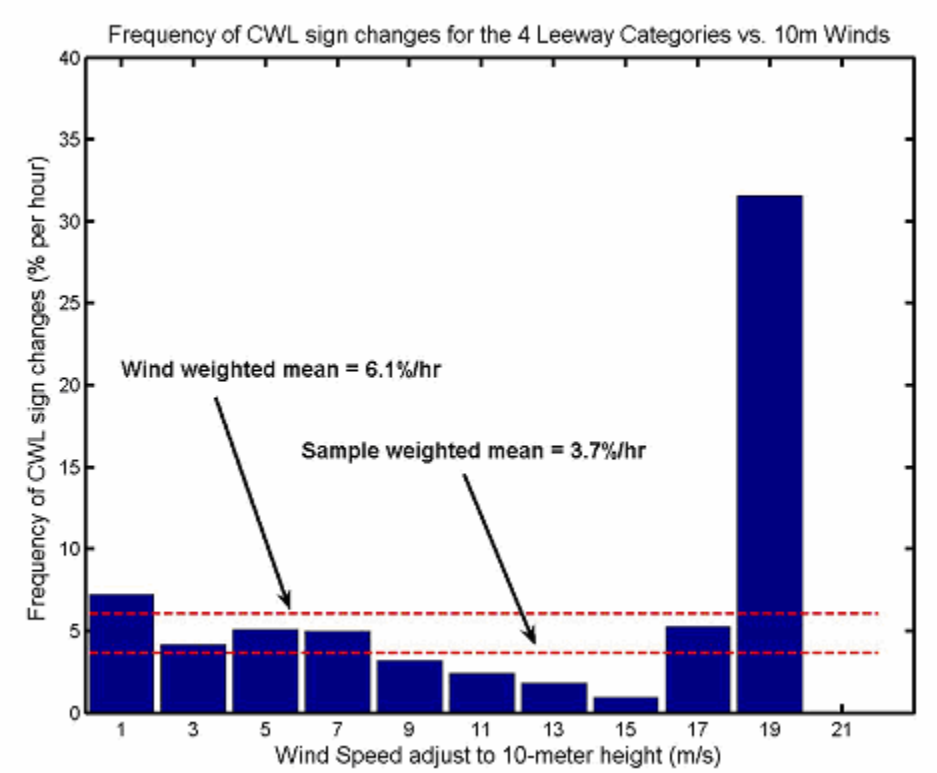

Figure 5-18. Histogram of the frequency of CWL sign changes per hour for the four leeway categories combined, versus 2 m/s groupings of the 10-meter wind speed.

Four schemes were used to investigate the frequency of CWL sign change per hour. First, a simple average of the 49 CWL sign changes was normalized by the 1332.2 hours of sampling to determine a sampled-weighted average of 3.7% chance of CWL sign change per hour. (This value is plotted as the lower red dashed line in Figure 5-18). The second averaging scheme was to average frequencies of CWL sign changes for the four leeway categories. This average is a 4.3% chance of CWL sign changes per hour, weighted by leeway category. The third method was to average the frequencies of CWL sign changes over the 2 m/s groupings of 10 meter wind speed as shown in Figure 5-18. This 10m wind speed grouped weighted average is 6.1% chance of CWL sign change per hour. (This value is plotted as the upper red dashed line in Figure 5-18). The fourth method was to average the 2 m/s groupings of the 10-meter wind speed for the four leeway categories. This 10-m wind speed and leeway category weighted average is 6.2% chance of CWL sign change per hour.

It appears from the above analysis that the frequency of CWL sign change per hour lies in the range of 3 to 7 %. However, before attempting to choose one value or the other as the "representative value" for the leeway object categories investigated, it is reasonable to first investigate the impact that varying the frequency from between 3 – 7 % has on the search area distributions generated using the DWL and CWL component models developed in Chapter 4.

5.4 Investigating The Effects Of Crosswind Component Sign Changes On Search Area Distributions

In the previous section the frequency of CWL sign change occurrence for four leeway categories was investigated in detail. In this section we will look at the effects of CWL sign change over the widest possible sign change frequency range to investigate the sensitivity of search area distributions predicted by current models to the frequency of CWL sign changes.

We will use a set of simplified search parameters to illustrate the effects of CWL sign changes. The leeway category chosen for this illustration is flat-bottom skiffs, (i.e. a Boston Whaler style outboard powerboat). The maximum divergence angle according to Allen and Plourde (1999) for this leeway category is 30 degrees. Winds are held constant from the south at 15 m/s (29 knots). Uncertainty in the wind speed of 0.25 m/s (1 sigma) and in wind direction of 1.0 degree (1 sigma) about the mean were applied to each replication. Mean surface currents were set to zero; however, biases of 5 cm/s sigma east and north currents were applied to each replication. Last known position (LKP) was set to zero, (zero coordinates in kilometers east and north) with 1000 replications, all starting at the same time, hour 0.0. Fifty percent of the replications were started to the left of the downwind direction with negative components of crosswind leeway and the other fifty percent were started to the right with positive components of crosswind leeway. No CWL sign changes were allowed to occur during the first one-hour time step. All time steps are one hour. The assigned probability for a replication to change crosswind component sign was held constant during a run, but changed from run to run. The percent change of CWL sign changes per hour per replication was varied from 0 % to 50 % (Figures 5-19 to 5-21).

In Figure 5-19 (A), no CWL sign changes were allowed to occur, showing the effect of leeway divergence and separating the two distributions based on negative (left) and positive (right) crosswind components of leeway. Each successive distribution also shows the spreading due to the uncertainty values of leeway, wind and sea current. What is clearly shown in this figure is the lack of replications between the two major left and right distributions.

For Figure 5-19 (B) the percent change of CWL sign change was set to 1.0 % per hour, which is very close to that observed for the 4-6 person life rafts and the wharf box. At this rate of CWL sign changes there are replications between the two major left and right distributions.

No CWL **sign changes** **1%** CWL **sign changes per Hour**

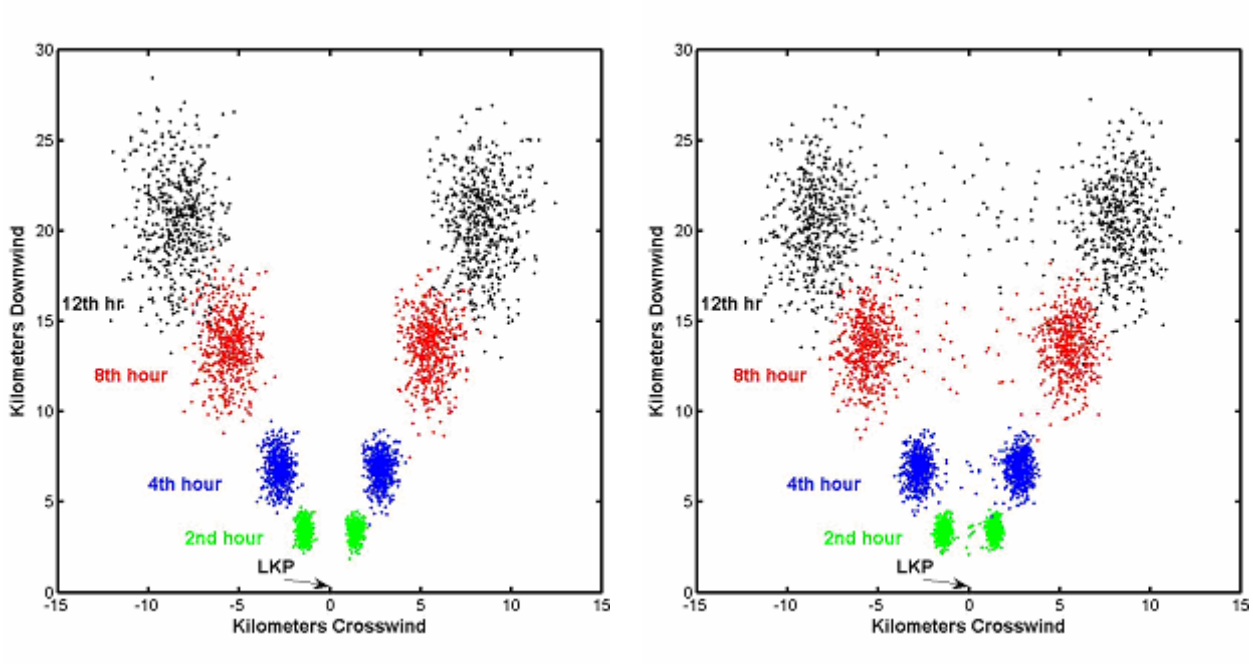

Figure 5-19. Probability distributions at 0, 2, 4, 8, and 12 hours after start of 1000 replications of a flat bottom skiff in 15 m/s of south wind. The percent change of CWL sign changes per hour per replication was set to zero [A] and 1% [B].

For figure 5-20, the percent change of CWL sign changes was increased to 4.0% (A) and 6.0% (B) per hour, which is very close to the averaged frequency of the four leeway categories combined. At these percentages, the middle of the distribution is being populated with a significant number of replications. At the second hour a small distribution on the order of 40 to 60 replications (or about 4% or 6% of the 1000) is now located half way between the two major distributions. During the next hour (3^{rd}) there are two intermediate distributions both on the order of 40 to 60 replications. Roughly, half came from the adjacent major distribution and half came from the center distribution.

Another effect is apparent in Figure 5-20. Those replications that have changed CWL sign and are filling in the area between the two major outside distributions do so along a straight line, between the centers of the two outside distributions, and not an arc. The pathways of replications with CWL sign changes have less net displacement from LKP then those replications that have not changed CWL sign. The CWL sign change replications zigzag their way downwind, thereby having less net displacement than those replications that remain in the same direction relative to the downwind direction.

4% CWL **sign changes per Hour** **6%** CWL **sign changes per Hour**

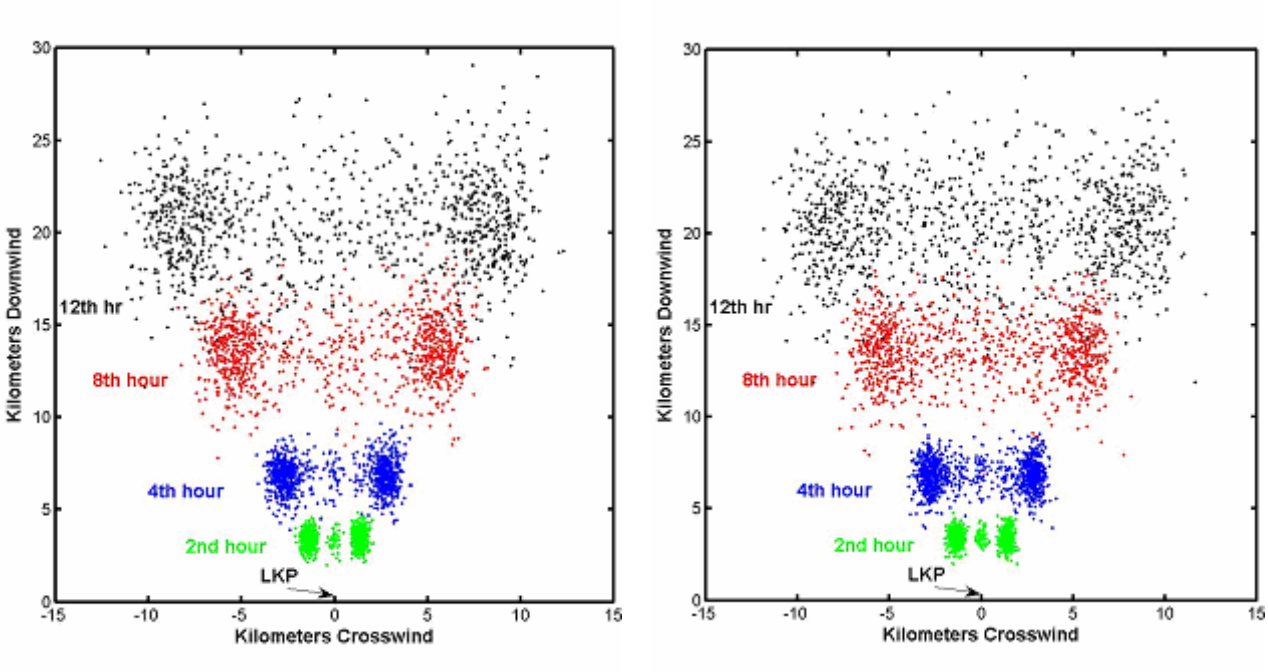

[A] [B]

Figure 5-20. Probability distributions at 0, 2, 4, 8, and 12 hours after start of 1000 replications of a flat bottom skiff in 15 m/s of south wind. The percent change of CWL sign changes per hour per replication was set to 4% [A] and 6% [B].

Figure 5-21 focuses on upper end of CWL sign changes (10% and 50% per hour). A 10% chance of CWL sign change is just above the observed frequency for 20-person life rafts (8.6 – 9.3%). At 10% CWL sign change per hour (Figure 5-21 A), the distribution shows the flattened, non-arc distributions evident in Figure 5-20. At this higher rate of CWL sign change, the two outer distributions have been severely reduced, and the overall distribution is more continuous from left to right.

The upper statistical limit for CWL sign change is 50% per hour, i.e., a CWL sign change could occur every time step. The effect of this is shown in Figure 5-21 [B]. This nicely illustrates the Central Limit Theorem, which will bring the replications back towards the downwind centerline. While this leeway category (small skiffs) has considerable leeway divergence (30 degrees), the effect of constant CWL sign changes completely cancels the effects of divergence after about nine hours.

10% CWL **sign changes per Hour** **50%** CWL **sign changes per Hour**

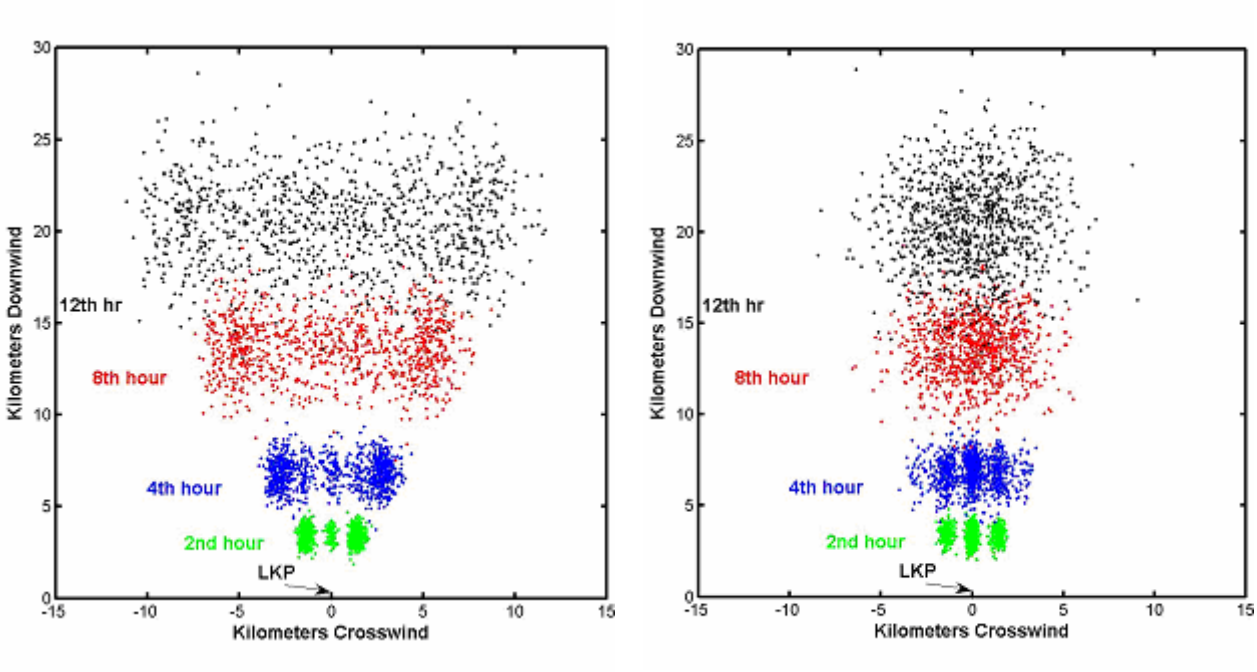

[A] [B]

Figure 5-21. Probability distributions at 0, 2, 4, 8, and 12 hours after start of 1000 replications of a flat bottom skiff in 15 m/s of south wind. The percent change of CWL sign changes per hour per replication was set to 10% [A] and 50% [B].

The most notable result of the analysis in this section is that there appears to be little variation in the search area distributions produced by 4% per hour CWL sign change frequency and 6% per hour CWL sign change frequency, which corresponds to the CWL sign frequency range identified in Section 5.3.5. (Roughly 3.7% to 6.2 %). In addition, the search area distributions generated by the DWL and CWL component linear regression models using CWL sign change frequencies of 4% per hour and 6% per hour correspond well with search area distributions generated using other Monte Carlo search area prediction models.

5.5 Summary Of Crosswind Component Sign Changes

In summary we have found:

3) For the four types of drift-objects studied, CWL sign changes did occur under a variety of wind conditions;

4) The experimental techniques used were not designed to investigate the dynamics of drift objects changing crosswind component signs,

5) At the present time there are no data that suggest a statistical relationship between crosswind sign changes and either wind speed or leeway object category,

6) The data analyzed for four leeway object categories suggest a CWL sign change frequency of 4-6% per hour, and

7) Search area distributions show little difference when CWL sign change frequency varies from 4 to 6% per hour.

Since we do not have a dynamic model of the physics of crosswind direction change (CWL sign change), and since the statistics of CWL sign changes for the four leeway categories investigated do not provide a rigorous enough basis for extrapolating to all leeway-object categories or indicate direct relationship between CWL sign change frequency and wind velocity or leeway object category, we recommend that search planning tools use a simple generic average CWL sign change frequency of 4% per hour for all leeway categories with no dependence on wind speed.

CHAPTER 6.

CONCLUSIONS AND RECOMMENDATIONS

6.1 Conclusions

The prediction of the divergence of search object trajectories from the downwind direction is a critical component to the accurate establishment of a search area. The somewhat murky relationship among leeway angle, divergence angle, and leeway divergence has hindered the proper implementation of leeway divergence into search planning tools. Based upon the leeway field studies of the 1990s, this report provides a review and analysis to determine a new approach to model leeway divergence based on computing the downwind (DWL) and crosswind (CWL) components of leeway. This is a different approach than that recommended in Allen and Plourde (1999), which provided coefficients for calculating leeway drift as a function of leeway speed and divergence angle (the traditional approach).

In Chapter 2, an empirical technique is developed to convert the leeway speed and divergence angle values of Allen and Plourde (1999) to a set of linear regression coefficients for computing the downwind and crosswind of leeway drift. This technique was used to determine the DWL and CWL coefficients for 38 leeway object categories for which actual leeway drift data are not available. These 38 sets of coefficients, combined with the initial set of 25 coefficients computed by linear regression analysis of actual data for 25 categories, forms a complete set of DWL and CWL coefficients for the 63 leeway object categories in the comprehensive leeway taxonomy developed by Allen and Plourde (1999). This complete set of coefficients for the unconstrained and constrained forms of the DWL and CWL component model is presented and explained in Chapter 3.

In Chapter 4, a DWL and CWL component leeway drift model is presented that uses the coefficients in Chapter 3 to compute leeway drift. Chapter 5 investigates the nature and impact of CWL sign changes in modeling leeway drift. Most of the drift objects studied during the 1990s field tests drifted to either the right or left of the downwind direction for the duration of the drift period. This behavior tends to generate two areas of high search probability that eventually separate over time. The use of downwind and crosswind components of leeway by Monte Carlo simulation techniques readily model this behavior. However, a closer inspection of four leeway categories that each contained over 100 hours of directly measured leeway revealed that the drift object did change crosswind leeway drift direction from either right of the downwind direction to the left or vice versa. These changes result in a change in the sign of the crosswind component of leeway.

The investigations in Chapter 5 show that the frequency of CWL sign change appears to be independent of wind speed. The frequency of the sign change was shown to vary among the four leeway object categories, but we were not able to generalize (or extrapolate) sign change occurrence to the 59 other leeway categories. The overall observed frequency of these sign changes in crosswind components based on the leeway drift of all four categories of leeway objects was approximately 4-6% per hour. It was further shown that while the difference between final search area probability distribution was significant for 0% and 50% sign change

frequency per hour, the difference between distributions resulting from 4% and 6% sign change frequency per hour was not. Based on past search area modeling, it appears that a 4-6% sign change frequency provides a search area distribution consistent with those generated by existing SAR planning tools. A "generic" value of 4% per hour is recommended for use in stochastic leeway models until further study provides a more complete picture of CWL sign phenomena.

6.2 Recommendations

1) Tables 3-1 and 3-2 provide a complete set of DWL and CWL coefficients for the 63 categories of leeway objects in the taxonomy developed by Allen and Plourde (1999). Although 38 sets of DWL and CWL coefficients were statistically derived from the empirical data, the Table 3-1 and 3-2 coefficients should be used in numerical search planning tools to determine the downwind and crosswind components of leeway (as a function of wind speed adjusted to the standard 10-meter height) in calculating search area distributions.
2) Incorporate into numerical search planning tools the use of a simple statistical model of switching between positive and negative crosswind component equations using a sign change frequency of 4% per hour, independent of wind speed or leeway category.
3) Incorporate into manual search planning tools the use of divergence angles provided by Allen and Plourde (1999) divided by an adjustment factor 1.35.
4) Continue efforts to fully understand and model the drift of survivors and survivor craft by studying targets over more drift runs and in a variety of wind conditions. The conditions should include wind speeds less than 3 m/s and greater than 20 m/s and periods of rapid wind direction shifts. With more drift run analysis, the subject of initial distribution between left and right divergence can be addressed. Collecting leeway data under a variety of wind conditions will also allow the observation of changes between left and right divergence. Data collection for the 38 leeway categories for which data are not available will allow direct computation and verification of the DWL and CWL coefficients for these categories.
5) Further refine the collection of leeway data collected in the field to minimize the effect that the instrumentation has on drift of the search test object. The use of current meters placed directly onboard the test object is likely to lessen the impact on the craft switching signs of the crosswind component. However, these directly mounted current meters should be verified against the more standard technique of a tethered current meter, which is well away from any local flow distortion effects. Additional insight into the behavior and dynamics of an object's CWL component sign change might come with further information of the wave field and from leeway dynamics modeling studies.

CHAPTER 7.

REFERENCES

Allen, A. A., 1996. "The Leeway of Cuban Refugee Rafts and a Commercial Fishing Vessel," U.S. Coast Guard Report No. CG-D-21-96.

Allen, A. A., and R.B. Fitzgerald, 1997. "The Leeway of an Open Boat and Three Life Rafts in Heavy Weather," U.S. Coast Guard Report No. CG-D-03-98.

Allen, A. A., and J.V. Plourde, 1999. "Review of Leeway: Field Experiments and Implementation," U.S. Coast Guard Report No. CG-D-08-99.

Allen, A.A., R.Q. Robe and E.T. Morton, 1999. "The Leeway of Person-In-the-Water and Three Small Craft," U.S. Coast Guard Report No. CG-D-09-00.

Chapline, W. E., 1960. "Estimating the Drift of Distressed Small Craft." Coast Guard Alumni Association Bulletin, U.S. Coast Guard Academy, New London, CT Vol. 22, No. 2, March-April 1960, pp 39-42.

Fitzgerald, R. B., D. J. Finlayson, and A. Allen, 1994. "Drift of Common Search and Rescue Objects - Phase III." Contract report prepared for Canadian Coast Guard, Research and Development, Ottawa, TP# 12179.

Hodgins, D. O. and S. L. M. Hodgins, 1998. "Phase II Leeway Dynamics Study Program Development and Verification of a Mathematical Drift Model for Liferafts and Small Boats." prepared for Canadian Coast Guard College, Dept. Fisheries and Oceans.

Hufford, G.L., and S. Broida, 1974. "Determination of Small Craft Leeway." U.S. Coast Guard Research and Development Center Report No. 39/74, December 1974.

Kang, S.Y., 1999. "A Field Experiment for the Determination of Drift Characteristics of Person-in-Water", 'Journal of the Society of Maritime Safety', Vol. 5, No.1, pp. 29-36 (Abstract in English, text in Korean).

Nash, L., and J. Willcox, 1985. "Summer 1983 Leeway Drift Experiment," U.S. Coast Guard Report CG-D-35-85.

Nash, L., and J. Willcox, 1991. "Spring 1985 Leeway Experiment," U.S. Coast Guard Report CG-D-12-92.

National Search and Rescue Committee, 2000, "U.S. National Search and Rescue Supplement to the International Aeronautical and Maritime Search and Rescue Manual," Washington D.C.

Neter, J., M.H. Kuter, C.J. Nachtsheim, and W. Wasserman, 1996. "Applied Linear Statistical Models" Fourth Edition, Irwin, Inc. Chicago, IL

Smith, S.D., 1988. “Coefficients for Sea Surface Wind Stress, Heat Flux, and Wind Profiles as a Function of Wind Speed and Temperature,” J. Geophysical Res. Vol. 93, No. C12, pp. 15,467-15,472, 5 December 1988.

APPENDIX A

LEEWAY COMPONENTS OF MARITIME LIFE RAFTS (DEEP BALLAST, CANOPY, 15-25 PERSON CAPACITY)

A.1 Introduction

A Beaufort 20-person circular life raft, shown in Figure A-1, was drifted six times in two configurations. Three leeway drift runs were performed with light loading and no drogue, and three drift runs were with heavy loading and a drogue deployed (Fitzgerald et al. (1994) and Allen and Plourde (1999)). Fitzgerald et al. (1994) presented results for the downwind component of leeway for the two configurations, while Allen and Plourde (1999) presented results for the combined class, i.e., both configurations. The results of the analysis for both components of leeway are presented here for the two configurations of the twenty-person life raft. The configurations follow the leeway taxonomy convention of Allen and Plourde (1999). The analysis procedure follows Allen (1996), Allen and Fitzgerald (1997), Allen and Plourde (1999) and Allen et al. (1999).

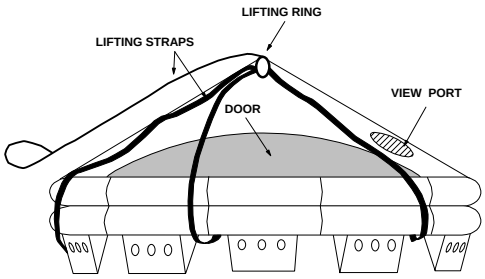

Figure A-1. Beaufort circular 20-person life raft.

A.1.1 MARITIME LIFE RAFT (Deep Ballast, Canopy, 15-25 Person Capacity, No Drogue, Light Loading).

The first leeway drift configuration of the Beaufort 20-person circular life raft was with light loading and no drogue attached. Three drift runs (Leeway Drift Runs 37, 43, and 48) in this configuration combined for a total of 816 ten-minute samples or 136 hours of data. In Figure A-2, the unconstrained linear regression of the downwind component of leeway (DWL, in cm/s) versus wind speed (m/s) adjusted by Smith (1988) to the 10-meter reference level ($\mathbf{W_{10m}}$). Also presented in Figure A-2 are the 95% prediction limits for the 20-person lifer raft with no drogue and light loading. The value of 0.94 for r^2 indicates that the regression of DWL versus $\mathbf{W_{10m}}$ accounts for 94% of the variance of the DWL, an excellent statistical fit.

For analysis purposes, drift runs were separated according to whether the total drift was positive or negative. The unconstrained linear regression of the crosswind components of leeway

(separated by positive (+CWL, in cm/s) and negative components (-CWL, in cm/s)) versus $\mathbf{W_{10m}}$ along with the 95% prediction limits are shown in Figure A-3. The r^2 value indicates that regression of +CWL (-CWL) versus $\mathbf{W_{10m}}$ accounts for 20% (38%)(what?) of the variance of the +CWL (-CWL), which is a poor (fair) fit. The intersection wind speed of the two crosswind regression equations occurs at a $\mathbf{W_{10m}}$ of 5.07 m/s. Below this wind speed, the data points were primarily described by the negative crosswind regression. Table A-1 summarized the coefficients for the three regression equations.

All regression analysis and parameters follow Allen and Fitzgerald (1998), Allen and Plourde (1999), and Allen et al. (1999), where r^2 and $S_{y/x}$ are the coefficients of determination and the standard errors of the estimate, respectively.

Table A-1. Unconstrained Linear Regression of the Downwind and Crosswind Components of Leeway (cm/s), Beaufort 20-person life raft, light loading, no drogue, $\mathbf{W_{10m}}$ (m/s).

Dependent Variable	# samples	Slope (%)	y-intercept (cm/s)	r^2	$S_{y/x}$ (cm/s)	W_{10m} (m/s)
DWL	816	3.9349	3.9349	0.9386	3.0070	2.0 – 16.3
+CWL	276	0.3847	-3.3346	0.1974	2.1583	2.0 – 14.1
-CWL	540	-0.5863	1.5915	0.3846	2.2767	2.3 – 16.3

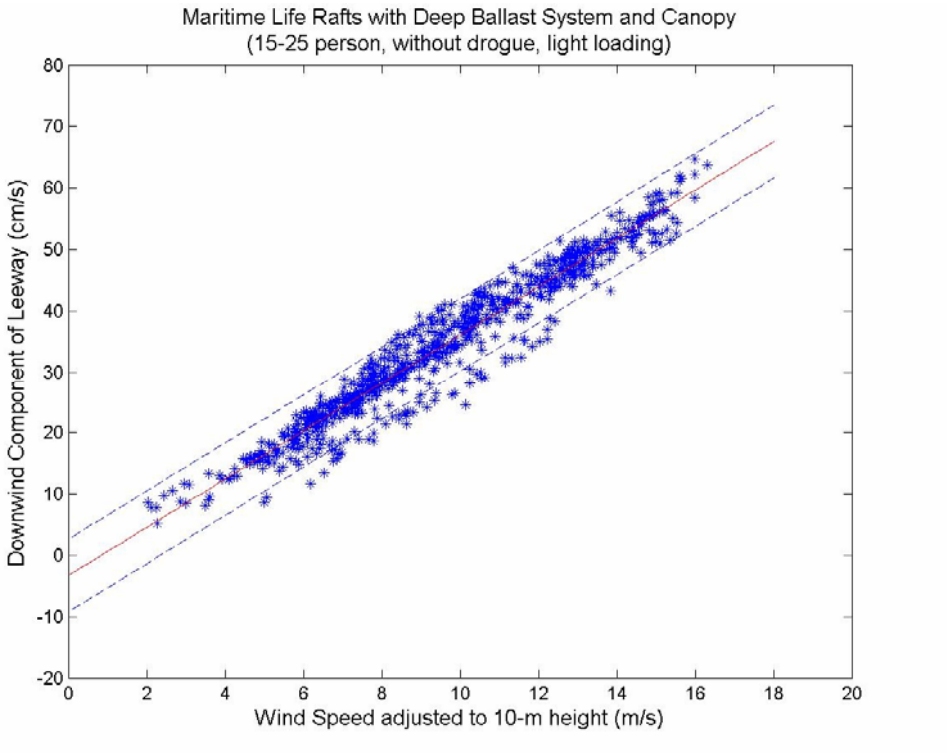

Figure A-2. The unconstrained linear regression and 95% prediction limits of the downwind component of leeway as function of wind speed at 10 m, maritime life rafts, deep ballast systems, canopy, 15-25 person capacity, no drogue, light loading.

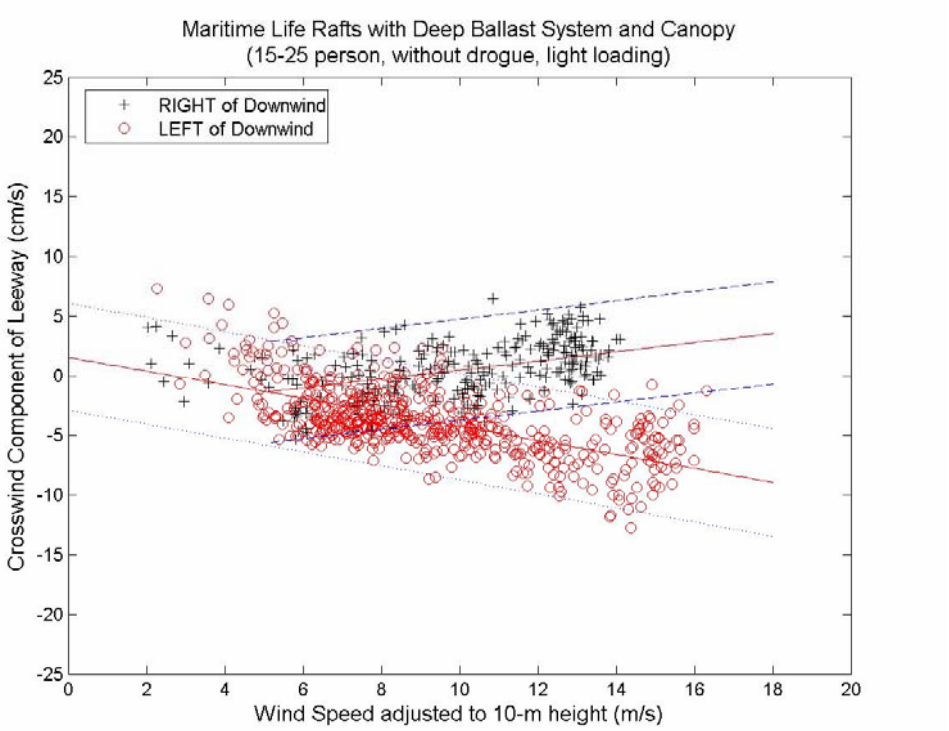

Figure A-3. The unconstrained linear regression and 95% prediction limits of the positive and negative crosswind components of leeway as function of wind speed at 10 m, maritime life rafts, deep ballast systems, canopy, 15-25 person capacity, no drogue, light loading.

A.1.2 Maritime Life Raft (Deep Ballast, Canopy, 15-25 Person Capacity, With Drogue, Heavy Loading)

The second leeway drift configuration of the Beaufort 20-person circular life raft was with heavy loading and with a drogue attached to the raft. Three drift runs (Leeway Drift Runs 40, 42, and 47) combined for a total of 794 ten-minute samples or 132.3 hours of data. In Figure A-4, the unconstrained linear regression of the downwind component of leeway as function of $\mathbf{W_{10m}}$ along with the 95% prediction limits are presented for the 20-person life raft with a drogue and heavy loading. The value of 0.94 for r^2 indicates that the regression of DWL versus $\mathbf{W_{10m}}$ accounts for 89% of the variance of the DWL, which is an excellent fit.

For analysis purposes, drift runs were again separated according to whether the total drift was positive or negative. However, during drift run 47 the life raft had a negative component of crosswind drift for the first 32 hours. After that, the crosswind component was positive. Therefore, this individual run was divided into two sections before being used in the crosswind regression. The unconstrained linear regression of the crosswind components (separated into positive and negative components) versus $\mathbf{W_{10m}}$, along with the 95% prediction limits, are shown in Figure A-5. The r^2 value indicate that regression of +CWL (-CWL) versus $\mathbf{W_{10m}}$ accounts for 20% (21%) of the variance of the +CWL (-CWL), a poor statistical fit, both positive and negative. The intersection wind speed of the two crosswind component regression equations occurs at a $\mathbf{W_{10m}}$ of 6.28 m/s. Below this wind speed, the data points were primarily described

by the positive crosswind regression. Table A-2 summarized the coefficients for the three regression equations.

Table A-2. Unconstrained Linear Regression of the Downwind and Crosswind Components of Leeway (cm/s), Beaufort 20-person life raft, heavy loading, with drogue $\mathbf{W_{10m}}$ (m/s).

Dependent Variable	# samples	Slope (%)	y-intercept (cm/s)	r^2	$S_{y/x}$ (cm/s)	W_{10m} (m/s)
DWL	794	3.1543	-4.4935	0.8942	3.3529	0.4 – 15.3
+CWL	601	0.3853	-1.7991	0.1974	2.5014	0.4 – 15.3
-CWL	193	-0.3756	2.9819	0.2092	1.6443	5.5 – 13.5

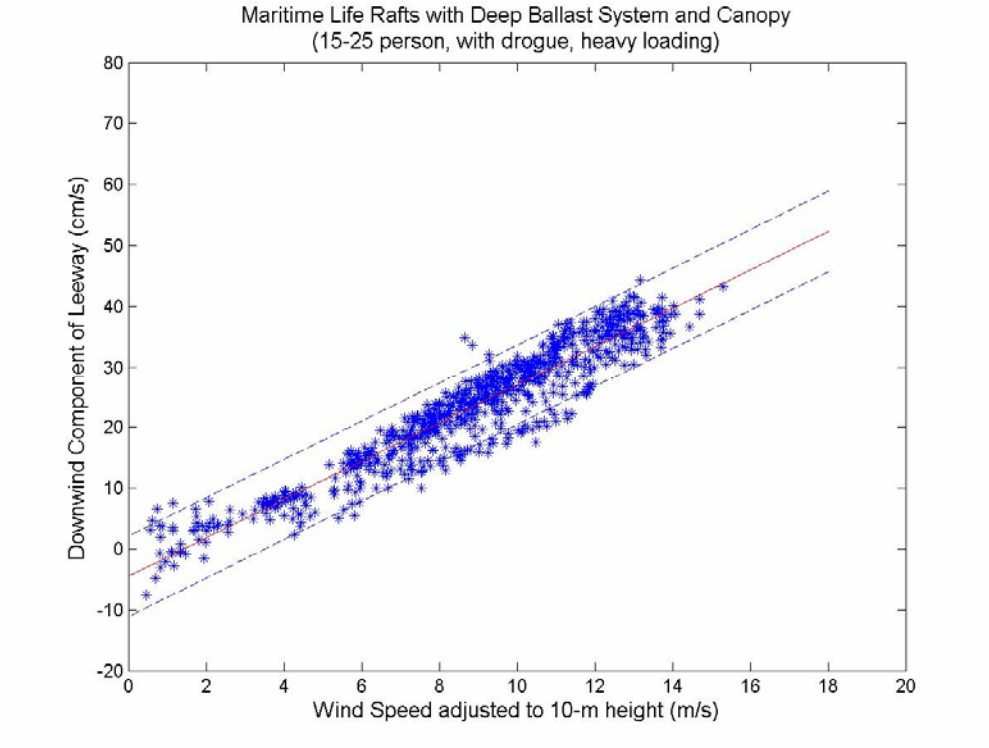

Figure A-4. The unconstrained linear regression and 95% prediction limits of the downwind component of leeway versus wind speed at 10 m, maritime life rafts, deep ballast systems, canopy, 15-25 person capacity, with a drogue, and heavy loading.

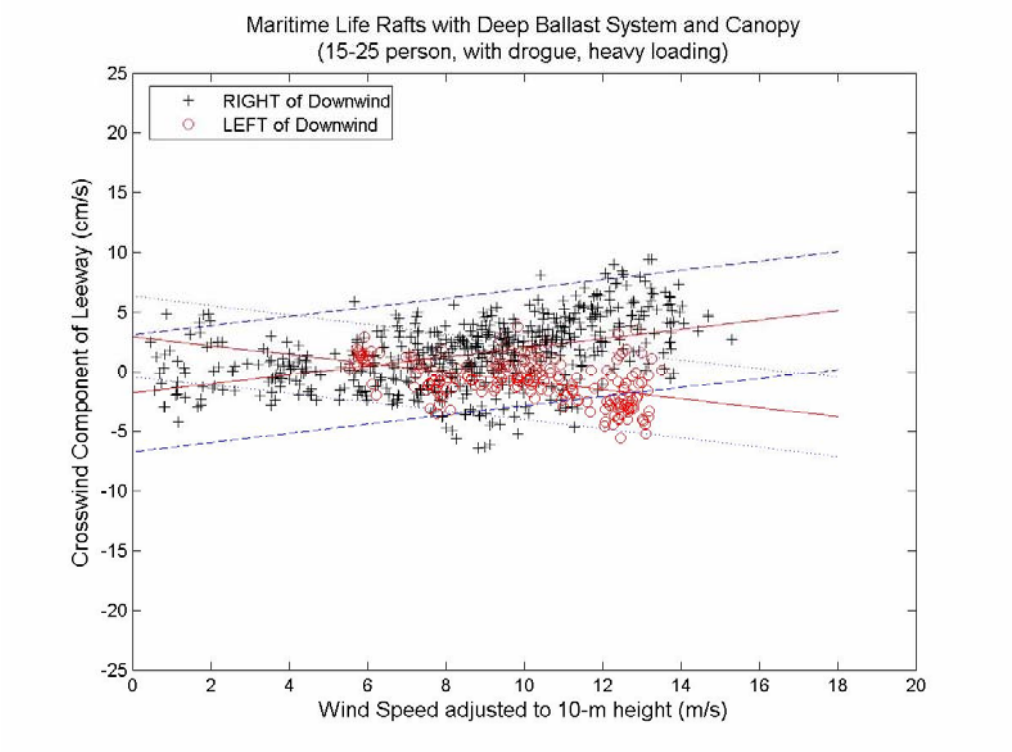

Figure A-5. Unconstrained linear regression and 95% prediction limits of the positive and negative crosswind components of leeway versus wind speed at 10 m, maritime life rafts, deep ballast systems, canopy, 15-25 person capacity, with drogue, heavy loading.

(This page intentionally left blank.)

APPENDIX B

ANALYSIS OF SELECTED LEEWAY CATEGORIES TO DETERMINE THE CONSTRAINED REGRESSION OF THE DOWNWIND AND CROSSWIND COMPONENTS OF LEEWAY AS FUNCTIONS OF THE 10-METER WIND SPEED

B.1 Maritime Life Rafts with no-ballast systems

There are five categories in Allen and Plourde's (1999) Table 8-1 with recommended values for Maritime Life Rafts, no ballast systems. Two of these categories are re-analyses of Hufford and Brodia's (1974) leeway data collected on a 12-foot open life raft. Hufford and Brodia (1974) provide the original data in a form that allowed the analysis to be conducted on the downwind and crosswind components of leeway. A third category is from Nash and Willcox (1991). The downwind and crosswind components of leeway were estimated from Allen (unpublished) report on Leeway Divergence and are used here. Allen and Plourde (1999-Chapter 7) used simple algebraic methods to extrapolate leeway values for two additional categories based upon the three categories above. In this report, we first re-analysis Hufford and Broida's two data sets for Maritime Life Rafts, no-ballast systems, no-canopy, with and without drogue. Then using the simple algebraic method of Allen and Plourde, we will use Nash and Willcox's (1991) values from Allen (unpublished), for Maritime Life Rafts, no-ballast systems, with canopy, without drogue; to extrapolate the downwind and crosswind components of leeway for two remaining leeway categories: (1) Maritime Life Rafts, no-ballast systems, with canopy, with drogue; and (2) the combined class of Maritime Life Rafts, no-ballast systems.

B.1.1 Maritime Life Rafts, no-ballast systems, no-canopy, with and without drogue

Hufford and Brodia (1974) 12-foot Rubber Raft without sea anchor were re-analyzed using the constrained linear regression method of Neter, Kuter, Nacjtsheim, and Wasserman (1996), page 161. Allen and Plourde (1999) contains an analysis of Hufford and Brodia's data using just the linear non-constrained method. The downwind and crosswind components of leeway as functions of wind speed are shown for Hufford and Broida's 12-foot raft without and with sea anchor in figures B-1 through B-4. Hufford and Broida's 12-foot raft are the only leeway drift values presently available for the Allen and Plourde's leeway categories: Maritime Life Rafts, no-ballast systems, no-canopy, without drogue; and Maritime Life Rafts, no-ballast systems, no-canopy, with drogue. The values of the constrained regressions are given in Table B-1.

Table B-1. Constrained linear regression of the leeway components (cm/s) on wind speed (m/s) Hufford and Broida's (1974) 12-foot rubber raft with and without sea anchor.

Leeway Craft	Dependent Variable	# samples	Slope (% wind)	r^2	$S_{y/x}$	Wind Speed (m/s)
12-ft Rubber raft Without Sea Anchor	**DWL**	21	7.10	0.507	10.39	1.1 – 8.2
	+CWL	21	2.45	0.225	8.86	1.1 – 8.2
	-CWL	21	-2.45	0.225	8.86	1.1 – 8.2
12-ft Rubber raft With Sea Anchor	**DWL**	10	2.53	0.692	3.93	3.9 – 9.8
	+CWL	10	1.51	0.524	5.02	3.9 – 9.8
	-CWL	10	-1.51	0.524	5.02	3.9 – 9.8

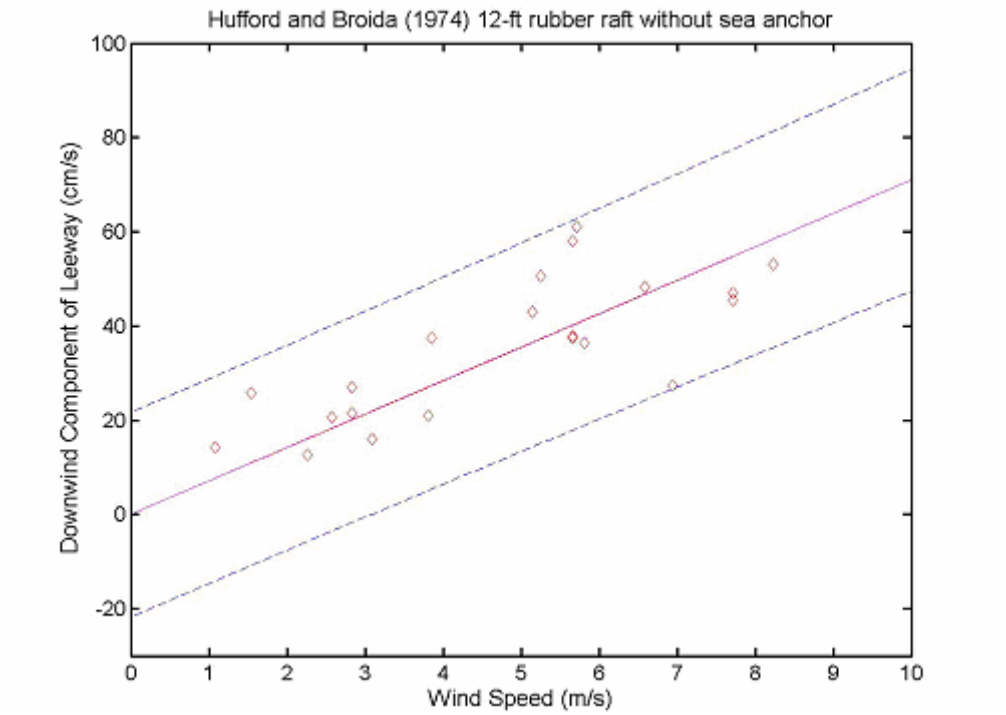

Figure B-1. Constrained linear regression and 95% prediction limits of the downwind components of leeway versus wind speed for maritime life rafts, no-ballast systems, no-canopy, without drogue, from Hufford and Broida (1974).

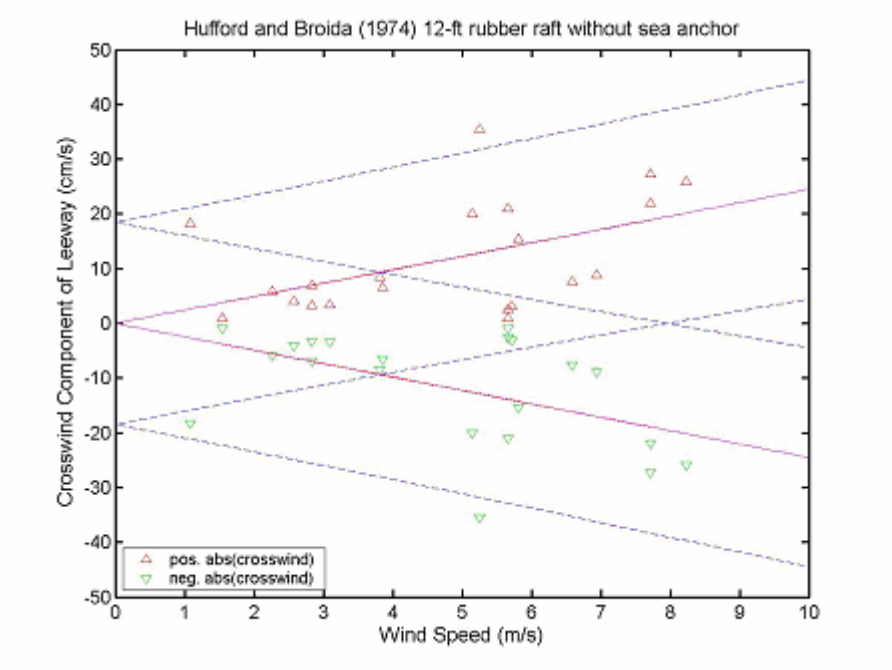

Figure B-2. Constrained linear regression and 95% prediction limits of the positive and negative crosswind components of leeway versus wind speed, maritime life rafts, no-ballast systems, no-canopy, without drogue, from Hufford and Brodia (1974).

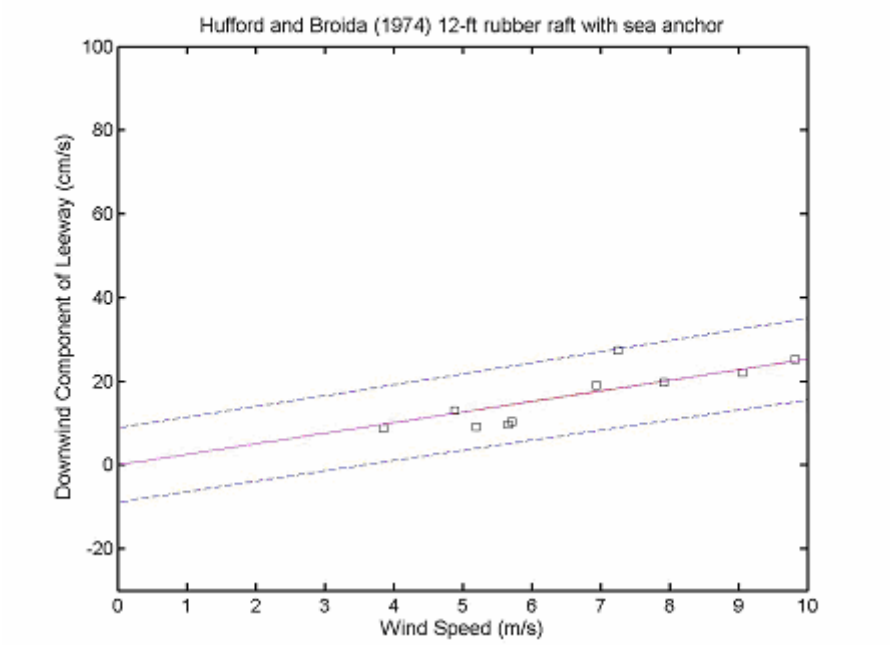

Figure B-3. Constrained linear regression and 95% prediction limits of the downwind components of leeway versus wind speed, maritime life rafts, no-ballast systems, no-canopy, with drogue from Hufford and Brodia (1974).

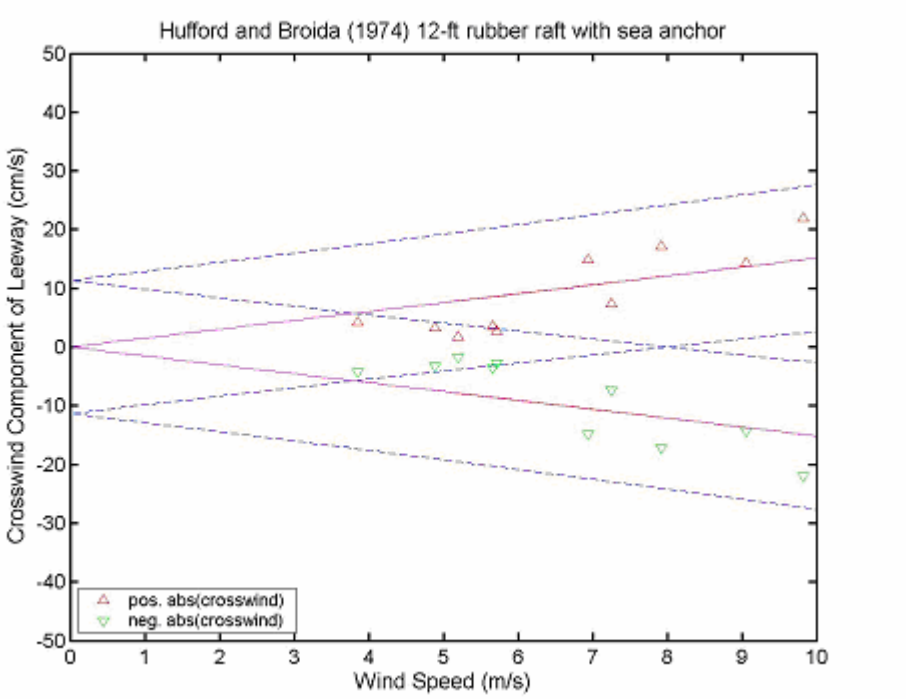

Figure B-4. Constrained linear regression and 95% prediction limits of the positive and negative crosswind components of leeway versus wind speed, maritime life rafts, no-ballast systems, no-canopy, with drogue from Hufford and Brodia (1974).

B.1.2 Maritime Life Rafts, no-ballast systems, canopy, without drogue

Three of the four categories for life rafts without ballast systems have references of leeway drift studies: Hufford and Brodia (1974) and Nash and Willcox (1991). Using the simple algebraic methods of Allen and Plourde (1999) the downwind and crosswind components of leeway for the leeway category Maritime Life Rafts, no-ballast systems, canopy, with drogue is extrapolated from the other three.

Maritime Life raft without Ballast Systems:

Without Canopy, Without Drogue	DWL 7.10 % $\mathbf{W_{10m}}$	CWL 2.45 % $\mathbf{W_{10m}}$
Without Canopy, With Drogue	DWL 2.53 % $\mathbf{W_{10m}}$	CWL 1.51 % $\mathbf{W_{10m}}$
With Canopy, Without Drogue	DWL 3.39 % $\mathbf{W_{10m}}$	CWL 1.49 % $\mathbf{W_{10m}}$

With Canopy, With Drogue

$\approx$ (2.53 % / 7.10 %) x 3.39 %

$\approx$ (1.51 % / 2.45%) x 1.49 %

$\approx$ DWL 1.21% $\mathbf{W_{10m}}$

≈ CWL 0.92% $\mathbf{W_{10m}}$

The value can now be computed for the entire class by the algebraic method.

Without Canopy, Without Drogue	DWL 7.10 % $\mathbf{W_{10m}}$	CWL 2.45 % $\mathbf{W_{10m}}$
Without Canopy, With Drogue	DWL 2.53 % $\mathbf{W_{10m}}$	CWL 1.51 % $\mathbf{W_{10m}}$
With Canopy, Without Drogue	DWL 3.39 % $\mathbf{W_{10m}}$	CWL 1.49 % $\mathbf{W_{10m}}$
With Canopy, With Drogue	DWL 1.21% $\mathbf{W_{10m}}$	CWL 0.92% $\mathbf{W_{10m}}$

≈ (2.53 + 7.10 + 3.39 + 1.21) / 4

≈ (1.51 + 2.45 +1.49 + 0.92) / 4

Maritime Life Rafts without Ballast Systems: DWL 3.56% $\mathbf{W_{10m}}$ CWL 1.59% $\mathbf{W_{10m}}$

B.2 Maritime Life Rafts with Deep Ballast Systems

Allen and Plourde (1999, Chapter 7) determined the unconstrained linear regression for 11 categories of maritime life rafts with deep ballast systems. Using the same naming conventions, data sets, and methodology, the constrained linear regressions were determined for this report.

B.2.1 Maritime Life Raft (deep ballast, canopy, without drogue, 4-6 person, light loading)

For this category, leeway data from the Tulmar life raft were combined with data from the Beaufort 5 and 6-sided life rafts. The leeway runs of the Tulmar were; 2, 3, 4, 16, 17, 19, 20 and 23 which included 1,166 ten-minute sample periods. The leeway runs of the Beaufort (5-sided) were 30, 32, 34, 35, 36, 38, 45 and 54, which included 747 ten-minute samples. The Beaufort (6-sided) runs were 44, 49 and 55, which provided 799 ten-minute samples for a total of 2,712 ten-minute samples or 18.8 days of leeway data. The results for all the data points combined equally are presented below. Regression parameters for this leeway category are listed in Table B-2.

Table B-2. Constrained linear regression of the leeway components (cm/s), 10-meter wind speed (m/s) 4-6 person life rafts, deep-ballast systems, canopy, without drogue, light loading.

Leeway Craft	Dependent Variable	# 10-min samples	Slope (% W_{10m})	r^2	$S_{y/x}$ (cm/s)	Wind Speed (m/s)
Light, without drogue	**DWL**	2712	3.53	0.91	4.60	0 - 17.4
	+CWL	1019	0.47	0.247	4.23	2.3 – 16.1
	-CWL	1693	-0.48	0.214	3.91	0 - 17.4

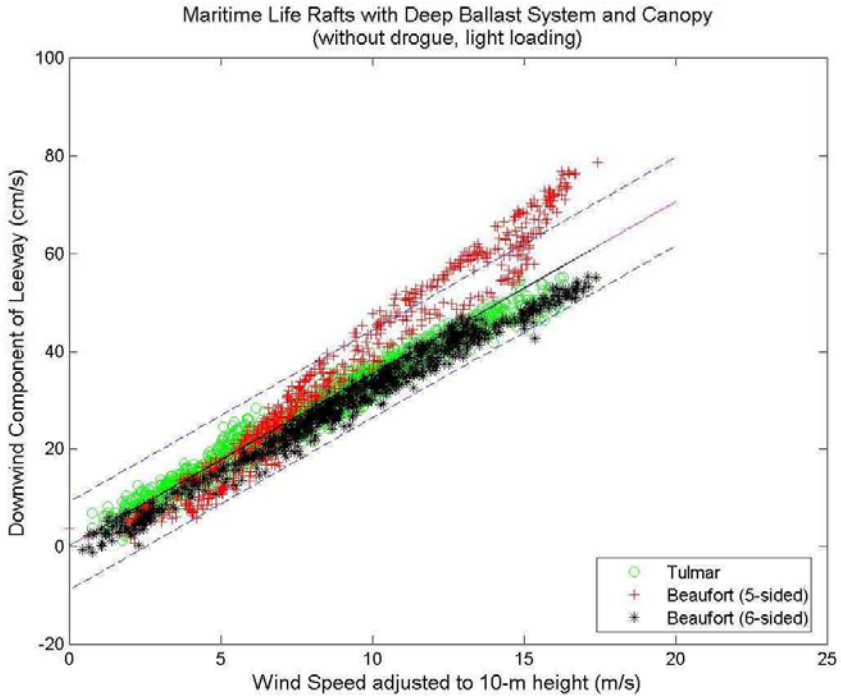

Figure B-5. Constrained linear regression and 95% prediction limits of the downwind components of leeway versus wind speed, 4-6 person maritime life rafts, deep-ballast systems, canopy, without drogue, light loading, from Allen and Plourde (1999).

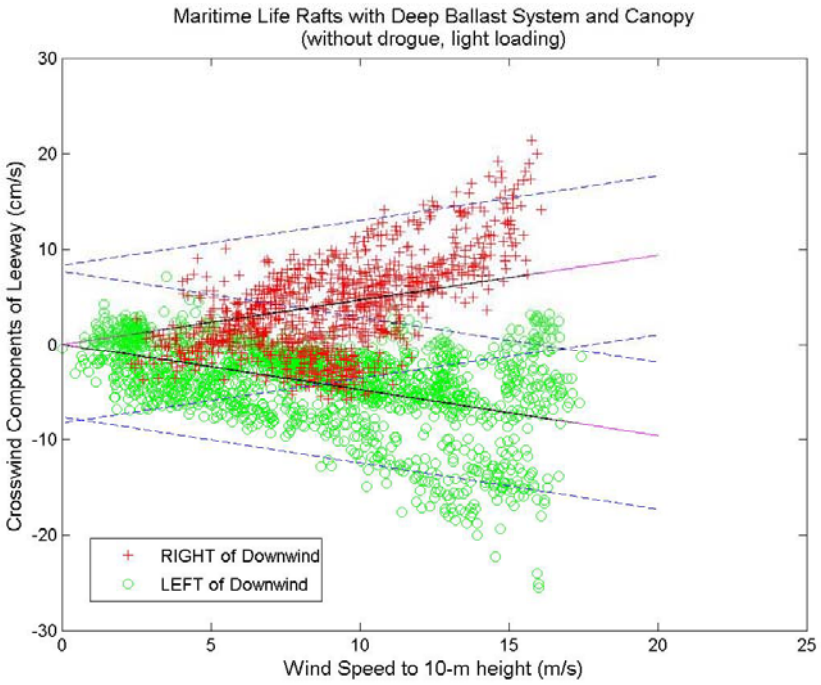

Figure B-6. Constrained linear regression and 95% prediction limits of the positive (+) and negative (o) crosswind components of leeway versus wind speed, from Allen and Plourde (1999) 4-6 person maritime life rafts, deep-ballast systems, canopy**,** without drogue, light loading.

B.2.2 Maritime Life Raft (deep ballast, canopy, w/ drogue, 4-6 person, light loading)

The data set as analyzed by Allen and Fitzgerald (1997) for the Switlik life raft "J" with a deep toroidal ballast bag was combined with run 5 of the Tulmar life raft from Fitzgerald et al. (1993). Three hundred thirty-three (333) points from run 63 of the Switlik were used for leeway speed, and 127 for leeway angle and the leeway components. From run 5 of the Tulmar, only the last 15 points were used in the analysis because there were a number of points where Smith's (1988) algorithm fails to provide a wind adjustment factor under low wind and stable conditions, rendering them not useable. The results for all data points combined equally are presented below. In Figures B-7 and B-8 the constrained linear regression of the downwind component and absolute values of the crosswind components of leeway versus $\mathbf{W_{10m}}$ are presented, along with the 95% prediction limits. In these two figures, the data are separated by life raft type. Regression parameters for this leeway category are listed in Table B-3.

Table B-3. Constrained linear regression of the leeway components (cm/s) on 10-meter wind speed (m/s) 4-6 person maritime life rafts, deep-ballast systems, canopy, with drogue, light loading.

Leeway Craft	Dependent Variable	# 10-min samples	Slope (% W_{10m})	r^2	$S_{y/x}$ (cm/s)	Wind Speed (m/s)
Light load, with drogue	**DWL**	143	1.91	0.85	3.59	6.7 - 20.4
	+CWL	143	0.30	0.12	2.19	6.7 - 20.4
	-CWL	0	-0.30	N/A	2.19	N/A

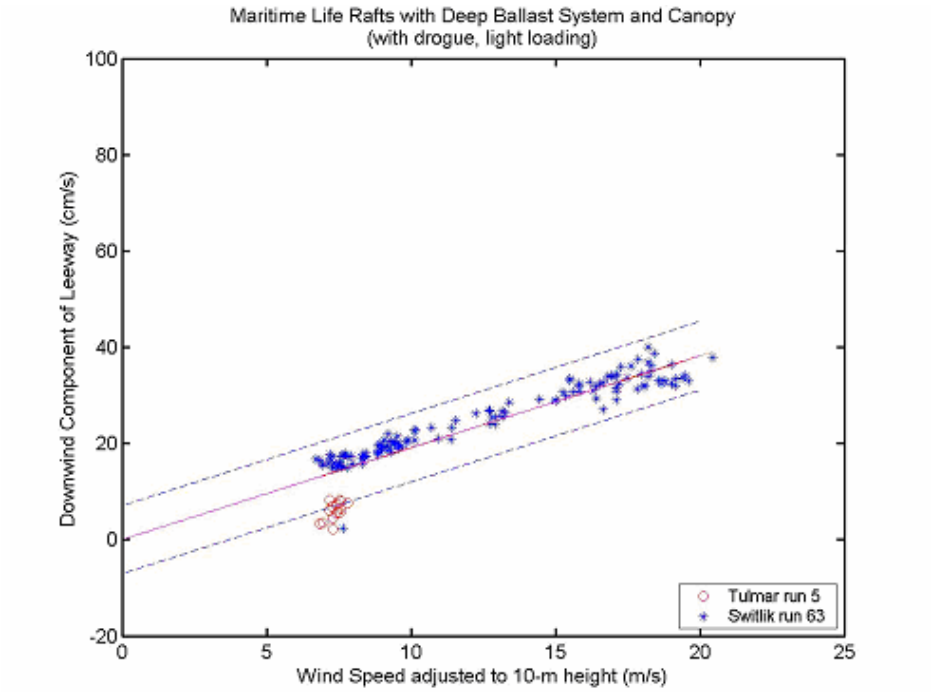

Figure B-7. Constrained linear regression and 95% prediction limits of the downwind components of leeway versus wind speed, 4-6 person maritime life rafts, deep-ballast systems, canopy, with drogue, light loading, from Allen and Plourde (1999).

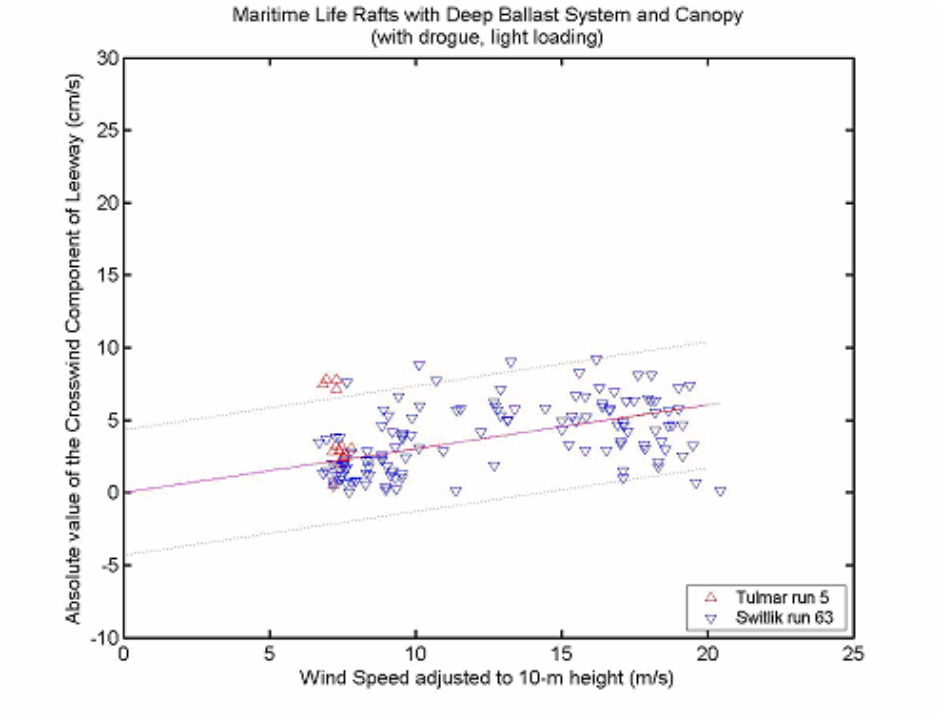

Figure B-8. Constrained linear regression and 95% prediction limits of the positive crosswind components of leeway versus wind speed, 4-6 person maritime life rafts, deep-ballast systems, canopy, with drogue, light loading, from Allen and Plourde (1999).

B.2.3 Maritime Life Raft (deep ballast, canopy, without drogue, 4-6 person, heavy loading)

Leeway data from Tulmar runs 6, 7, and 8 were combined with Beaufort (5-sided) runs of 9 and 10 after runs 9 and 10 were edited to remove winds that could not be converted to $\mathbf{W_{10m}}$ by Smith (1988). The Tulmar runs contained 104 ten-minute samples and 24 ten-minute samples were used from the Beaufort life raft for a total of 128 ten-minute samples or 21.3 hours of data. The results for all the data points combined equally are presented below. In Figures B-9 and B-10 the constrained linear regression of the downwind and crosswind component of leeway versus $\mathbf{W_{10m}}$ are presented, along with the 95% prediction limits. In these two figures, the data are separated by life raft type. Regression parameters for this leeway category are listed in Table B-4.

Table B-4. Constrained linear regression of leeway components (cm/s) on 10-meter wind speed (m/s) 4-6 person maritime life rafts, deep-ballast systems, canopy, without drogue, light loading.

Leeway Craft	Dependent Variable	# 10-min samples	Slope (% W_{10m})	r^2	$S_{y/x}$ (cm/s)	Wind Speed (m/s)
Heavy without drogue	**DWL**	128	3.35	0.94	2.67	2.2 - 12.9
	+CWL	128	0.49	0.24	1.80	2.2 - 12.9
	-CWL	0	-0.49	N/A	1.80	N/A

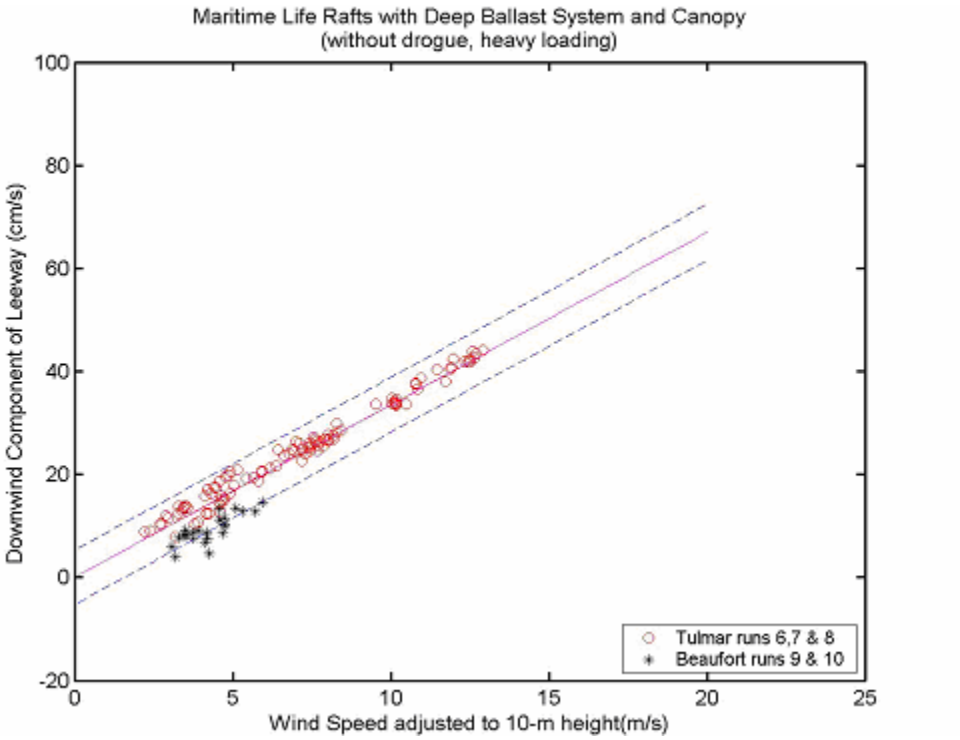

Figure B-9. Constrained linear regression and 95% prediction limits of the downwind components of leeway versus wind speed, 4-6 person maritime life rafts, deep-ballast systems, canopy, without drogue, heavy loading, from Allen and Plourde (1999).

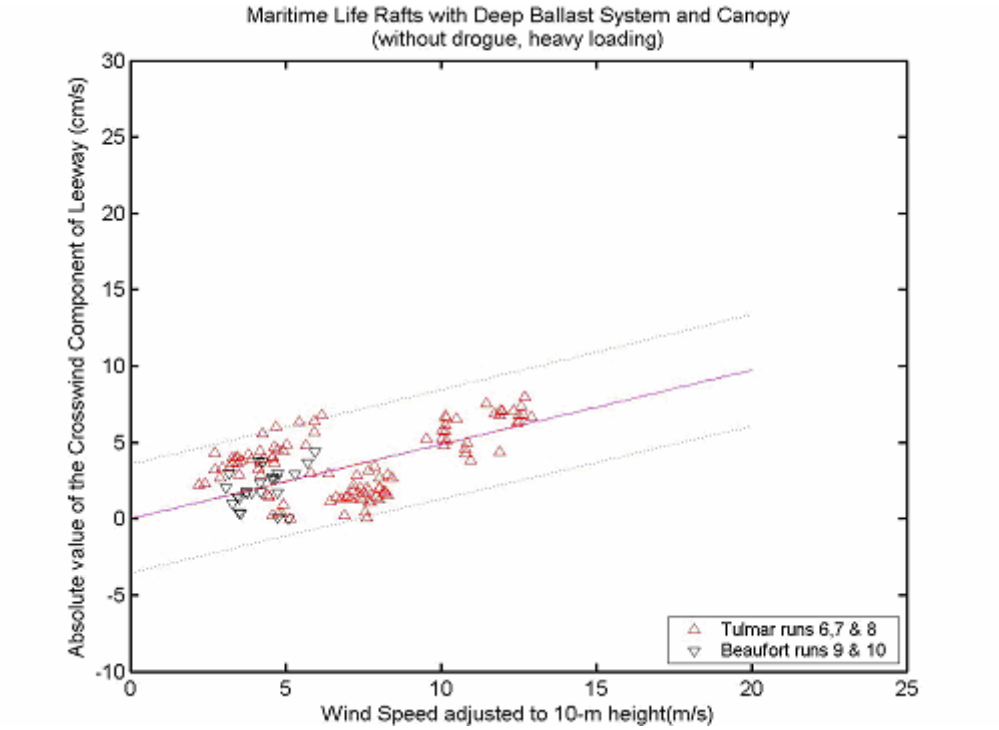

Figure B-10. Constrained linear regression and 95% prediction limits of the positive crosswind components of leeway versus wind speed, 4-6 person maritime life rafts, deep-ballast systems, canopy, without drogue, heavy loading, from Allen and Plourde (1999).

B.2.4 Maritime Life Raft (deep ballast, canopy, w/ drogue, 4-6 person, heavy loading

For this category, leeway runs 15 (138 ten-minute samples) and 22 (296 ten-minute samples) of the Beaufort (5-sided) were combined with run 24 (146 ten-minute samples) of the Tulmar life raft. Thus, leeway **speed** is based upon 580 ten-minute samples or about 4.0 days. However, run 22 was not used for leeway **angle**, **DWL** and **CWL** therefore these values are based upon 284 ten-minute samples, or about 2.0 days of data. The results for all the data points combined equally are presented below. In Figures B-11 and B-12 the constrained linear regression of the downwind and crosswind components of leeway versus $\mathbf{W_{10m}}$ are presented, along with the 95% prediction limits. In these two figures, the data are separated by life raft type. Regression parameters for this leeway category are listed in Table B-5.

Table B-5. Constrained Linear Regression of the Leeway Components (cm/s) on 10-meter Wind Speed (m/s) 4-6 person Maritime Life Rafts, deep-ballast systems, canopy, with drogue, heavy loading.

Leeway Craft	Dependent Variable	# 10-min samples	slope (% W_{10m})	r^2	$S_{y/x}$ (cm/s)	Wind Speed (m/s)
Heavy with drogue	**DWL**	284	2.08	0.96	1.05	2.0 - 11.8
	+CWL	284	0.34	0.30	3.00	2.0 - 11.8
	-CWL	0	-0.34	N/A	3.00	N/A

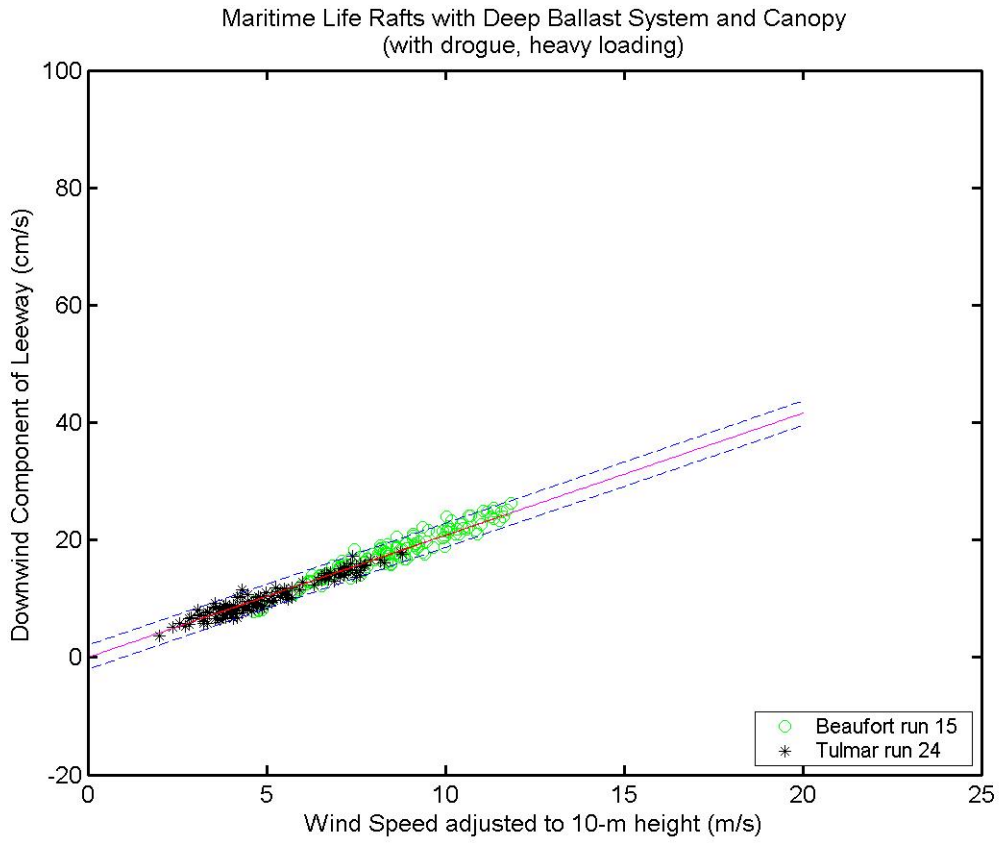

Figure B-11. Constrained linear regression and 95% prediction limits of the downwind components of leeway versus wind speed, 4-6 person maritime life rafts, deep-ballast systems, canopy, with drogue, heavy loading, from Allen and Plourde (1999).

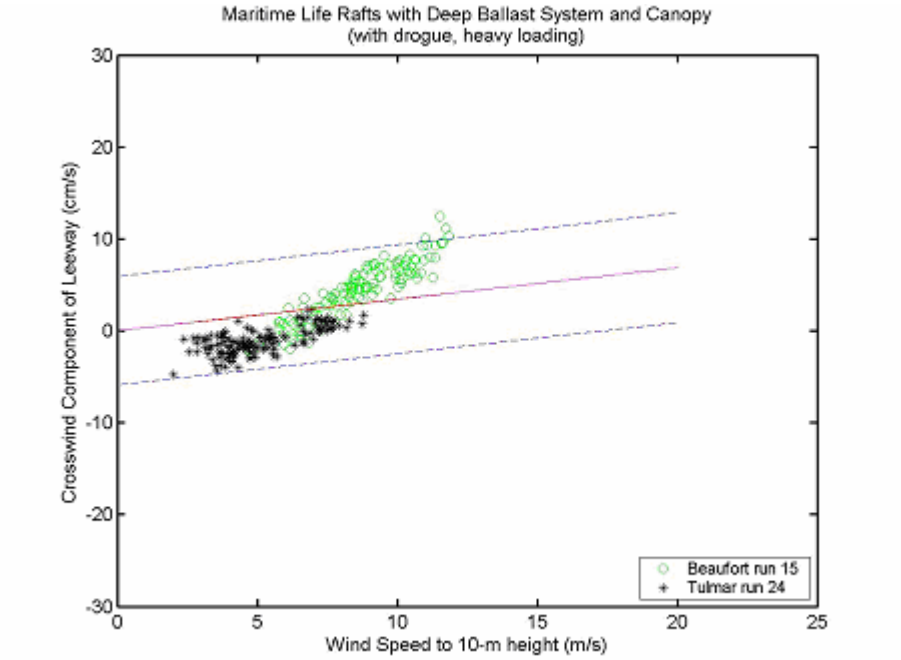

Figure B-12. Constrained linear regression and 95% prediction limits of the crosswind components of leeway versus wind speed, 4-6 person maritime life rafts, deep-ballast systems, canopy, with drogue, heavy loading, from Allen and Plourde (1999).

B.2.5 Maritime Life Raft (deep ballast, canopy, 4-6 person, with and without drogue)

The data sets for 4-6 person deep draft life rafts without drogues that were lightly and heavily loaded were combined together. There is a considerable difference between the number of data points of the lightly loaded (2712) life rafts as compared to number of data points with heavily loaded (128) life rafts. The constrained linear regression of downwind and crosswind components of leeway versus 10-m wind speed along with the 95% prediction limits are shown in Figure B-13 and Figure B-14.

Within the combined data set of lightly and heavy loaded 4-6 person deep draft life rafts with drogues, there was sufficient parity of data points that statistics would not be affected by the combination. The number of data points of the lightly loaded (349 for leeway speed, 143 for leeway angle, DWL and CWL) life rafts compared well to the number of data points for the heavily-loaded (580 and 284 respectively) life rafts. Constrained linear regression of downwind and crosswind leeway components versus 10-m wind speed are shown in Figures B-15 and B-16.

Regression parameters for both leeway categories are listed in Table B-6.

Table B-6. Constrained linear regression of the leeway components (cm/s) on 10-meter wind speed (m/s) 4-6 person maritime life rafts, deep-ballast systems, canopy, with and without drogue.

Leeway Craft	Dependent Variable	# 10-min samples	slope (% W_{10m})	r^2	$S_{y/x}$ (cm/s)	Wind Speed (m/s)
Without Drogue	**DWL**	2840	3.52	0.91	4.54	0 – 17.4
	+CWL	1147	0.47	0.25	4.05	2.2 – 16.1
	-CWL	1693	-0.48	0.21	3.91	0 - 17.4
With Drogue	**DWL**	427	2.00	0.96	1.67	2.0 - 20.4
	+CWL	427	0.30	0.32	2.97	2.0 - 20.4
	-CWL	0	-0.30	N/A	2.97	N/A

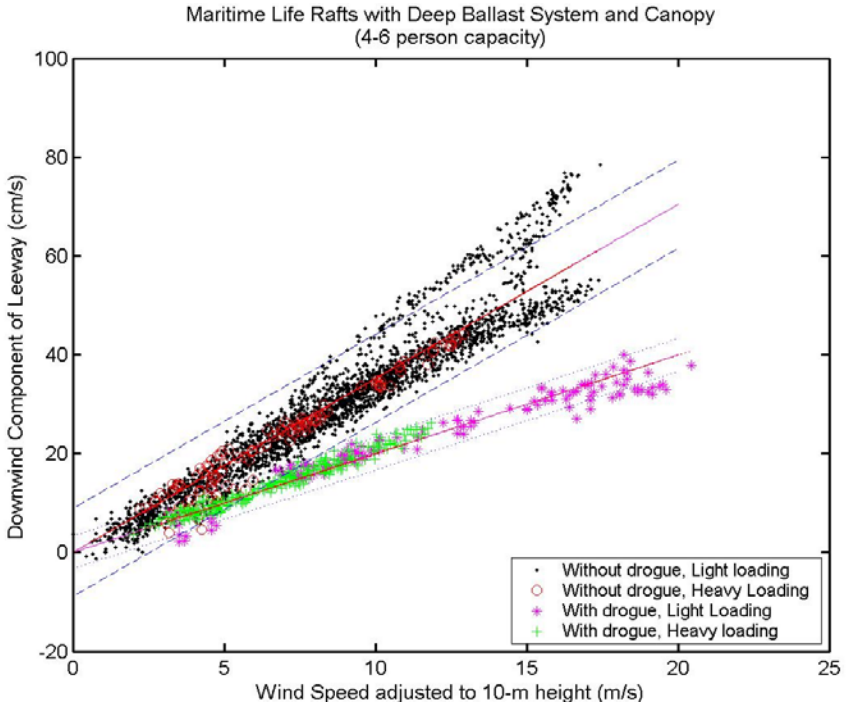

Figure B-13. Constrained linear regression and 95% prediction limits of the downwind components of leeway versus wind speed, 4-6 person maritime life rafts, deep-ballast systems, canopy, with ('+, *', lower curve) and without ('o, •' upper curve) drogue, from Allen and Plourde (1999).

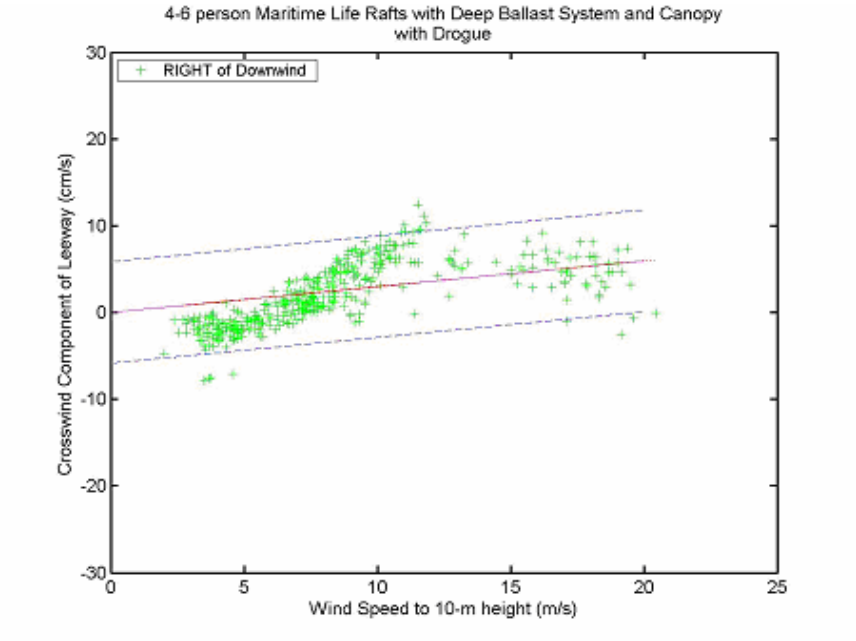

Figure B-14. Constrained linear regression and 95% prediction limits of the crosswind components of leeway versus wind speed, 4-6 person maritime life rafts, deep-ballast systems, canopy, with drogue, from Allen and Plourde (1999).

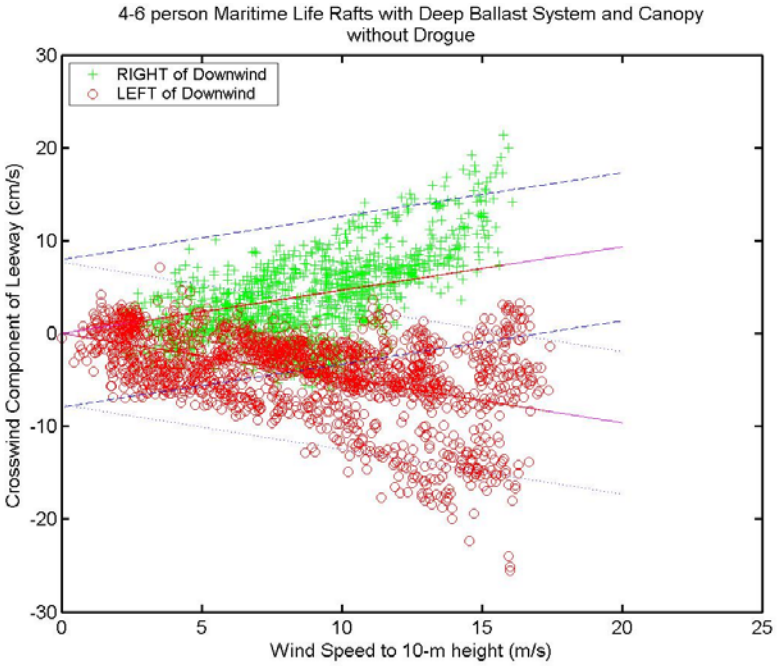

Figure B-15. Constrained linear regression and 95% prediction limits of the crosswind components of leeway versus wind speed, 4-6 person maritime life rafts, deep-ballast systems, canopy, without drogue, from Allen and Plourde (1999).

B.2.6 Maritime Life Raft (deep ballast, canopy, 4-6 person)

For this category the data sets of the four sub-categories, 4-6 person deep draft life rafts with and without drogues that were lightly and heavily loaded were combined together. This produced a data set that contained 3,769 ten-minute samples of leeway speed and 3,267 samples of leeway angle, downwind and crosswind components of leeway. This represents more than 26.2 and 22.7 days of leeway samples, respectively.

The constrained linear regression of downwind and crosswind components of leeway versus 10-m wind speed along with the 95% prediction limits are shown in Figures B-16 and B-17, respectively. For analysis purposes, drift runs were separated according to whether the total drift was positive or negative. Regression parameters for this leeway category are listed in Table B-7.

Table B-7. Constrained linear regression of the leeway components (cm/s) on 10-meter wind speed (m/s) 4-6 person maritime life rafts, deep-ballast systems, canopy, with and without drogue.

Leeway Craft	Dependent Variable	# 10-min samples	slope (% W_{10m})	r^2	$S_{y/x}$ (cm/s)	Wind Speed (m/s)
4-6 man Life Raft	**DWL**	3267	3.32	0.82	6.43	0 – 20.4
	+CWL	1574	0.42	0.26	3.86	2.0 – 20.4
	-CWL	1693	-0.48	0.21	3.91	0 - 17.4

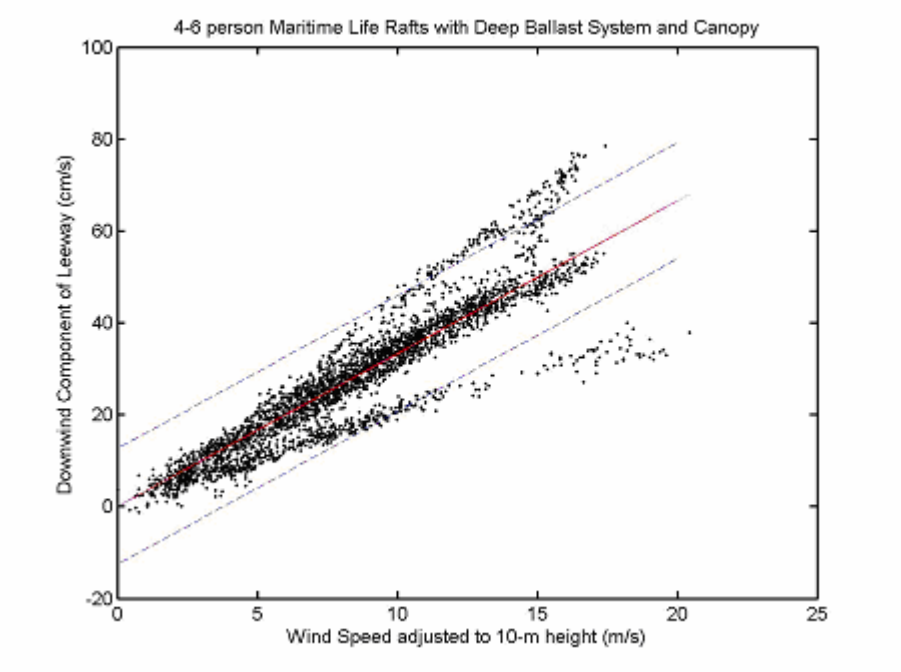

Figure B-16. Constrained linear regression and 95% prediction limits of the downwind components of leeway versus wind speed, 4-6 person maritime life rafts, with deep-ballast systems, canopies, from Allen and Plourde (1999).

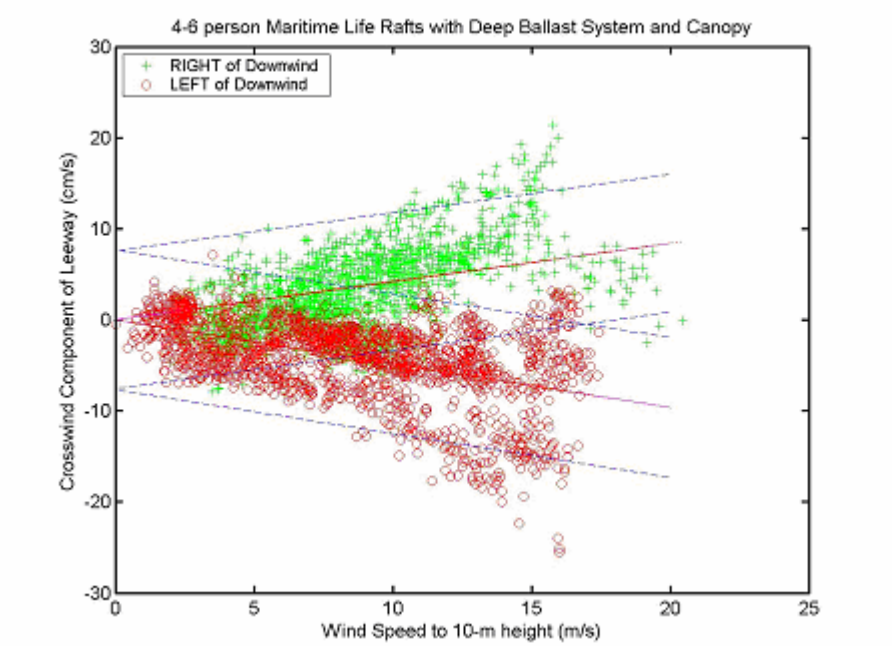

Figure B-17. Constrained linear regression and 95% prediction limits of the positive (+) and negative (o) crosswind components of leeway versus wind speed, 4-6 person maritime life rafts, with deep-ballast systems and canopies from Allen and Plourde (1999).

B.2.7 Maritime Life Raft (deep ballast, canopy, 15-25 person)

A Beaufort 20-person circular life raft was drifted six times, three times with light loading and no drogue (runs 37, 43, and 48) and three times with heavy loading with a drogue deployed (runs 40, 42, and 47). For this leeway category, there is sufficient parity between the number of data points for lightly-loaded, without drogue (816) and the number of data points for heavily-loaded, with drogue (794) that the two data sets were combined for a total of 1610 ten-minute samples, or about 11.2 days of data.

The constrained linear regressions of the downwind component of leeway versus $\mathbf{W_{10m}}$ are presented for the 15-25 person life rafts, first with light loading and without a drogue (Figure B-18), then for heavy loading with a drogue, (Figure B-19) and finally for the combined class, (Figure B-20).

The crosswind components separated by drift runs into positive and negative components and then constrained regressions against versus $\mathbf{W_{10m}}$ were determined.. The constrained linear regressions of positive and negative crosswind components of leeway versus $\mathbf{W_{10m}}$ along with the 95% prediction limits are shown for light loading, no drogue case (Figure B-21), heavy loading with a drogue (Figure B-22) and the combined case (Figure a-23).

Regression parameters for the three leeway categories for 15-25 person life rafts are listed in Table B-8.

Table B-8. Constrained linear regression of the leeway components (cm/s) on 10-meter wind speed (m/s) 15-25 person maritime life rafts, deep-ballast systems, canopy, (without drogue and light loading), (with and heavy loading), (combined).

Leeway Craft	Dependent Variable	# 10-min samples	slope (% W_{10m})	r^2	$S_{y/x}$ (cm/s)	Wind Speed (m/s)
Combined Class	**DWL**	1610	3.19	0.80	5.59	0.4 – 16.3
	+CWL	877	0.15	0.10	2.57	0.4 – 15.3
	-CWL	733	-0.34	0.20	2.67	2.3 - 16.3
W/o Drogue Light	**DWL**	816	3.62	0.93	3.16	2.0 – 16.3
	+CWL	276	0.07	0.06	2.33	2.0 – 14.1
	-CWL	540	-0.43	0.35	2.33	2.3 - 16.3
With Drogue Heavy	**DWL**	794	2.70	0.87	3.67	0.4 – 15.3
	+CWL	601	0.20	0.14	2.58	0.4 – 15.3
	-CWL	193	-0.09	0.09	1.76	5.5 – 13.5

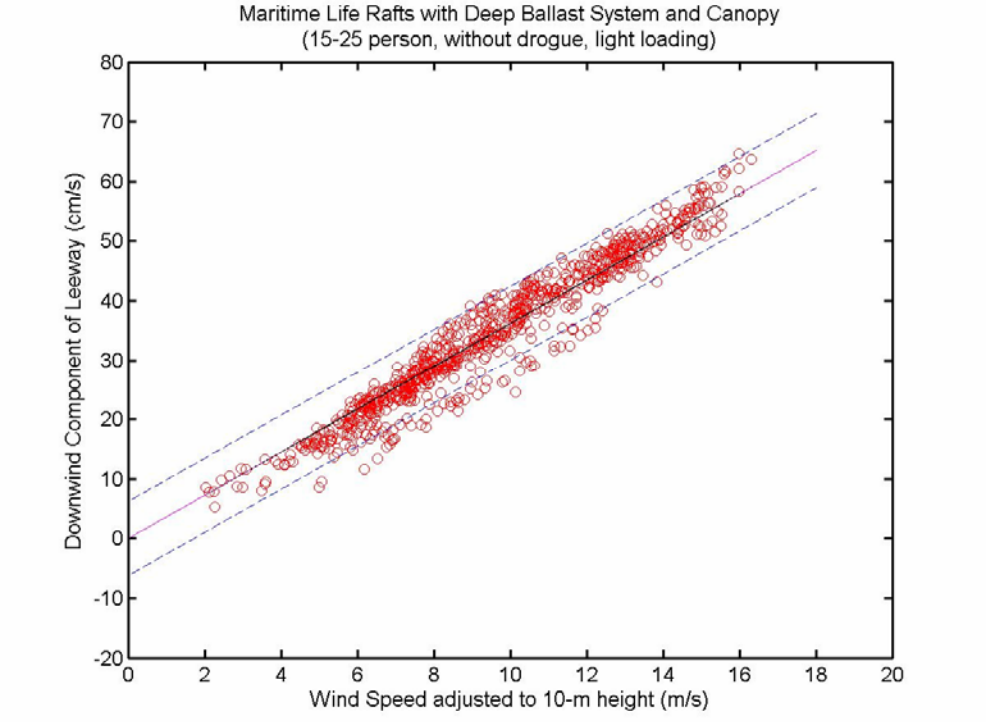

Figure B-18. Constrained linear regression and 95% prediction limits of the downwind components of leeway versus wind speed, 15-20 person maritime life rafts, with deep-ballast systems, canopies, with light loading and no drogue, from Allen and Plourde (1999).

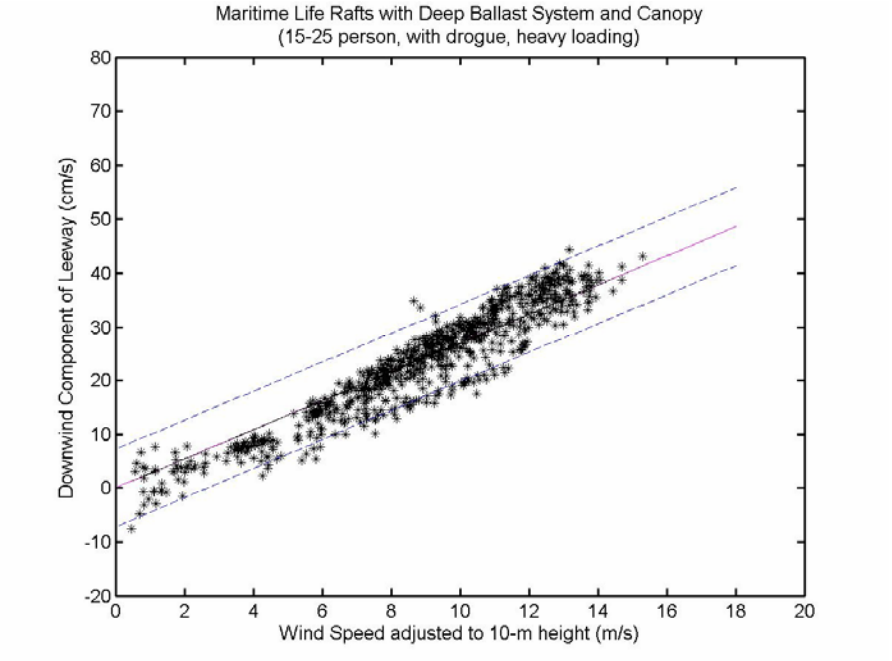

Figure B-19. Constrained linear regression and 95% prediction limits of the downwind components of leeway versus wind speed, 15-20 person maritime life rafts, with deep-ballast systems, canopies, with heavy loading and with a drogue, from Allen and Plourde (1999).

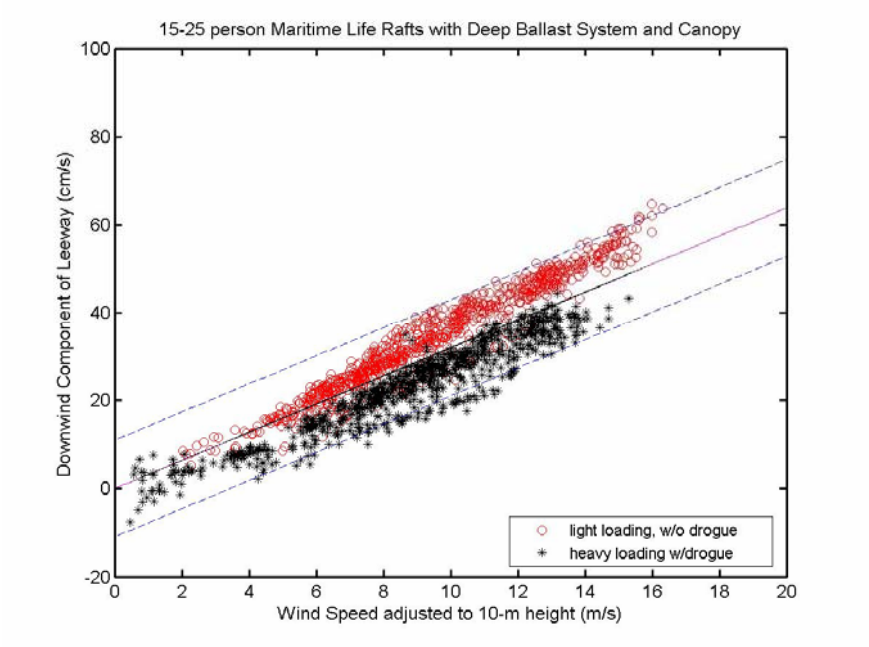

Figure B-20. Constrained linear regression and 95% prediction limits of the downwind components of leeway versus wind speed, 15-20 person maritime life rafts, with deep-ballast systems, canopies, combined class, Allen and Plourde (1999).

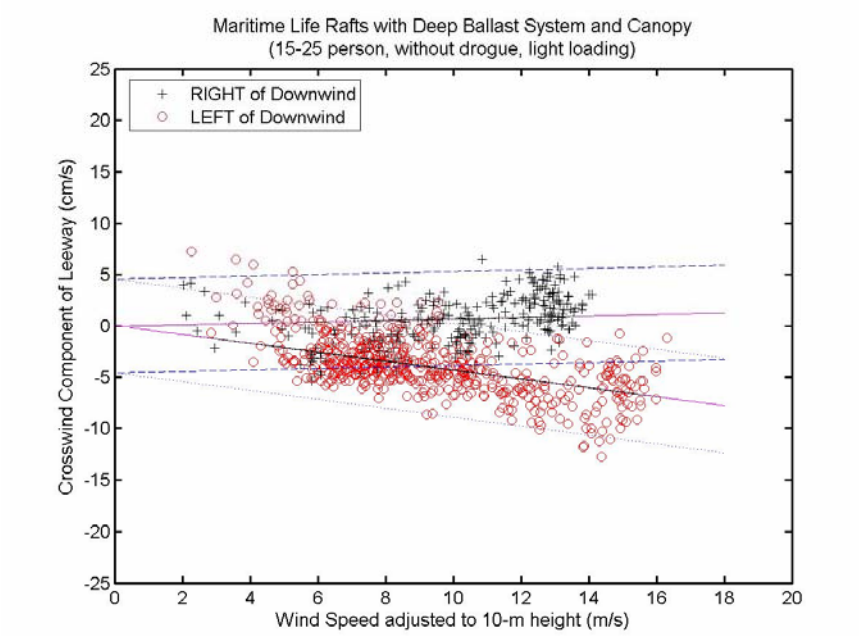

Figure B-21. Constrained linear regression and 95% prediction limits of the crosswind components of leeway versus wind speed, 15-20 person maritime life rafts, with deep-ballast systems, canopies, with light loading and no drogue, from Allen and Plourde (1999).

Figure B-22. Constrained linear regression and 95% prediction limits of the crosswind components of leeway versus wind speed, 15-20 person maritime life rafts, with deep-ballast systems, canopies, with heavy loading and with a drogue, from Allen and Plourde (1999).

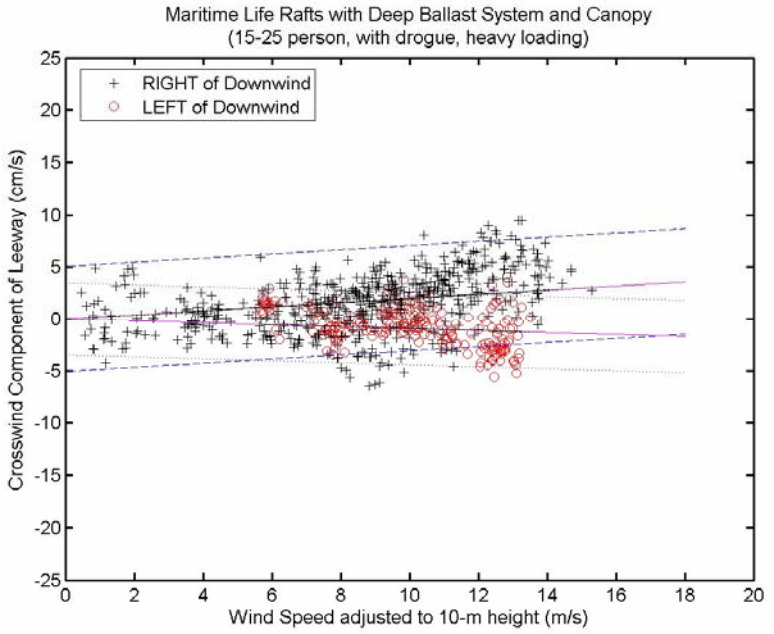

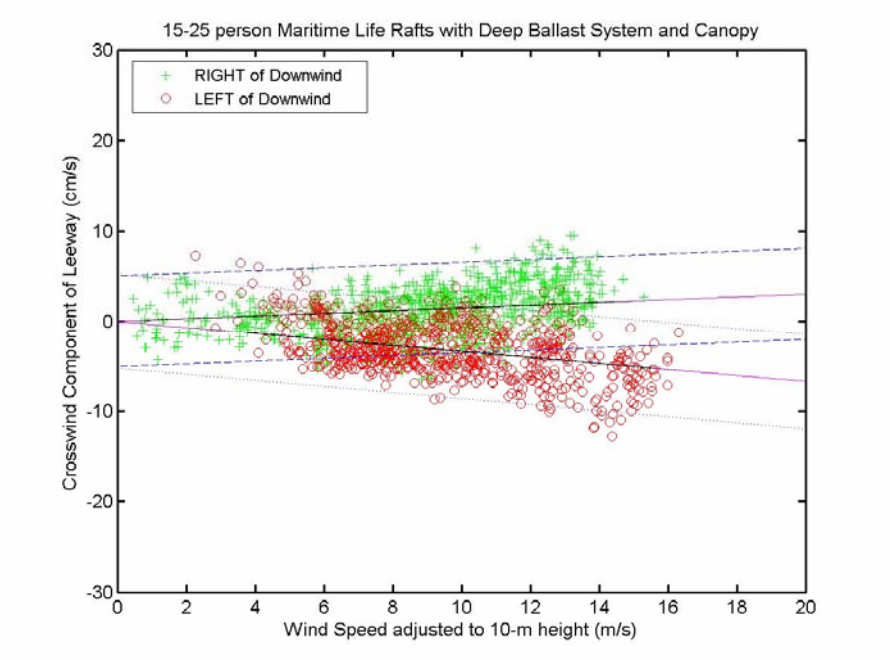

Figure B-23. Constrained linear regression and 95% prediction limits of the crosswind components of leeway versus wind speed, 15-20 person maritime life rafts, with deep-ballast systems canopies, combined class, from Allen and Plourde (1999).

B.2.8 Maritime Life Raft (deep ballast, canopy)

For this category the data sets of the six sub-categories were combined together. Four were 4-6 person deep draft life rafts with and without drogues that were lightly and heavily loaded, and two were 15-25 person life rafts heavy loaded with drogue and lightly loaded without drogue. This produced a data set containing 5,379 ten-minute leeway speed data points and 4,877 samples of leeway angle, downwind and crosswind components of leeway. This represents more than 37.4 and 33.9 days of leeway samples, respectively.

The constrained linear regression of downwind component of leeway versus 10-m wind speed along with the 95% prediction limits are shown in Figure B-24.

Crosswind components were then separated by drift runs into positive and negative crosswind components. Constrained linear regression of the positive and negative crosswind components versus 10-m wind speed along with the 95% prediction limits are shown in Figure B-25.

Regression parameters for Maritime Life rafts with deep ballasts systems and canopies are listed in Table B-9.

Table B-9. Constrained linear regression of leeway components (cm/s) on 10-meter wind speed (m/s) maritime life rafts, deep-ballast systems, canopy.

Leeway Craft	Dependent Variable	# 10-min samples	slope (% W_{10m})	r^2	$S_{y/x}$ (cm/s)	Wind Speed (m/s)
Deep Ballast rafts	**DWL**	4877	3.28	0.81	6.20	0 – 20.4
	+CWL	2451	0.32	0.19	3.66	0.4 – 20.4
	-CWL	2426	-0.43	0.20	3.64	0 - 17.43

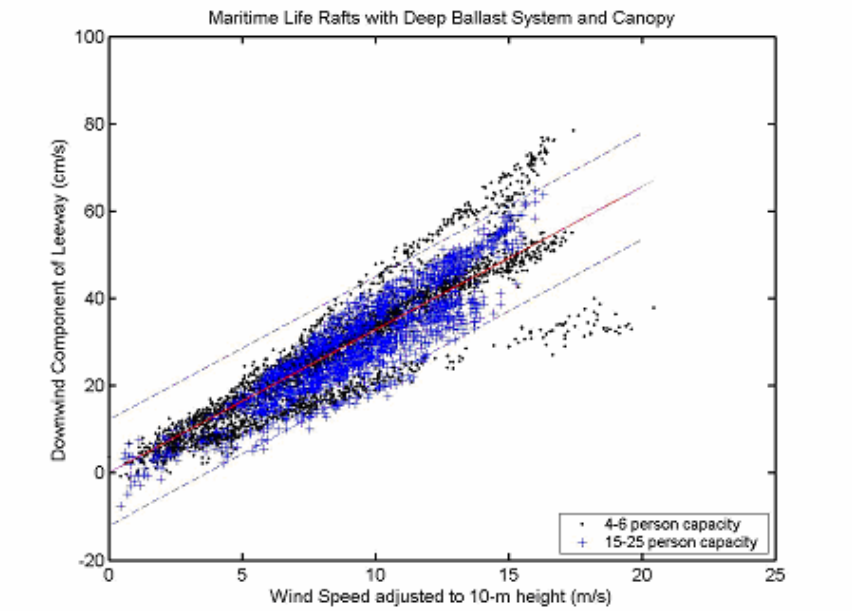

Figure B-24. Constrained linear regression and 95% prediction limits of the downwind components of leeway versus wind speed, maritime life rafts, with deep-ballast systems canopies, combined class, from Allen and Plourde (1999).

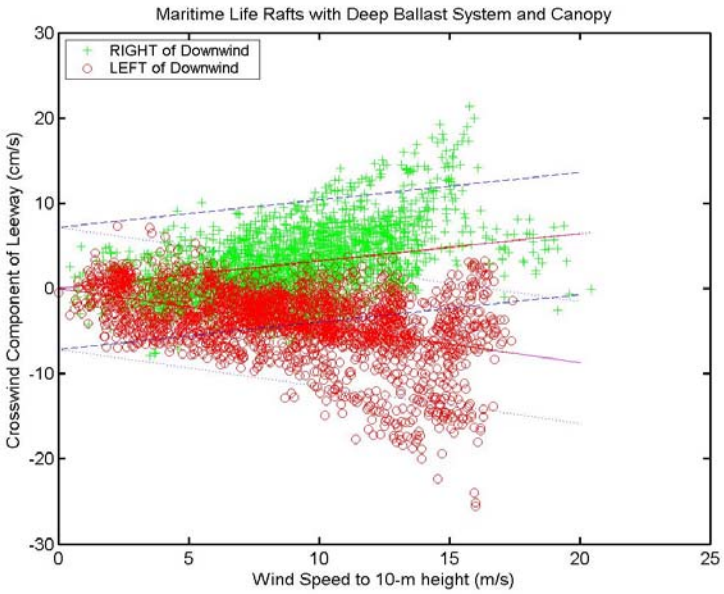

Figure B-25. Constrained linear regression and 95% prediction limits of the crosswind components of leeway versus wind speed, maritime life rafts, with deep-ballast systems canopies, combined class, from Allen and Plourde (1999).

(This page intentionally left blank.)

APPENDIX C

STATISTICAL COMPARISON OF EXPERIMENTAL DATA WITH 0 – MODEL AND Y- MODEL GENERATED PREDICTIONS

This appendix provides additional statistical comparisons of the experimental leeway data and 0-Model and Y-Model predictions for Maritime Life Rafts with Deep Ballast Systems and Canopies. These comparisons are presented as an extension of the analysis in Section 4.2 to show the performance of the 0-Model and Y-Model in predicting leeway at both low and high wind speeds. In the following comparisons the experimental leeway data are presented in blue, the 0-Model predictions in red and the Y-Model predictions in green. The number of replications generated for each model is 1000.

In Figure C-1, we show slices of the 0-Model (a) and the Y-Model (b) at 2 m/s intervals of wind. The leeway data have been grouped by wind speed plus and minus 0.5 m/s about each of these two-meter per second wind intervals to provide comparisons. A listing of the number of 10-minute wind/leeway samples in each slice is given in Table C-1.

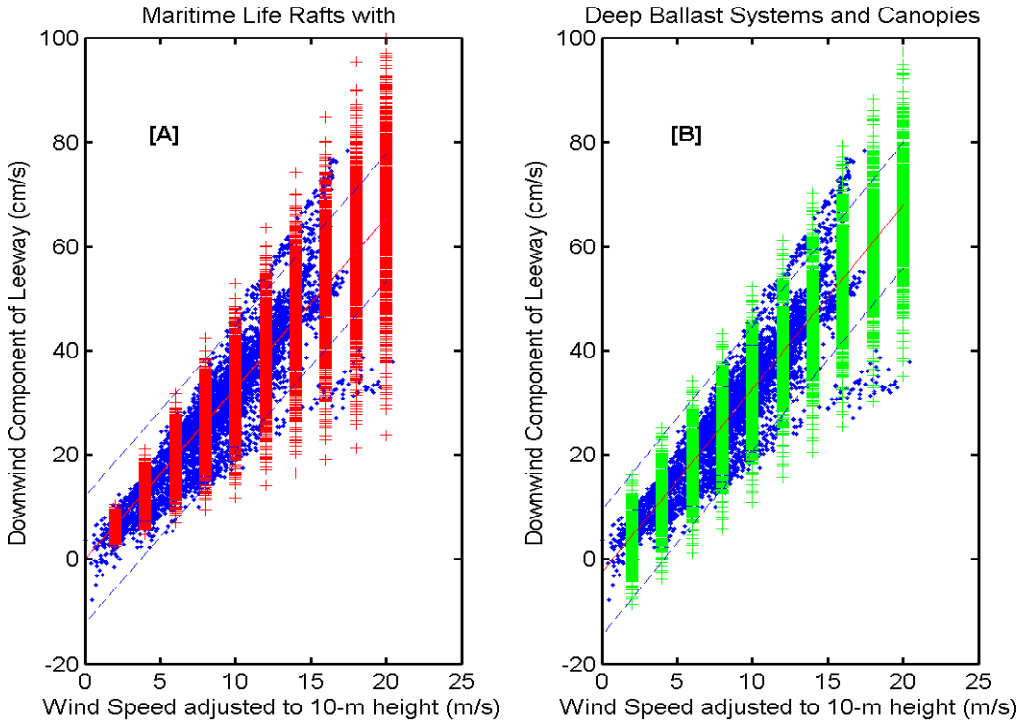

Figure C-1. Downwind leeway data (blue) from maritime life rafts with deep ballast system and canopies versus 10-meter wind speed; (A) compared with 1000 0-Model (red), and (B) with 1000 Y-Model (green) generated leeway equation values at 2, 4, 6, 8, 10, 12, 14, 16, 18, and 20 m/s of wind.

Table C-1. Summary of Wind Speed Slices for Maritime Life Rafts with Deep Ballast System and Canopies.

Wind Range (m/s)	# of 10-min. samples Life Rafts w/ Deep Ballast Systems & Canopies
3.5 – 4.5	264
5.5 – 6.5	361
7.5 – 8.5	557
9.5 - 10.5	489
11.5 - 12.5	303
13.5 – 14.5	166

From these "slices," we generate a series of statistical plots comparing the models' leeway values at given wind speed with the actual leeway values with 0.5 m/s of that wind speed. Histograms (Figures C-2 and C-3) provide cross-sectional views of the distributions. The paired histograms show both models doing reasonably well at reproducing the leeway data distributions for winds 6 m/s and higher. Figure C-2 (a) shows that the 0-Model (shown in red) would overestimate the downwind leeway at 4 m/s compared with the values observed from the field tests (shown in blue), while the Y-Model (green bars) has a spread that encompasses the leeway data (blue bars) at 4 m/s (figure C-2 (d)). It should be noted that for these histograms the models' data set was sub-selected to equal that of the experimental data subset, so that each paired histogram would have an equal number of values.

The notched whisker-box plots Figures C-4 show the median value, the horizontal red line, the 25^{th} and 75^{th} percentiles of the sample, with the "whiskers" showing the extent of the rest of the samples. Any values greater than 1.5 of the inter-quartile range are considered outliers and are shown as red pluses. The notches define the confidence interval about the median. When viewed side-by-side, notched whisker box plots are the graphical equivalent of a "T-test," comparing the mean of one population to the mean of another population. The results of the T-test between the experimental data and 0-model predictions at the 95% confidence level are shown on the y-axis (where 1 fails (means not equal) and 0 passes the T-test (means equal)). The T-tests results are tabulated in Table C-2. One advantage of this type of plot over the paired histograms is that the full 1000 values from the each model are included.

The whisker-box plots show the Y-Model doing a better job at covering the mean, middle 50%, and the range of leeway values than the 0-Model for winds from 4 to 10 m/s. Above 10 m/s wind, the 0-Model spread covers the leeway data better between the 25 and 75% percentile levels and also at the extremes. However, the 0-Model clearly overestimates the leeway data at the lower wind speeds, (4 and 6 m/s). The T-tests support these comparisons, indicating that the Y-Models' means are not significantly different from the data's means between 6 and 12 m/s, while the means for the 0-Model are equivalent to the data only for winds between 10 and 12 m/s.

The vertical separation of overlaid Empirical Cumulative Distribution Function (CDF) plots graphically represent the Kolmogorov-Smirnov statistic for comparing the distributions between two samples. When two distributions are the same at 95% confidence level for the Kolmogorov-Smirnov test, h = 0, and when they are different, h = 1. The Kolmogorov –Smirnov statistic is

the maximum difference over all values. Figure C-5 shows the CDF plots for the downwind leeway data (blue) from the Deep-ballasted life rafts with canopies, the 0-Model (red) and the Y-Model (green), for the 6 wind slices. The Kolmogorov-Smirnov test is also shown in the plots and again in Table C-3.

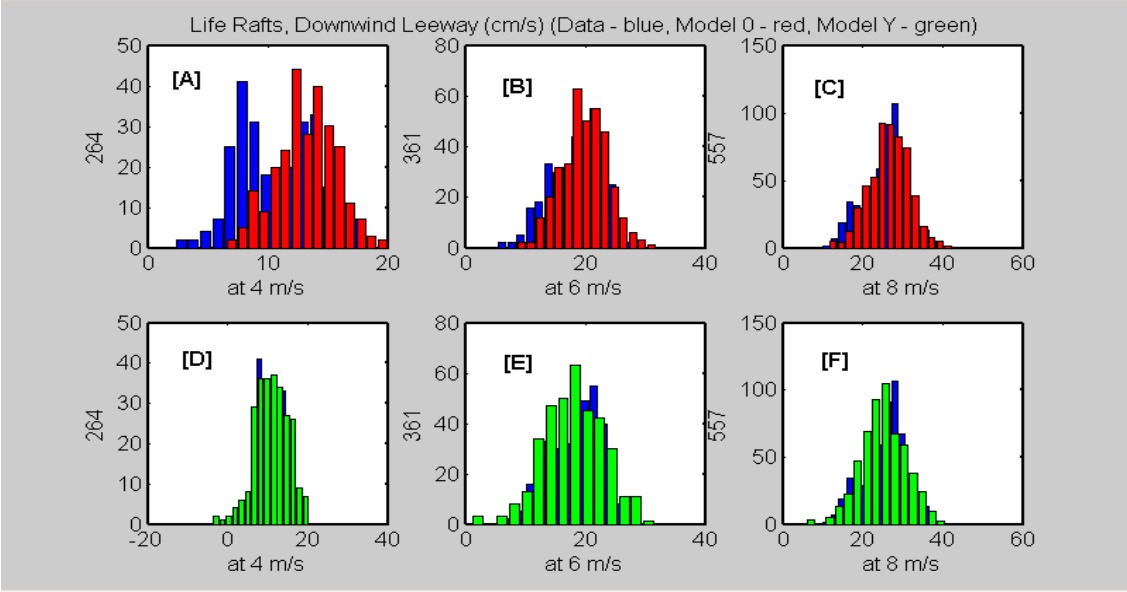

Figure C-2. Histograms of downwind leeway data (blue) of maritime life rafts with deep ballast system and canopies with histograms with (A, B, C) 0-Model (red), and (D, E, F) with Y-Model (green) generated leeway equations leeway values at 4, 6, and 8 m/s of wind. The number of data points and equal number of model values are listed on the y-axis.

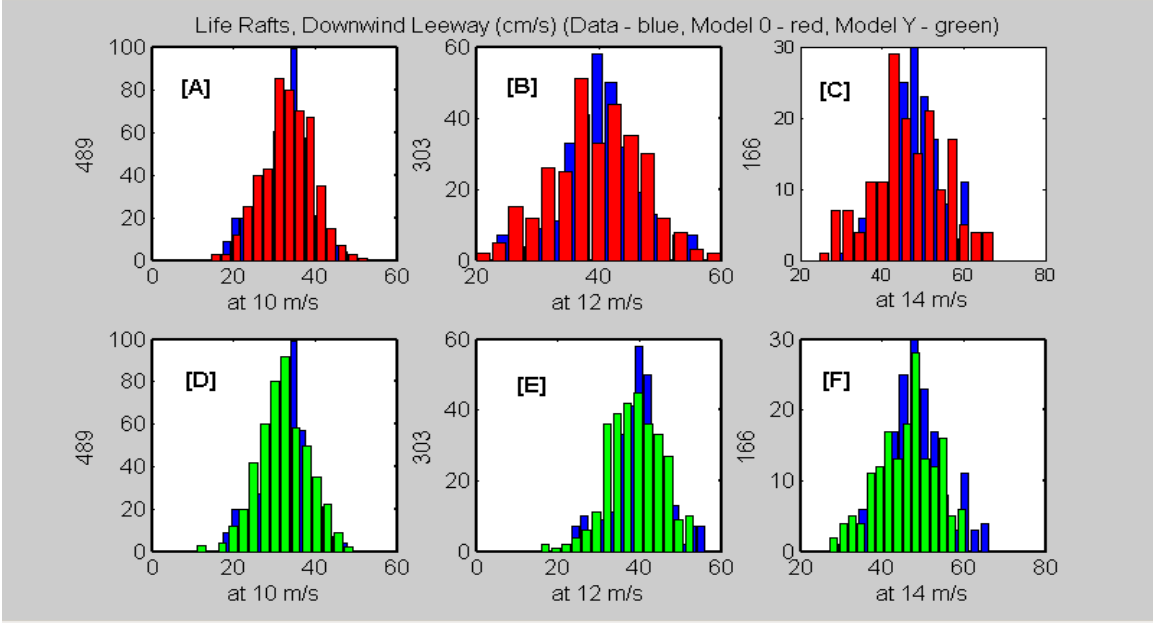

Figure C-3. Histograms of downwind leeway data (blue) of maritime life rafts with deep ballast system and canopies with histograms with (A, B, C) 0-Model (red), and (D, E, F) with Y-Model (green) generated leeway equations leeway values at 10, 12, and 14 m/s of wind. The number of data points and equal number of model values are listed on the y-axis.

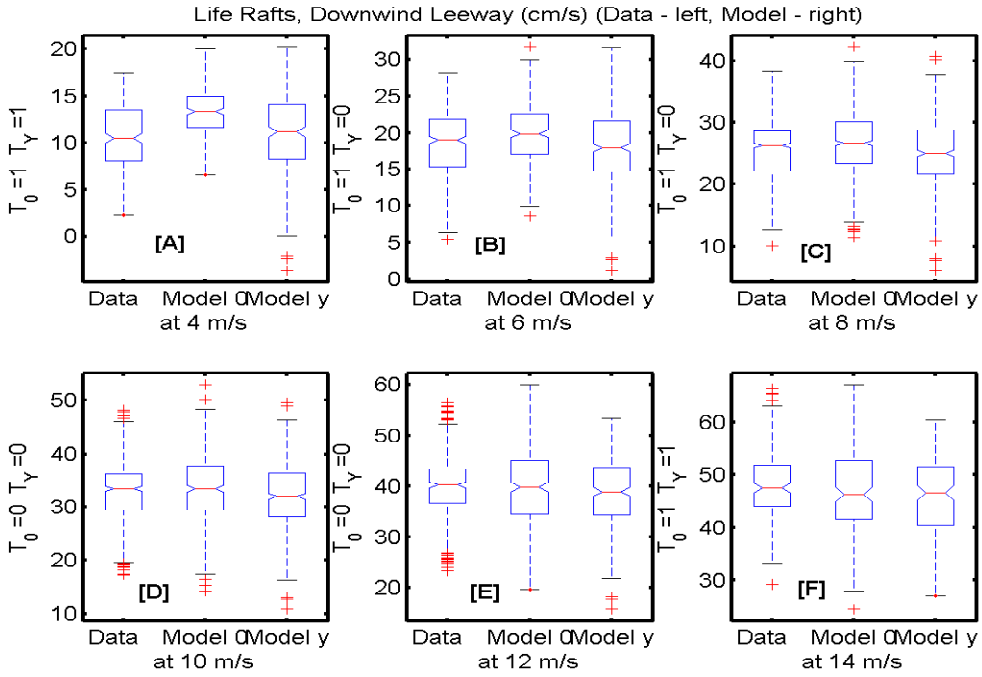

Figure C-4. Box plots of downwind leeway data (left) of maritime life rafts with deep ballast system and canopies; 0-Model (center), and Y-Model (right) generated leeway equations leeway values at (A) 4, (B) 6, (C) 8, (D) 10, (E) 12, and (F) 14 m/s of wind. Results of the T-Test are shown along the y-axis.

Table C-2. Summary of T-tests for Models of Downwind Components of Leeway for Maritime Life Rafts with Deep Ballast System and Canopies at different Wind Speed Slices.

Wind Range (m/s)	O-Model	Y-Model
3.5 – 4.5	1	1
5.5 – 6.5	1	0
7.5 – 8.5	1	0
9.5 - 10.5	0	0
11.5 - 12.5	0	0
13.5 – 14.5	1	1

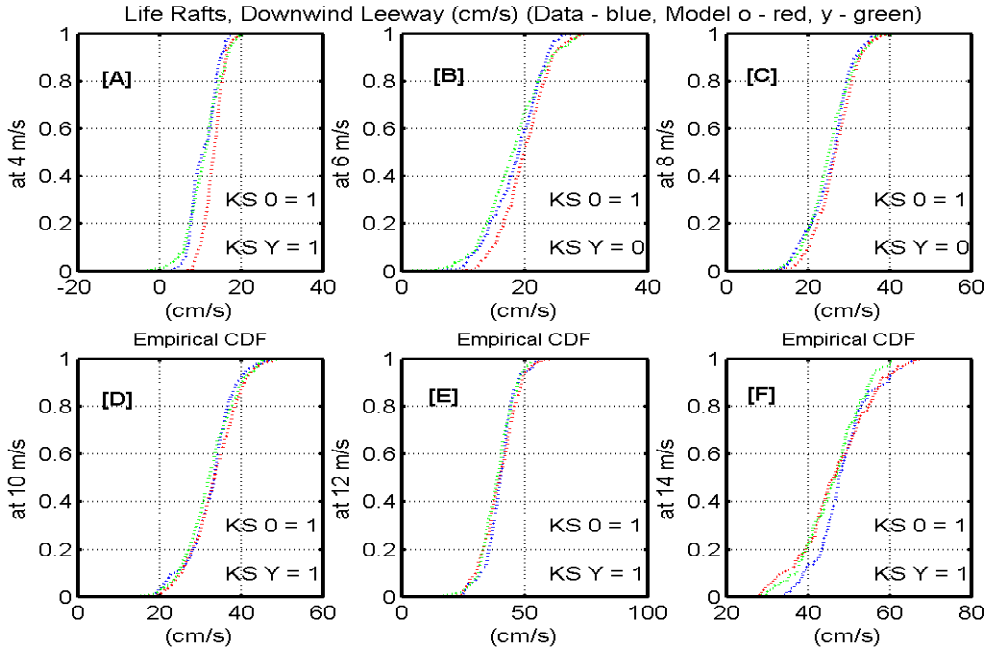

Figure C-5. Plot of empirical cumulative distributions functions (cdf) of downwind leeway (cm/s) data (blue) of maritime life rafts with deep ballast system and canopies; 0-Model (red), and Y-Model (green) generated leeway equations leeway values at (A) 4, (B) 6, (C) 8, (D) 10, (E) 12, and (F) 14 m/s of wind.

The CDF plots and the Kolmogorov-Smirnov tests indicate again that the Y-Model does a slightly better job at generating leeway values that are distributed similarly to the original leeway data than the 0-Model.

Table C-3. Summary of Kolmogorov-Smirnov tests for models of downwind components of leeway for maritime life rafts with deep ballast system and canopies at different wind speed slices.

Wind Range (m/s)	O-Model	Y-Model
3.5 – 4.5	1	1
5.5 – 6.5	1	0
7.5 – 8.5	1	0
9.5 - 10.5	1	1
11.5 - 12.5	1	1
13.5 – 14.5	1	1

In summary, the three methods of statistical analysis comparisons presented here show that though the 0-Model converges to zero, it doesn't cover the data distribution at low wind speeds as well as the Y-Model. Overall, the Y-Model does a slightly better job than the 0-Model covering the data (particularly at low wind speeds).

APPENDIX D

RESULTS OF ANALYSIS OF CROSSWIND COMPONENT SIGN CHANGES FOR FOUR CATEGORIES OF LEEWAY OBJECTS

D.1 5.5-Meter Open Skiff

Progressive Vector Diagrams (PVDs) of the downwind and crosswind components of leeway were plotted for the seven drift-runs of the 5.5 m open skiff. (The drift runs for *all* leeway drift objects were consecutively numbered during the Canadian/US leeway field tests (Fitzgerald, et al., 1994), and that numbering is retained here.) Of the seven drift-runs, PVD plots and analyses are shown here only for those runs where at least one change in CWL was noted.

Drift run 60 contained four distinct, significant changes in sign of the crosswind leeway component, as shown by the arrows in Figure D-1. The corresponding time series of the crosswind component of leeway and the 10-meter wind speed are shown in Figure D-2. Vertical dashed lines indicate the time of the four CWL sign changes. The 10-meter wind speeds at the time of these changes in CWL were 16.7 18.3, 19.6 and 18.1 m/s.

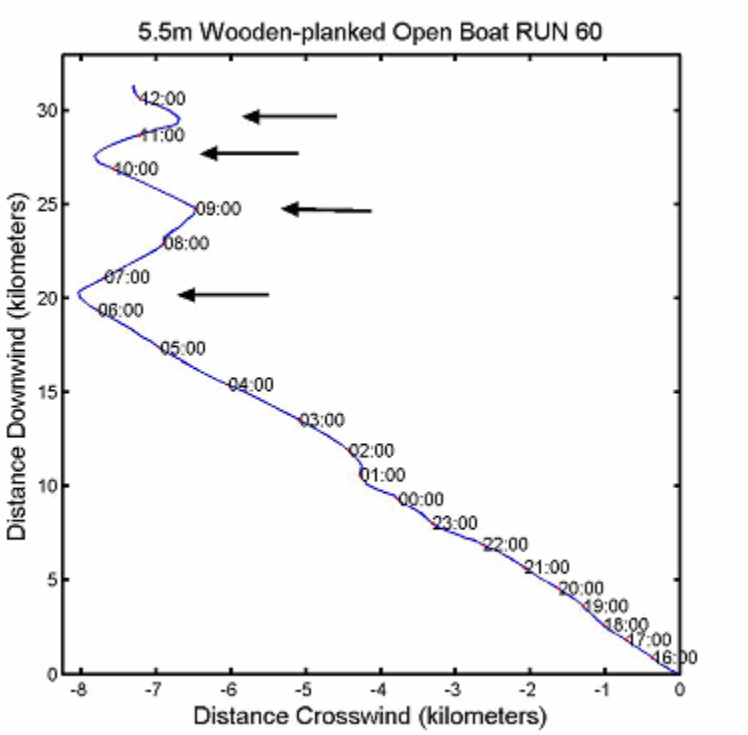

Figure D-1. Progressive Vector Diagram of the leeway displacement vectors for Drift Run 60, 5.5 m open V-hull skiff starting at 15:00, 26 November 1995. Times of day are marked along the PVD.

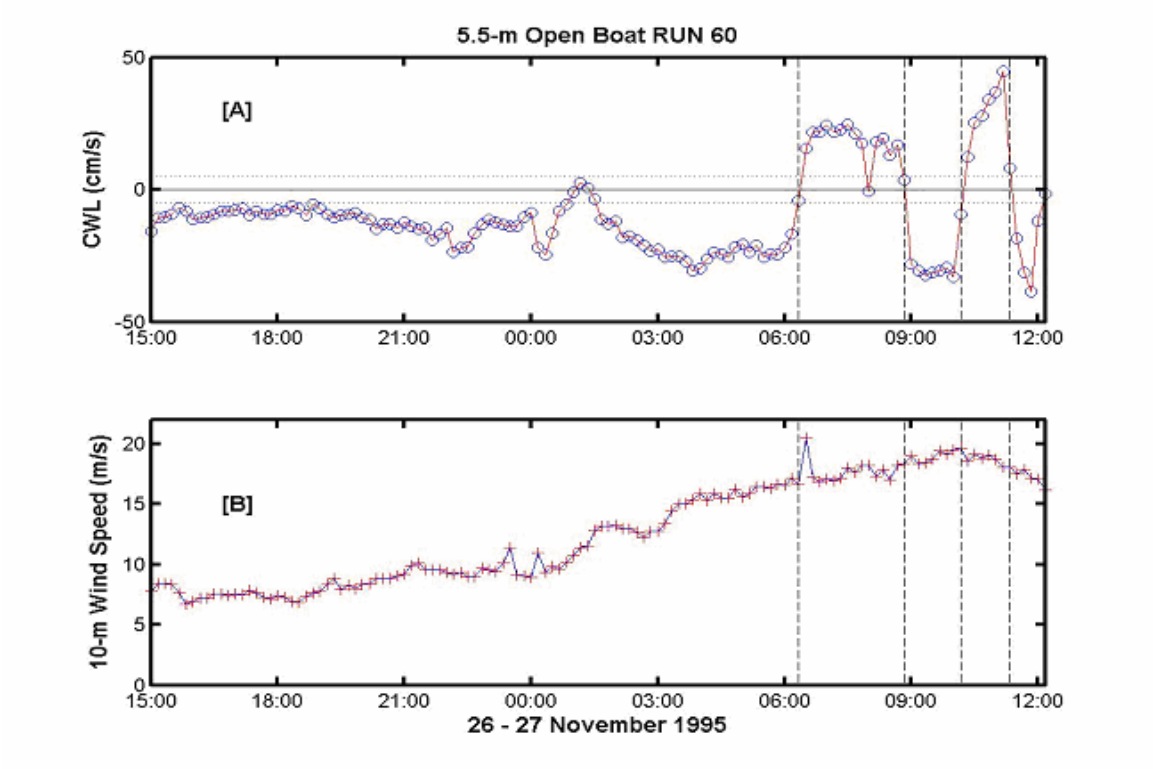

Figure D-2. Time series of [A] the crosswind component of leeway (cm/s) and [B] the wind speed adjusted to the 10-meter height, during drift run 60, 5.5 m open boat. Vertical-dashed lines indicate CWL sign changes.

Four additional leeway drift runs (21, 31, 46, and 52) contained twelve total changes in sign of the crosswind leeway component that were less pronounced than those observed during drift run 60. The arrows in Figure D-3 indicate changes in the sign of CWL during leeway drift runs 21, 31, 46, and 52. The corresponding time series of the CWL and the 10-meter wind speed are shown in Figures D-4 through D-7. Vertical dashed lines indicate the times of the twelve CWL sign changes (seven for Run 21, one for Run 31, one for Run 46, and three for Run 52). The 10-meter wind speeds at time of these changes in CWL were 2.3, 4.9, 6.5, 3.1, 4.2, 4.1, 0.3, 5.5, 7.0, 11.2, 6.5, and 7.4 m/s; all considerably lower than wind speeds of Run 60.

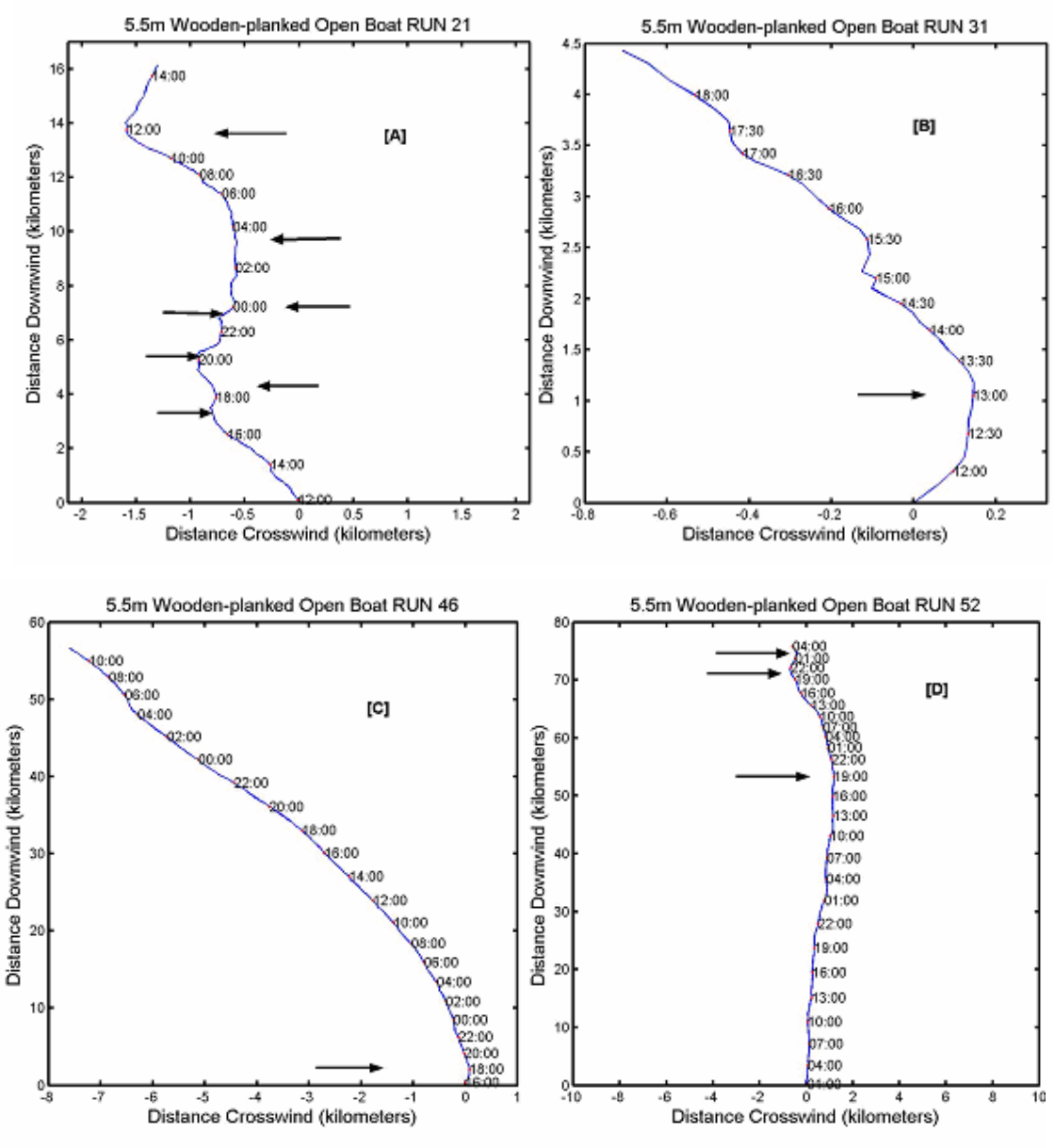

Figure D-3 Progressive Vector Diagrams of the leeway displacement vectors for Drift Runs [A] 21, [B] 31, [C] 46, and [D] 52; 5.5 m open V-hull skiff on 21 (Run 27) and 25 (Run 33) August, 1993. Times of day are marked along the PVDs.

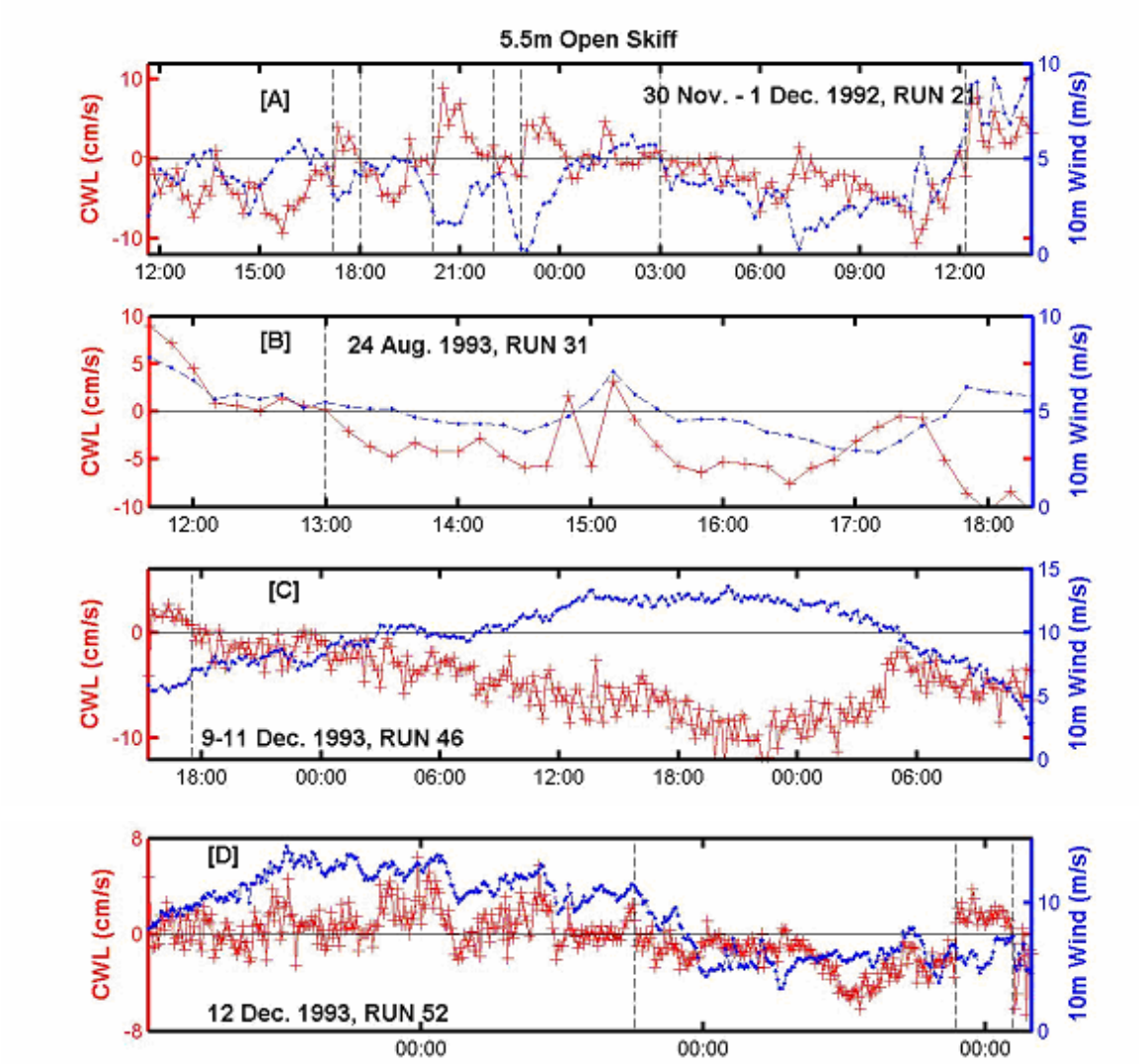

Figure D-4. Time series of the crosswind component of leeway (cm/s) (red crosses) and the wind speed adjusted to the 10-meter height (m/s) (blue dots), during drift run [A] 21, [B] 31, [C] 46, and [D] 52 of the 5.5m open skiff. Vertical-dashed lines indicate the CWL sign changes.

D.2 Person Life Rafts (Deep Ballast Systems, Canopy)

Three separate 4-6 person life rafts with deep ballast system and canopies were studied by Fitzgerald, Finlayson, and Allen (1994); and Allen and Plourde (1999). For this general leeway category, the life rafts were lightly or heavy loaded and with or without a drogue. A total of 656.0 hours of leeway data that resolved the crosswind component of leeway was collected on this category. Progressive Vector Diagrams of the downwind and crosswind components of leeway were plotted for the 31 drift runs of the 4-6 person life rafts. Of these, seven runs were identified as having significant sign changes in the crosswind component of leeway.

During Drift run 38, a lightly–loaded Beaufort 4-person, 5-sided life raft with no drogue attached, there was a significant change in the crosswind component of leeway at 1930Z on 29 November 1993, as shown in Figure D-6. The arrow in Figure D-5 indicates the distinct changes in sign of CWL during leeway drift run 38. The corresponding time series of the crosswind component of leeway and the 10-meter wind speed are shown in Figure D-7. A vertical dash line indicates the time of the CWL sign changes. The 10-meter wind speed at time of this change in CWL was 15.1 m/s.

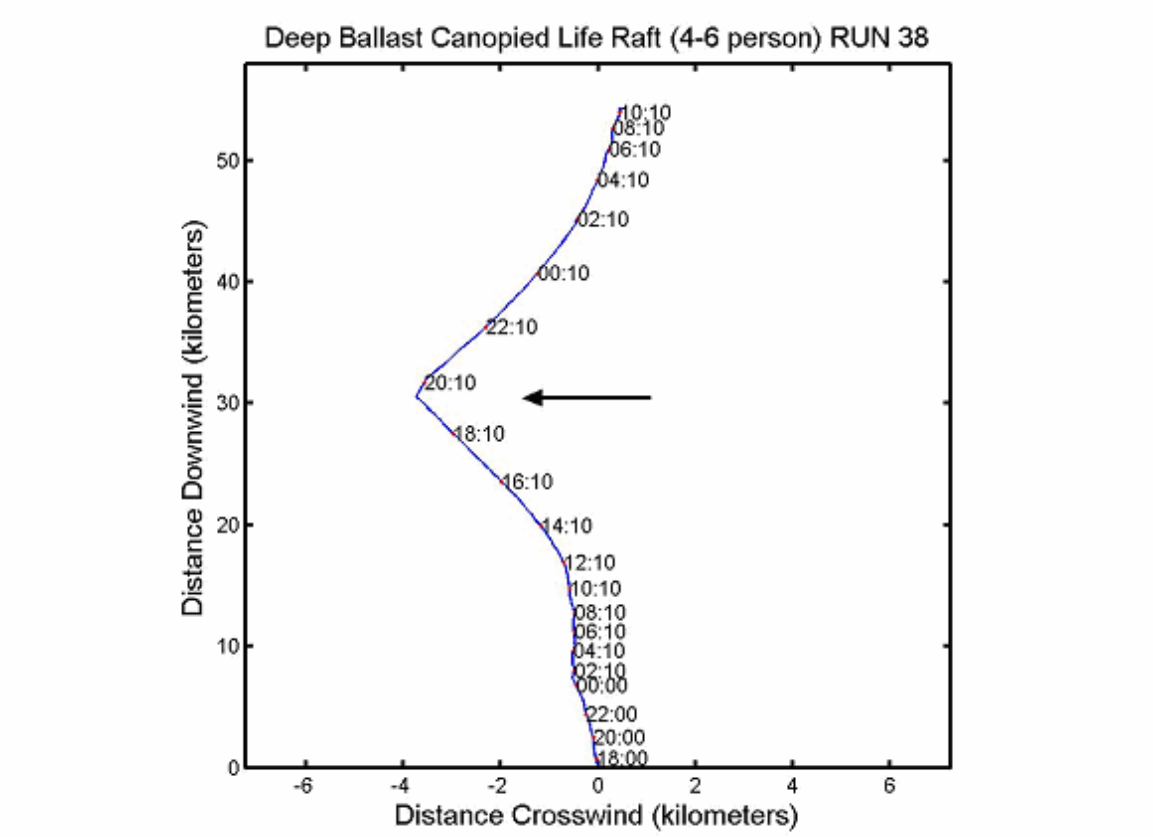

Figure D-5. Progressive Vector Diagram of the leeway displacement vectors for Drift Run 38, 4-6 person Life Raft starting at 1720Z 28 November 1993. Times of day are marked along the PVD.

Six other leeway drift runs contained seven additional changes in sign of the crosswind leeway component that were less pronounced that those observed during drift run 38. The descriptions of the life rafts are provided in Table D-1. The arrows in Figures D-7 and D-8 indicate changes in sign of CWL during leeway drift runs. The corresponding time series of the crosswind component of leeway and the 10-meter wind speed are shown in Figures D-9 and D-10. Vertical dash lines indicate the time of these seven CWL sign changes. The 10-meter wind speeds at the time of these changes in CWL were 6.2, 8.4, 4.6, 6.4, 12.7, 16.0, and 7.3 m/s.

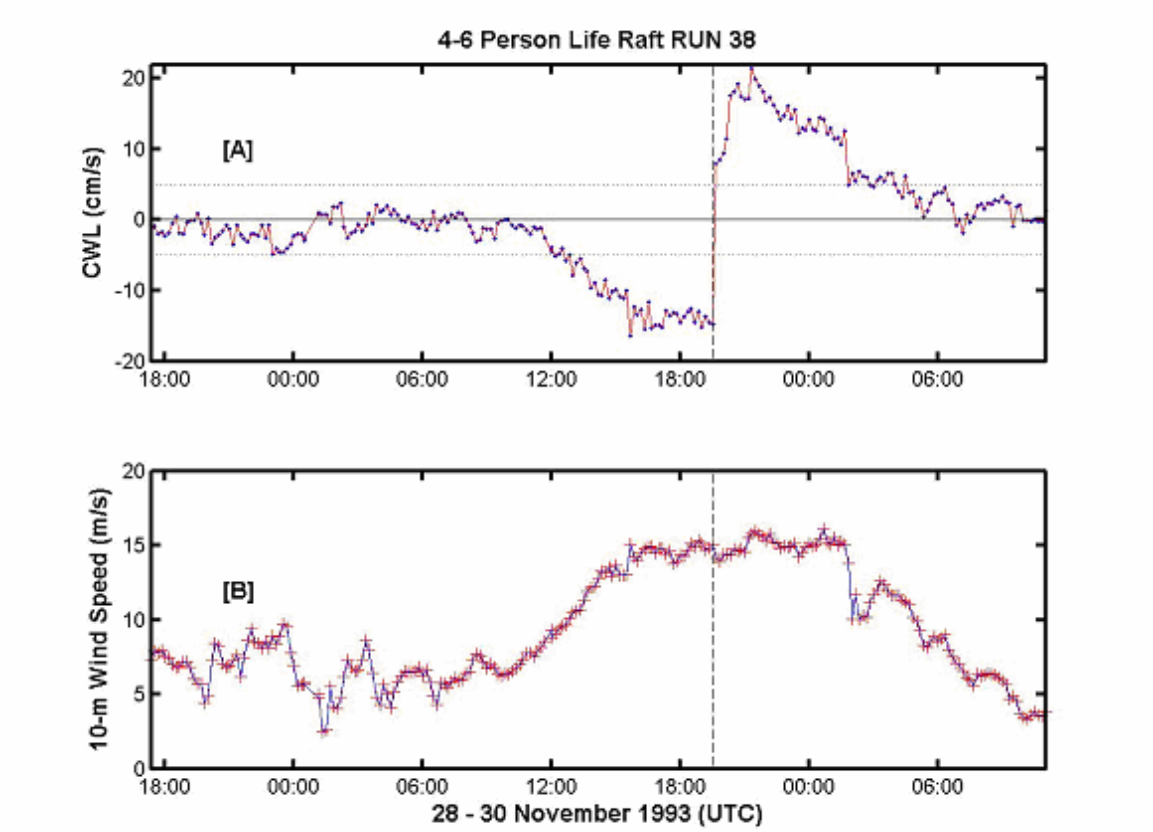

Figure D-6. Time series of [A] the crosswind component of leeway (cm/s) and [B] the wind speed adjusted to the 10-meter height, during drift run 38, 4-6 person life raft. A vertical-dashed line indicates the CWL sign change.

Table D-1. Characteristics of the 4-6 person Life Rafts that had Significant Changes in CWL sign.

RUN #	Life Raft Manufacturer	Description	Loading	Drogue
15	Beaufort	5-sided	Heavy	Yes
16	Tulmar	Round	Light	No
17	Tulmar	Round	Light	No
24	Tulmar	Round	Heavy	Yes
38	Beaufort	5-sided	Light	No
54	Beaufort	5-sided	Light	No
55	Beaufort	6-sided	Light	No

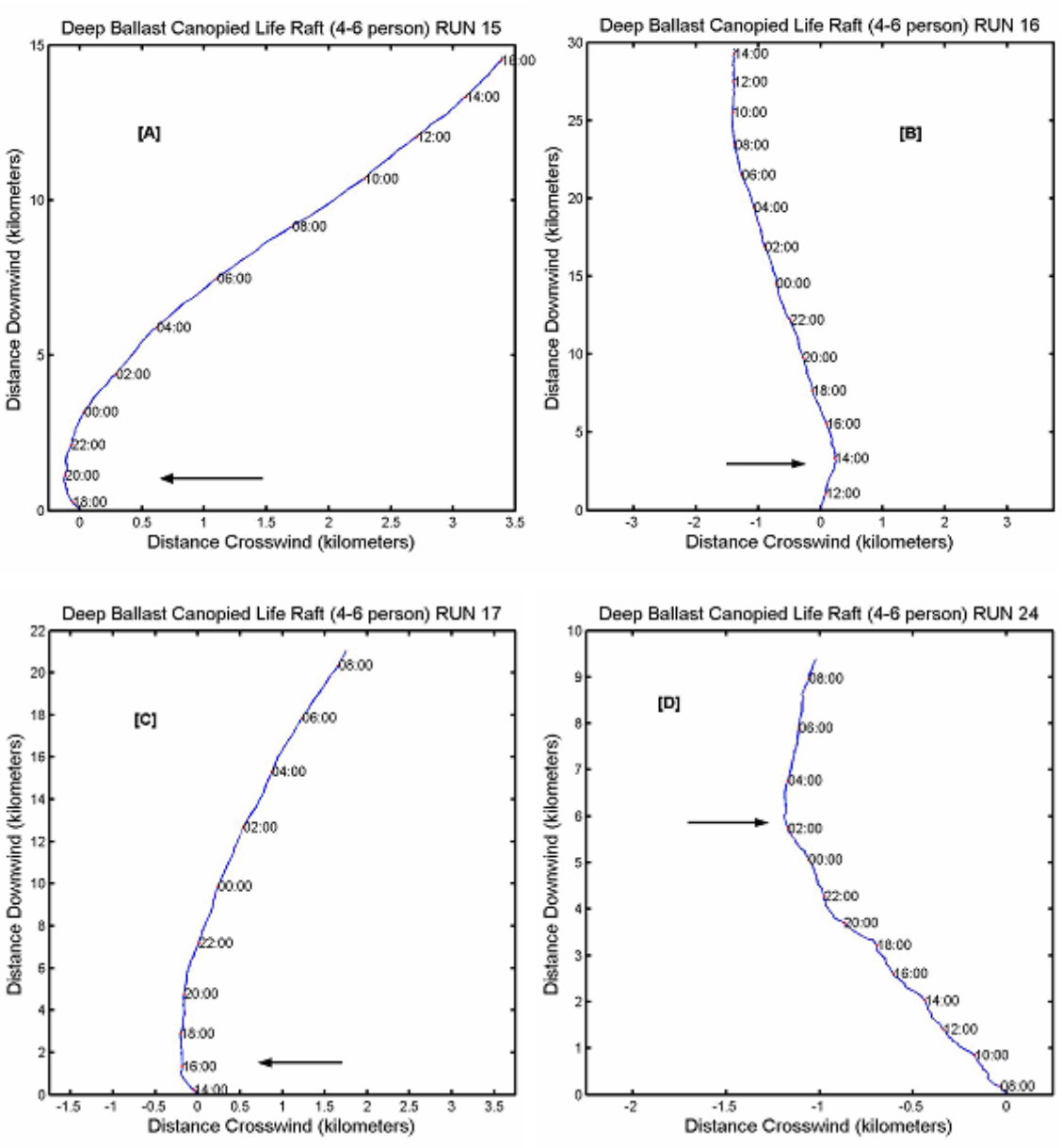

Figure D-7. Progressive Vector Diagrams of the leeway displacement vectors for Drift Runs [A] 15, [B] 16, [C] 17, and [D] 24; 4-6 person life rafts. Times of day are marked along the PVDs.

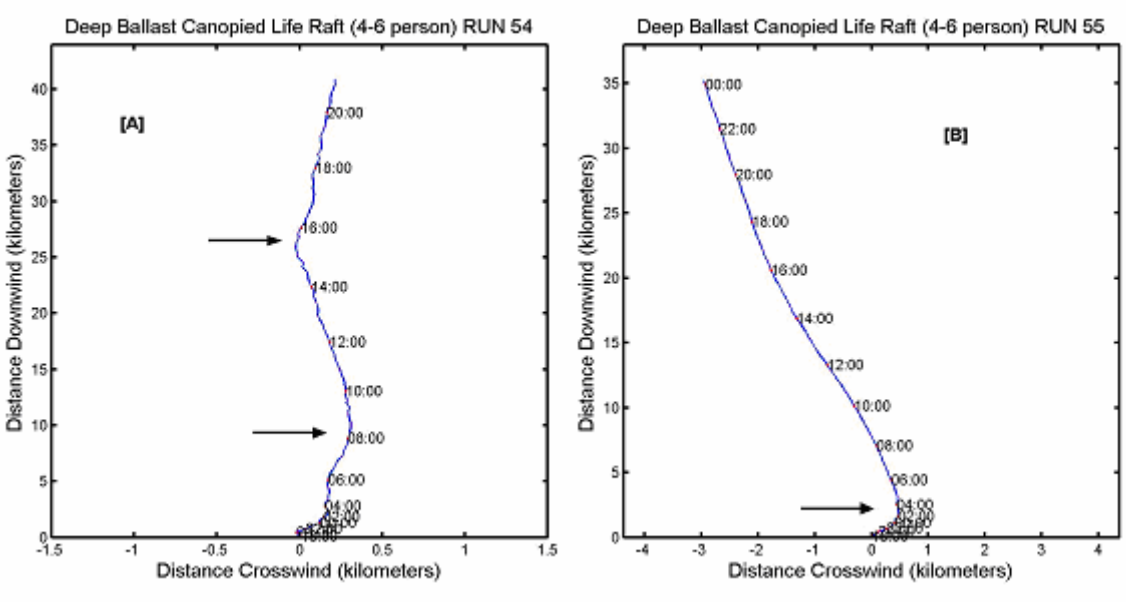

Figure D-8. Progressive Vector Diagrams of the leeway displacement vectors for Drift Runs [A] 54, and [B] 55, 4-6 person life rafts. Times of day are marked along the PVDs.

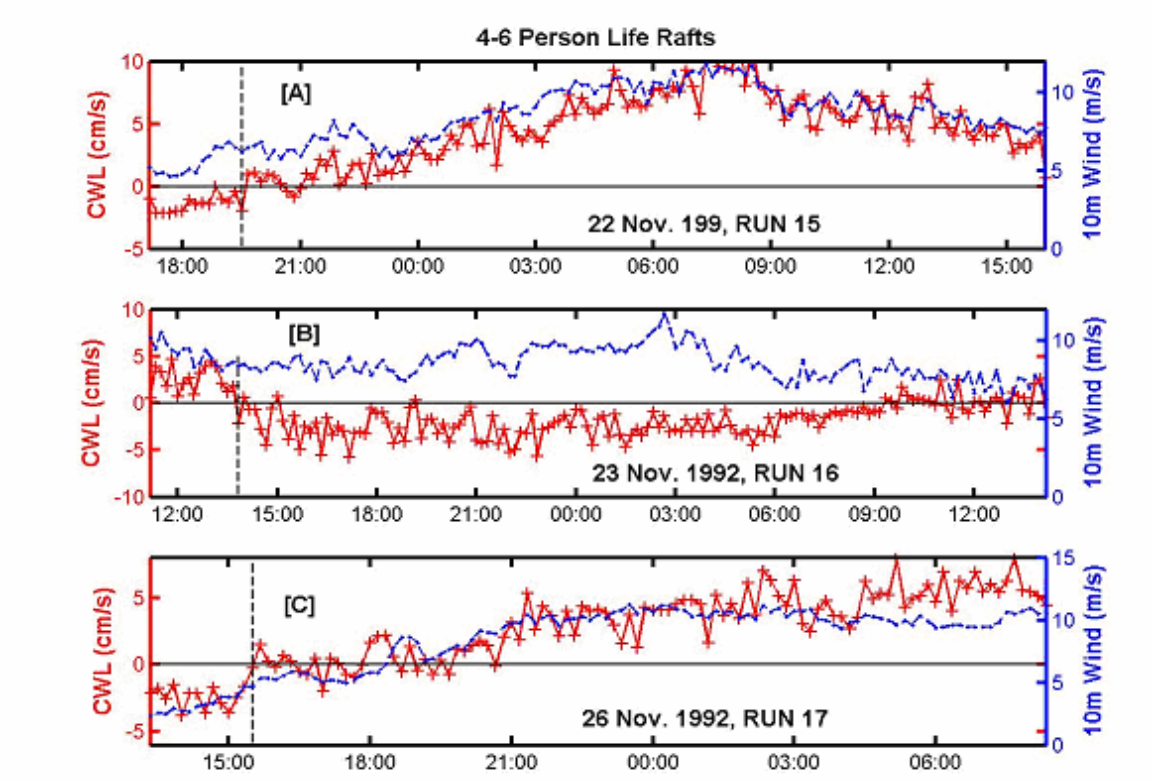

Figure D-9. Time series of the crosswind component of leeway (cm/s) (red crosses) and the wind speed adjusted to the 10-meter height (m/s) (blue dots), during drift run [A] 15, [B] 16, and [C] 17 of the 4-6 person life rafts. Vertical-dashed lines indicate the CWL sign changes.

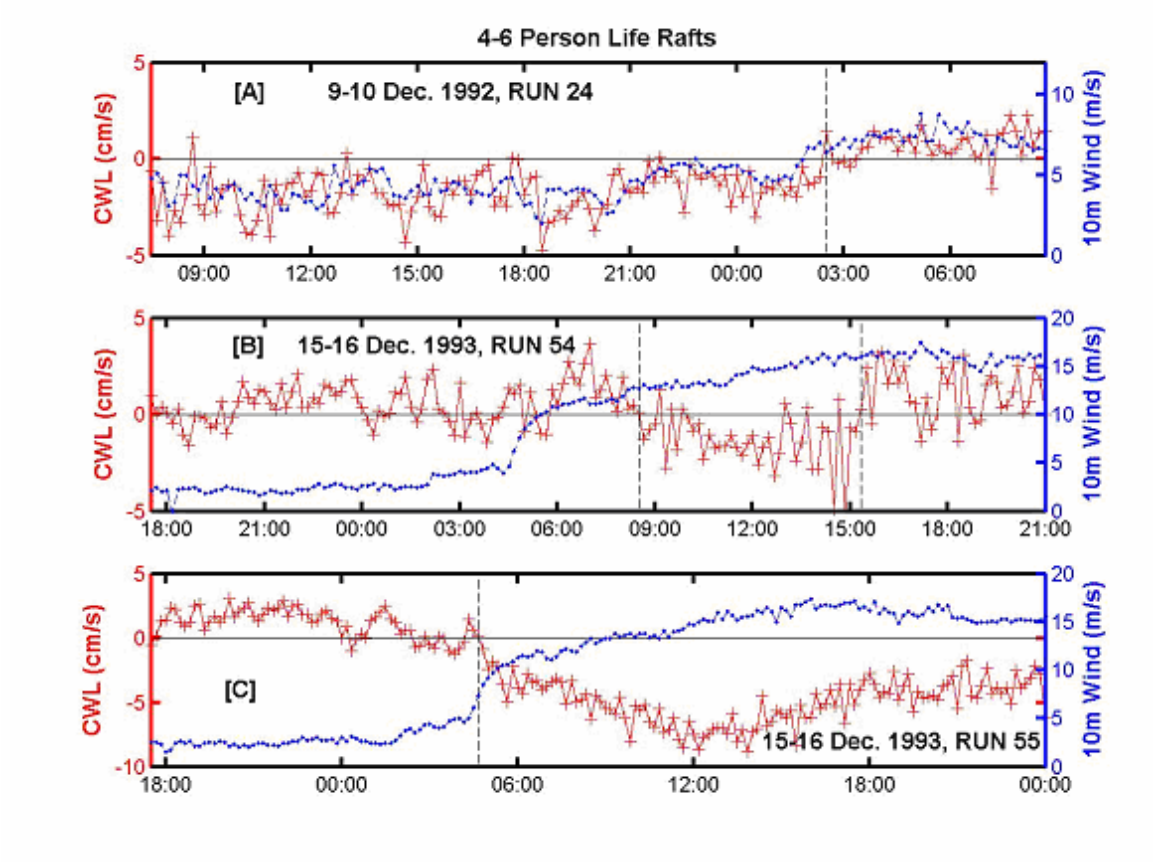

Figure D-10. Time series of the crosswind component of leeway (cm/s) (red crosses) and the wind speed adjusted to the 10-meter height (m/s) (blue dots), during drift run [A] 24, [B] 54, and [C] 55 of the 4-6 person life rafts. Vertical-dashed lines indicate the CWL sign changes.

D.3 20-Person Life Rafts

Twenty-person life rafts with deep ballast system and canopies were studied by Fitzgerald, Finlayson and Allen (1994), and Allen and Plourde (1999). For this general leeway category the life rafts were either lightly loaded without a drogue or heavy loaded with a drogue. A total of 268.3 hours of leeway data that resolved the crosswind component of leeway was collected on this category. Progressive Vector Diagrams of the downwind and crosswind components of leeway were plotted for the six drift runs of the 20-person life rafts. From these, five runs were identified as having significant sign changes in the crosswind component of leeway (Figures D-11 through D-15).

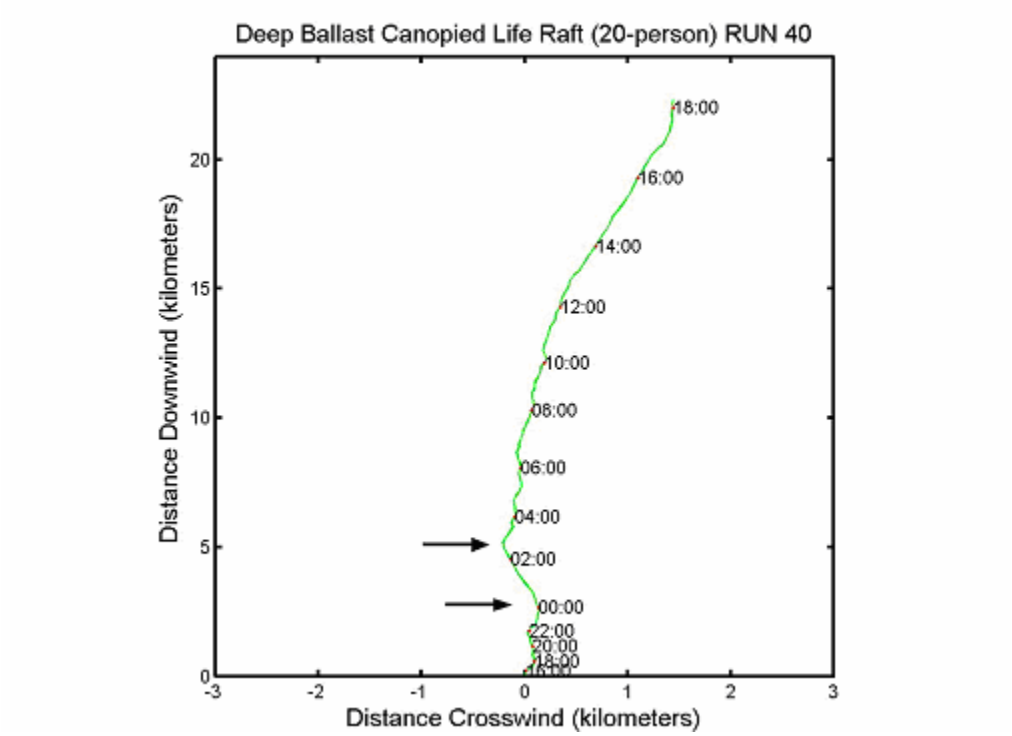

Figure D-11. Progressive Vector Diagram of the leeway displacement vectors for Drift Run 40, 20-person life raft starting at 1510Z, 30 November 1993. Times of day are marked along the PVD.

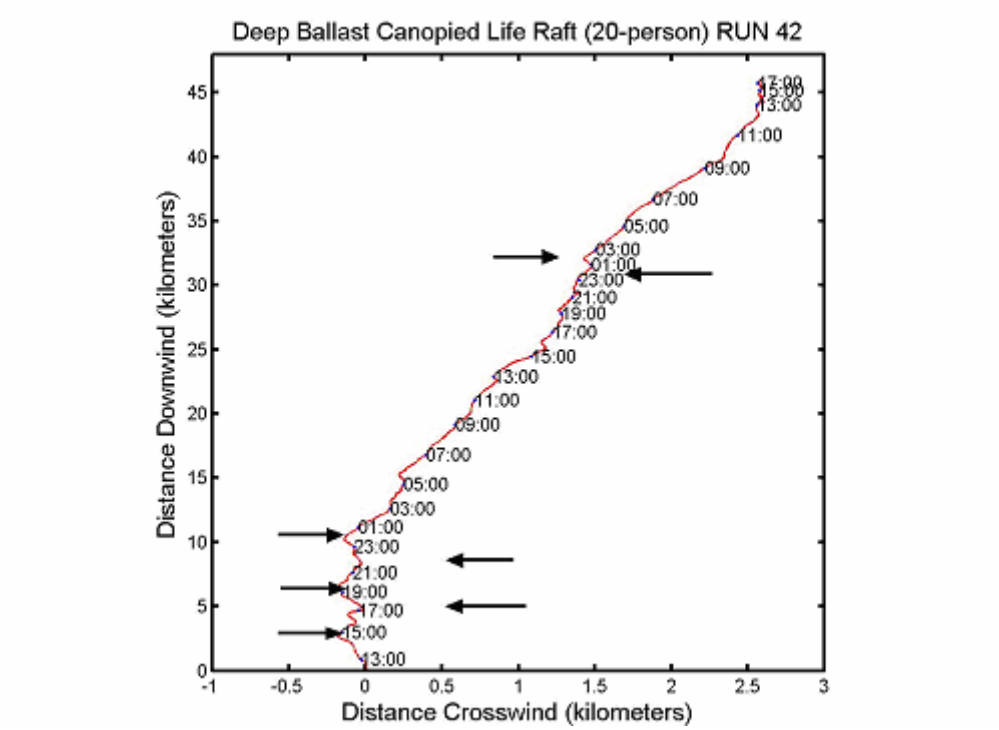

Figure D-12. Progressive Vector Diagram of the leeway displacement vectors for Drift Run 42, 20-person life raft starting at 1210Z, 2 December, 1993. Times of day are marked along the PVD.

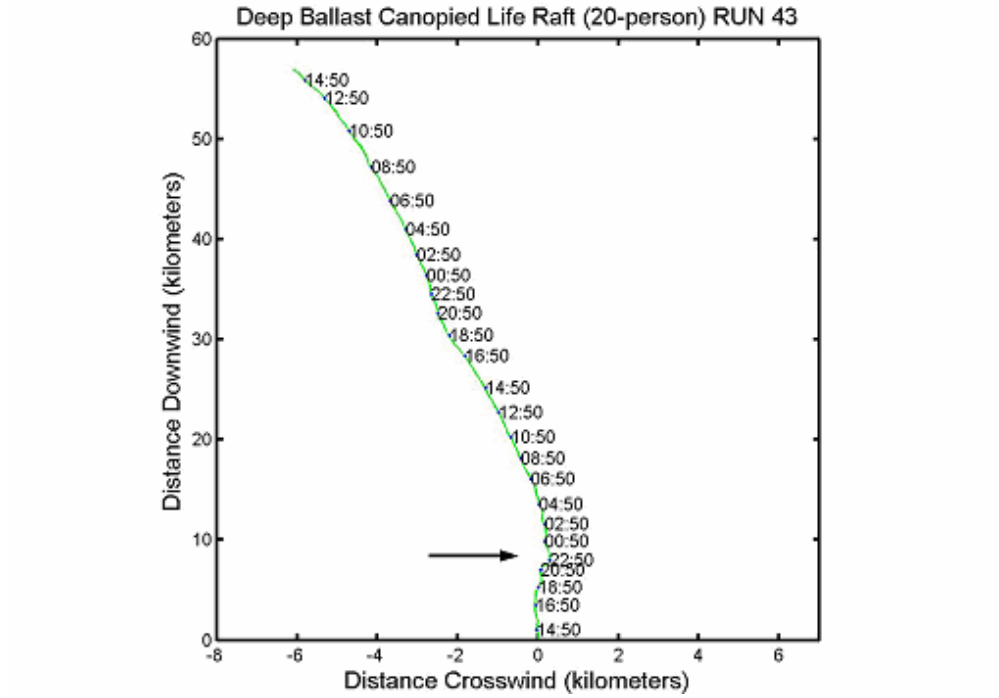

Figure D-13. Progressive Vector Diagram of the leeway displacement vectors for Drift Run 43, 20-person life raft starting at 1400Z, 2 December 1993. Times of day are marked along the PVD.

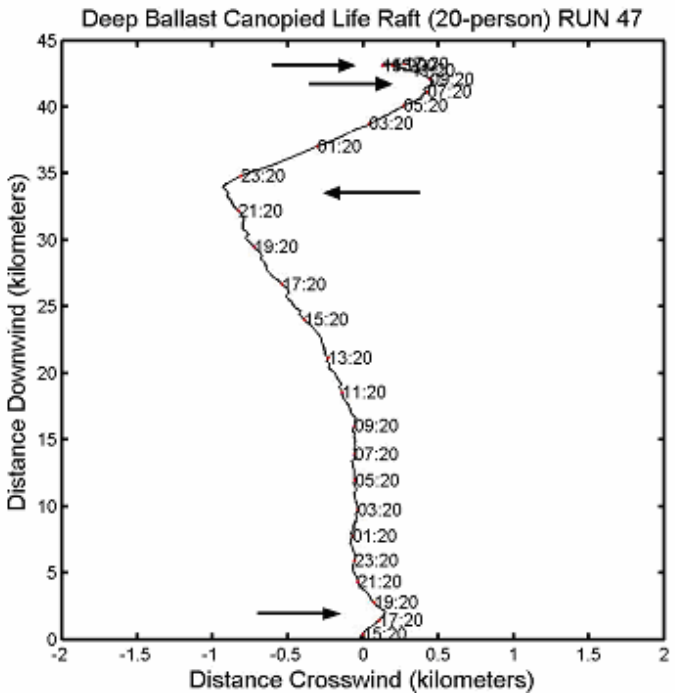

Figure D-14. Progressive Vector Diagram of the leeway displacement vectors for Drift Run 47, 20-person life raft starting at 1430Z, 9 December 1993. Times of day are marked along the PVD.

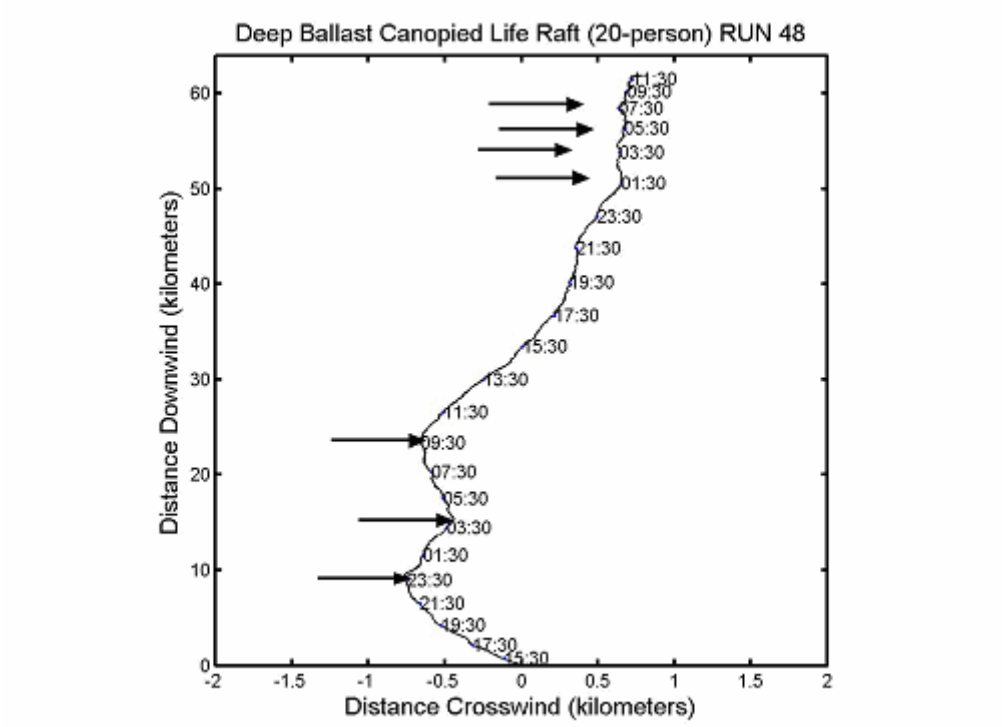

Figure D-15. Progressive Vector Diagram of the leeway displacement vectors for Drift Run 48, 20-person life raft starting at 1440Z 9 December 1993. Times of day are marked along the PVD.

The corresponding time series of the crosswind component of leeway and the 10-meter wind speed are shown in Figure D-17. Vertical dash lines indicate the time of the twenty-three CWL sign changes. The 10-meter wind speeds at time of these changes in CWL were 13.3, 9.8, 9.4, 8.3, 8.7, 5.7, 8.7, 6.7, 5.9, 4.7, 7.1, 11.7, 7.1, 0.7, 8.1,10.8, 11.1, 12.1, 11.2, 8.3, 7.5, 3.9, and 2.4 m/s.

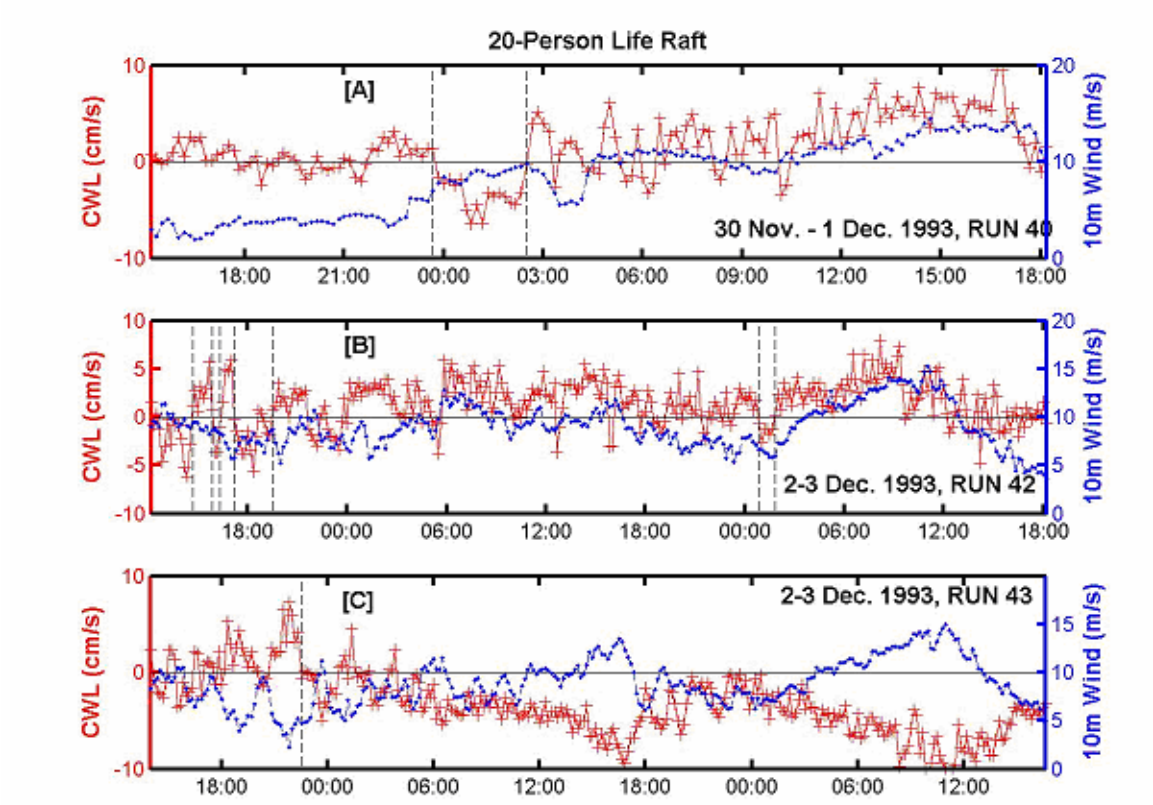

Figure D-16. Time series of the crosswind component of leeway (cm/s) (red crosses) and the wind speed adjusted to the 10-meter height (m/s) (blue dots), during drift run [A] 40, [B] 42, [C] 43, [D] 47 and [E] 48 of the 20-person life rafts. Vertical-dashed lines indicate the CWL sign changes.

D.4 One-Cubic Meter Wharf Box

Allen, Robe and Morton (1999) conducted leeway field tests on a one-cubic meter wharf box used by commercial fisherman to store ice and bait. Four drift runs were conducted, two with 1-person loading and two with four-person loading. A total of 102.2 hours of leeway data was collected on the wharf box. Progressive Vector Diagrams of the down and crosswind components of leeway were plotted for the 4 drift runs of the wharf box. From these, one run was identified as having significant sign changes in the crosswind component of leeway.

During Drift run 117, a lightly–loaded wharf box, there were two significant changes in the crosswind component of leeway at 0745Z and 1955Z on 22 January 1998, as shown in Figure D-17. The arrows in Figure D-17 indicate the changes in sign of CWL during leeway drift run 117. The corresponding time series of the crosswind component of leeway and the 10-meter wind speed are shown in Figure D-18. Vertical dash lines indicate the time of the CWL sign changes. The 10-meter wind speeds at time of these changes in CWL were 4.2 and 3.0 m/s.

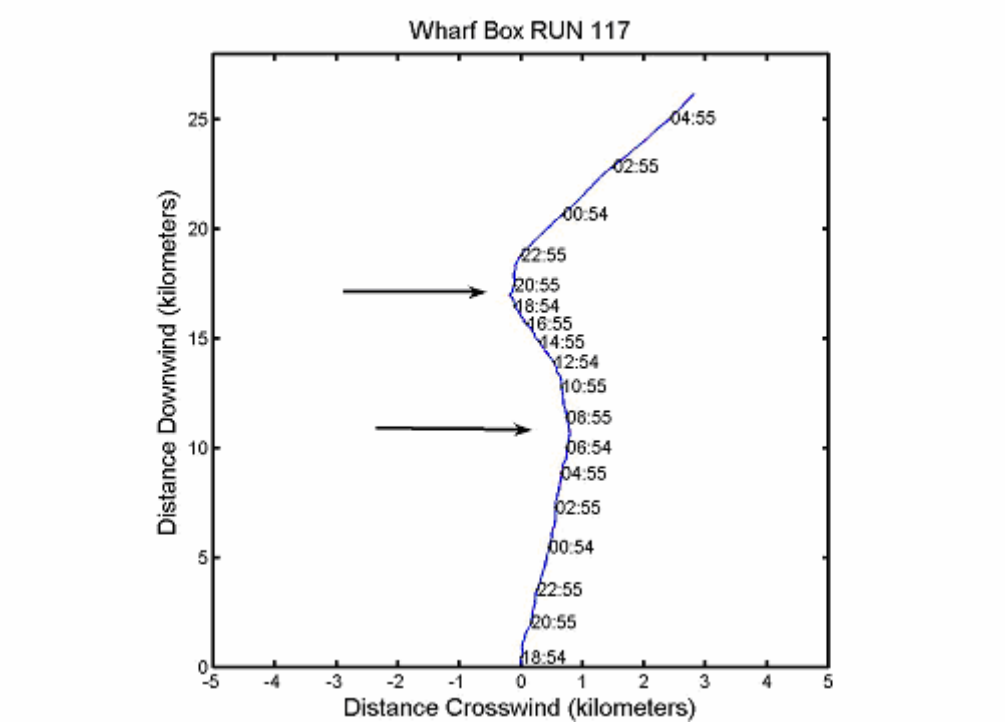

Figure D-17. Progressive Vector Diagram of the leeway displacement vectors for Drift Run 117, 1-cubic meter Wharf Box starting at 1820Z, 21 January 1998. Times of day are marked along the PVD.

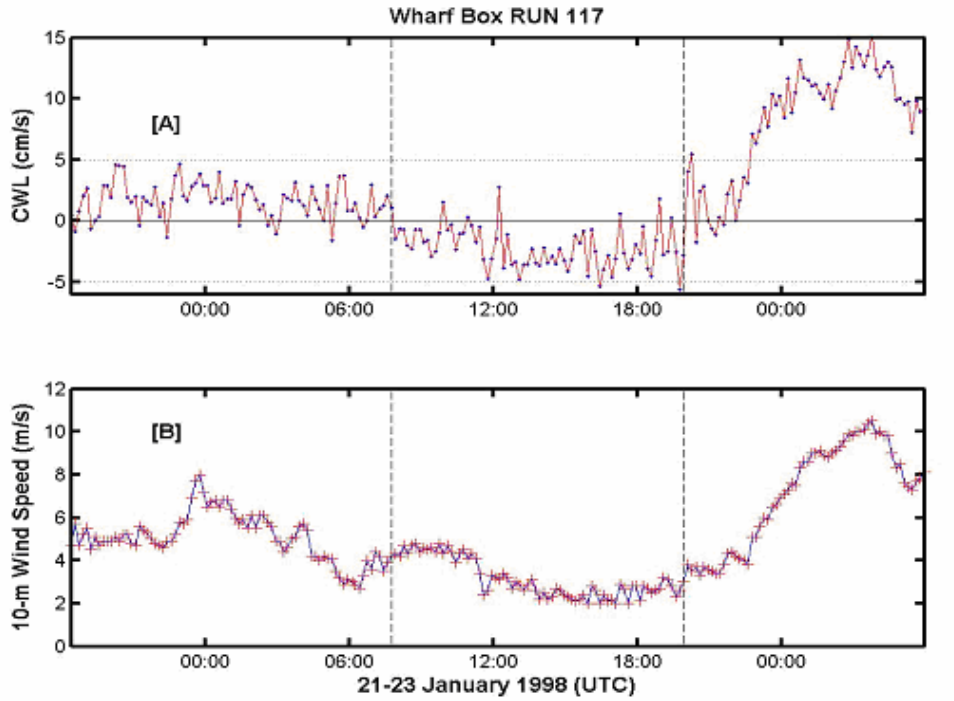

Figure D-18. Time series of [A] the crosswind component of leeway (cm/s) and [B] the wind speed adjusted to the 10-meter height, during drift run 117, 1-cubic meter wharf box. Vertical-dashed lines indicate the CWL sign changes.